Identification and characterization of proteomic regulations in the cerebellum region of brain in MM1 and VV2 subtypes of sporadic Creutzfeldt-Jakob disease (sCJD)

Dissertation

for the award of the degree

"Doctor rerum naturalium" (Dr.rer.nat.)

(alternatively: "Doctor of Philosophy" Ph.D. Division of Mathematics and Natural Sciences)

of the Georg-August-Universität Göttingen

within the doctoral program “Biology”

of the Georg-August University School of Science (GAUSS)

Submitted by

WAQAS TAHIR

from Pakpattan, Pakistan

Göttingen, 2016

Thesis Committee

Anleiter/in: Dr. rer. nat. Saima Zafar

Prion research group, Department of Neurology, UMG, Goettingen.

Betreuer and Referent: Prof. Dr. Mikael Simons

Max Planck Institute for Experimental Medicine, Goettingen.

Betreuer and Korreferent: PD Dr. Michael Hoppert

Dept. of General Microbiology, Georg August University Göttingen.

Further members of the Examination Board

1- **Prof. Dr. Tiago Fleming Outeiro**

   Dept. of Neuro-Degeneration and Restaurative Research, University Medical Center Göttingen.

2- **Prof. Dr. Uwe Groß**

   Institute for Medical Microbiology, University Medical Center Göttingen.

3- **Prof. Dr. Markus Zweckstetter**

   Protein structure determination using NMR, Max Planck Institute for Biophysical Chemistry.

4- **Prof. Dr. E. A. Wimmer**

   Dept. of Developmental Biology, Georg-August-University Goettingen.

Date of the oral examination: 02 June, 2016

DECLARATION

I hereby declare that the PhD thesis entitled “Identification and characterization of proteomic regulations in the cerebellum region of brain in MM1 and VV2 subtypes of sporadic Creutzfeldt-Jakob disease (sCJD)” is exclusively my own work. It is solely written by my-self and it does not contain any already published / written material except quoted with references.

Waqas Tahir Göttingen, 09 May, 2016

Dedicated to

Holy Prophet Muhammad (Peace be upon Him)

Table of Contents

List of Figures

List of Tables

1 List of Abbreviations

2-DE	Two Dimensional Electrophoresis
Ab	Antibody
AD	Alzheimer's Disease
ARE	Antioxidative Response Element
cDNA	Complimentary deoxyribonucleic acid
Ct	Threshold cycle
dd H_2O	Double distilled water
DTT	Dithiothreitol
HRP	Horse Reddish Peroxidase
IEF	Isoelectric Focusing
IFN-γ	Interferon gamma
IgG	Immunoglobulin G
IL	Interleukin
IL-17	Interleukin 17
IL-1β	Interleukin 1 Beta
kDa	Kilodalton
Keap1	Kelch-like ECH-associated protein 1
Min	Minutes
MS	Multiple Sclerosis
Nrf2	Nuclear factor (erythroid-derived 2)-like 2
OD	Optical density
PBS	Phosphate buffered saline
PCR	Polymerase chain reaction
PD	Parkinson's Disease
pI	Isoelectric Point
PrP^{C}	Cellular Prion Protein
PrP^{SC}	Scrapie form of Prion Protein
ROS	Reactive Oxygen Species
RPM	Rounds per minute

RT	Room temperature
RT-PCR	Reverse transcriptase-PCR
sCJD	Sporadic Creutzfeldt-Jakob disease
SDS	Sodium dodecylsulfate
SDS-PAGE	SDS-polyacrylamide gel electrophoresis
SEM	Standard error of the mean
TEMED	N, N, N´, N´-tetramethylethylenediamine
Tris	Tris-(hydroxymethyl)-aminomethane
TSE	Transmissible Spongiform Encephalopathies
WB	Western Blot

2 Abstract

Sporadic Creutzfeldt–Jakob disease (sCJD) is a fatal, transmissible spongiform encephalopathy (TSE) characterized by broad range of clinical and pathological manifestations. Pathological features of sCJD are largely dependent on the presence of misfolded form of cellular prion protein (PrP^{C}); known as PrP^{SC} and polymorphism (methionine and valine) at codon 129 of *PRNP* gene that encodes PrP^{C}. Exact etiological factors of sCJD are still unknown. Codon 129 genotype of *PRNP* gene and the type of PrP^{SC} (type 1 or type 2) influence the heterogeneity of disease as defined by regional specific pathological features potentially regulating the molecular pathways which lead to development of subtype dependent disease phenotypes. In this study, we have investigated the whole proteomic regulations in cerebellum region of brain of the two most prevalent subtypes (MM1 and VV2) of sCJD patients using two dimensional gel electrophoresis (2DE) and mass spectrometry. Analysis of all protein spots on 2DE gels with DECODON Delta2D software, revealed twenty five differentially regulated protein spots and identification of these spots with MALDI-TOF MS/MS revealed eighty three differentially regulated proteins in both subtypes in cerebellum region of brain from sCJD patients. Forty proteins in MM1 subtype and forty three proteins in VV2 subtype were found regulated. Twelve proteins were commonly regulated in both subtypes with five of those showed inverse expressional regulation and rest seven showed similar expressional regulation in both subtypes. Top three regulated cellular molecular mechanisms in both subtypes included, i)- cell cycle; gene expression and cell death, ii)- cellular stress response/ oxidative stress and iii)- signal transduction and synaptic functions Most of the proteins under the classification of cellular stress responses, were associated with oxidative stress related cellular molecular functions. DJ-1 which is a well-known sensor of oxidative stress, was also found regulated under the category of cellular stress responses. DJ-1 protects the cells against oxidative stress directly by translocalizing to nucleus for activation of antioxidative genes and indirectly by activating the Nrf2/ARE pathway. Our experimental results demonstrated the activation of Nrf2/ARE pathway in both MM1 and VV2 subtypes of sCJD. DJ-1 also showed significant upregulation in its mRNA expression in both MM1 and VV2 subtypes but protein expression only in VV2 subtype in cerebellum of brain of sCJD patients. Furthermore, DJ-1 protein expression was also found to be increased during the pre-symptomatic and symptomatic stages in cerebellum of brain of mice models of sCJD (MM1 and VV2) and

during the clinical stage in CSF samples of sCJD patients as well. These results suggest the implication of oxidative stress during the pathophysiology of sCJD and use of DJ-1 as a potential sensor of oxidative stress during the clinical phase of sCJD.

3 Introduction

3.1 Neurodegenerative Diseases

Human Central nervous system (CNS) which includes brain and spinal cord is comprised of 100 billion of neurons. Neurons are responsible for the relay of information in the form of electric impulses throughout the whole body. Any condition leading to the impairment of the structure or function of the neurons or leading to the death of the neurons is known as neurodegeneration which may lead to various neurodegenerative diseases. Neurodegenerative diseases are one of the most serious and inexorable health challenges faced by modern day world leaving behind either physical debilitations or sudden mortality. Few examples of neurodegenerative diseases include Alzheimer's disease (AD), Parkinson's disease (PD), and Prion diseases.

Neurodegenerative diseases are not easy to be exactly diagnosed due to inaccessibility to the brain so many times patients with various neurodegenerative signs lose their lives even without precise diagnosis and hence treatment. Every neurodegenerative disease may differ from others in its pathophysiology resulting either from any of the following factors or combination of any of these factors

- Genetic mutations (Huntington's disease)
- Protein misfolding and aggregation (Prion diseases and Alzheimer's disease)
- Intracellular mechanisms including impairment in protein degradation pathways, membrane damage, mitochondrial dysfunction, deregulation of axonal transport and programmed cell death

A unique group of neurodegenerative diseases which arise from protein misfolding are known as Prion diseases resulting in the malfunctioning of proteins in the CNS. The exact etiology of such diseases is still not clear.

3.2 Prion Diseases

Prion diseases are also known as transmissible spongiform encephalopathies (Prusiner and DeArmond, 1994) which can be sporadic, inherited or acquired in their origin (Gambetti et al.,

2003). Prion diseases are characterized by neurodegeneration and aggregation of proteins in CNS (Linden et al., 2008). Prion diseases can affect individuals of any age group and carry a variety of motor or cognitive clinical manifestations. In spite of their low prevalence rate, Prion diseases are still invariably fatal and incurabe (Knight and Will, 2004).

3.2.1 Prion diseases in animal

Many of the animal species suffer from prion diseases like scrapie in sheep and goat, transmissible mink encephalopathy (TME) in mink, chronic wasting diseases (CWD) in cervids, bovine spongiform encephalopathy (BSE) in bovines, exotic ungulate encephalopathy (EUE) in nyala and kudu, feline spongiform encephalopathy (FSE) in cats and non-human primate TSE (NHP) in lemurs. Prion diseases in animals mostly occur due to infection with Prions of unknown origin (Imran and Mahmood, 2011).

3.2.2 Human prion diseases

Other than animals, humans also suffer equally from prion diseases and have different variants of the prion diseases with characteristic clinical and pathological manifestations. Prion diseases in human can be sporadic, genetic/ familial or acquired.

3.2.2.1 Sporadic prion diseases in human

Sporadic prion diseases make most of the proportion of human prion diseases that is up to 85% and arise due to spontaneous conversion of cellular form of prion protein (PrP^{C}) in to its pathogenic form known as scrapie form of prion protein (PrP^{SC}) (Puoti et al., 2012). Sporadic prion diseases include three phenotypes: Creutzfeldt-Jakob disease (CJD), fatal insomnia, and variably protease-sensitive prionopathy (VPSPr). Sporadic form of CJD (sCJD) comprises of more than 85-90% of all sporadic prion diseases (Puoti et al., 2012).

3.2.2.2 Genetic/ familial prion diseases in human

Familial forms of prion diseases comprise 10-15% of total prion diseases and are caused by mutation in prion protein gene. Familial Creutzfeldt-Jakob disease (fCJD) and fatal familial insomnia (FFI) are two familial forms of prion diseases which arise due to the polymorphism at D178N (replacement of asparagine- N with aspartic acid- D) but disease phenotype is segregated for both types by the presence of polymorphism at codon 129 of *PRNP* gene. fCJD is linked to the presence of valine and FFI is linked to the presence of methionine at codon 129 of mutant

allele (Goldfarb et al., 1992) showing opposite lesion topography in thalamus and cerebral cortex respectively. Gerstmann-Sträussler-Scheinker (GSS) is another genetic form of human prion diseases but is quite rare. It is an autosomal dominant linked to mutations in the *PRNP* gene (at codons 102 and 198 of *PRNP* gene being the most common ones). Clinical manifestations include rapidly progressive dementia in familial form of CJD (fCJD), slowly progressive ataxia accompanied by later onset of dementia in GSS, and insomnia, hallucinations and motor signs in FFI (Mead, 2006).

3.2.2.3 Acquired prion diseases in human

Acquired forms of prion diseases arise due to the transmission of infectious agent. Transmission of prion diseases occurs by the transfer of the agent mostly from the brain extracts from affected individuals into susceptible host species. Evidences about the transmission of prion disease into humans date back to 1950 when kuru epidemics occurred by ritual cannibalism in Papua New Guinea (Gajdusek and Zigas, 1957) followed by occurrence of 450 cases of iatrogenic Creutzfeldt–Jakob disease (iCJD) after growth hormone treatment or surgical interventions (Duffy et al., 1974). Finally, variant CJD (vCJD) in humans occurred by consuming meat of cattle affected with bovine spongiform encephalopathy (BSE) (Will, 1994).

3.2.3 Biology of PrP^{C}

Cellular form of prion protein (PrP^{C}) is the protein which serves as a substrate during the conversion of PrP^{C} into PrP^{SC}.

3.2.3.1 Expression of PrP^{C}

Efforts to identify the characteristics of PrP^{SC} led to the discovery of *PRNP* gene encoding PrP^{C} (Basler et al., 1986;Chesebro et al., 1985) on chromosome 20 in humans. PrP^{C} is expressed throughout the whole body (Ford et al., 2002) but it is highly expressed in CNS (Harris et al., 1993b;Manson et al., 1992) and localized more at both pre- and post-synaptic vesicles (Brown et al., 1996) and glial cells (Moser et al., 1995). Cellular prion protein is also constitutively expressed in peripheral nervous system as well as immune cells, lymphoid organs and intestinal system (Linden et al., 2008).

3.2.3.2 Biosynthesis and Intracellular Trafficking of PrP^C

After its synthesis in endoplasmic reticulum (ER), PrP^C makes its way to the plasma membrane through Golgi network (Harris, 2003), where PrP^C is anchored into lipid rafts with Glycosyl-phosphatidylinositol (GPI) anchor on its C-terminal (Stahl et al., 1987). PrP^C undergoes posttranslational modifications during its stay in the ER and Golgi, which include glycosylation at two asparagine residues (Haraguchi et al., 1989), formation of a disulfide bond between two cysteine residues at amino acid residues 179 and 214 in human PrP (Turk et al., 1988) and the addition of a GPI anchor at the carboxy-terminus of PrP (Stahl et al., 1992). Localization of PrP^C at cell surface is short lived and PrP^C is internalized back into the cytosol for recycling or degradation in lysosomes (Taraboulos et al., 1992). This process of internalization and trafficking of PrP^C takes by both clathrin-coated pits and/or caveolin mediated endocytic pathways (Harris et al., 1993a;Shyng et al., 1994;Shyng et al., 1993;Vey et al., 1996) (Fig. 3.1). In addition, PrP^C can also exist in extracellular spaces after cleavage at GPI anchor resulting in the release of PrP^C from the cell surface (Hay et al., 1987).

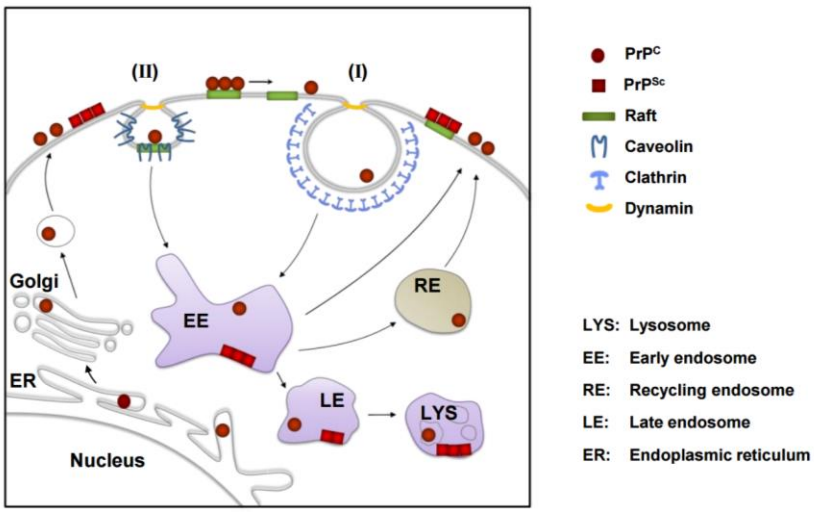

Figure 3-1: Biosynthesis and Intracellular trafficking of PrP^C
PrP^C is synthesized in the endoplasmic reticulum (ER) and passes through the secretory pathway to the cell surface, where it resides in lipid rafts. In many cells, PrP^C leaves lipid rafts prior to being internalized by clathrin-dependent endocytosis **(I)**. Clathrin-independent raft/caveolae-dependent internalization **(II)** of PrP^C has also been proposed for some cells. PrP^C can be degraded by lysosomes or rapidly recycled back to the cell surface by recycling endosomes (RE). In cultured scrapie-infected cells the conversion of PrP^C to PrP^{SC} is believed to take place on the cell surface and/or in vesicles along the endolysosomal

pathway. After conversion PrP^{SC} can accumulate at the cell surface or in intracellular vesicles (e.g. lysosomes). Source modified: (Grassmann et al., 2013)

3.2.3.3 Physiological functions of PrP^{C}

Conserved sequence of PrP^{C} during evolution (Rivera-Milla et al., 2006) suggests important putative functions of this protein. But, the exact biological functions of PrP^{C} are still obscure. Localization of PrP^{C} on cell surface implicates regulation of important transmembrane signal transduction cascades (Taylor and Hooper, 2006;Tsui-Pierchala et al., 2002) through PrP^{C} and presumably it requires adopter proteins for transmitting signals into the cytoplasm. These transmembrane signaling pathways may potentiate several cellular mechanisms including neuronal survival, neurite outgrowth and neurotoxicity. PrP^{C} is found to modulate the activity of glutamate receptors like NMDA and thus suppressing the neuronal excitotoxicity. Activation of the NMDA receptors can induce nerve cell damage leading to neuronal death in several acute and chronic neurological disorders by inducing abnormal entry of Ca^{+2} ions into neurons, resulting in neuronal excitotoxicity (Gillessen et al., 2002). Interaction of PrP^{C} (at residues 113–128) with secretory form of cytoplasmic co-chaperone; stress-inducible protein 1 (STI1), also promote neuronal survival and differentiation (Zanata et al., 2002). PrP^{C} mediated neuroprotective role of PI3 kinase/Akt signaling pathways protects the cells against oxidative stress (Vassallo et al., 2005;Weise et al., 2006). Interaction of PrP^{C} with neural cell adhesion molecule (N-CAM) (Schmitt-Ulms et al., 2001) promotes neurite outgrowth by recruiting N-CAM to lipid rafts, thus activating fyn kinase (Santuccione et al., 2005) as shown in figure 3.2.

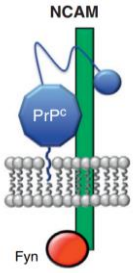

Figure 3-2: A role for the PrP^{C} in cell adhesion
Interaction of PrP^{C} with neural cell adhesion molecule (NCAM), which results in activation of Fyn kinase and enhancement of neurite outgrowth in cultured hippocampal neurons. Source modified: (Biasini et al., 2012)

Expression of PrP^{C} at axons and pre-synaptic terminals (Ford et al., 2002) suggests its role in synapses formation by increasing the number of synaptic contacts (Kanaani et al., 2005). Behavioral studies of $PrP^{-/-}$ mice show various neurobiological abnormalities implicating role of PrP^{C} in organization of nerve fibers (Colling et al., 1997), circadian rhythm (Tobler et al., 1996), and spatial learning (Criado et al., 2005). In addition, PrP^{C} is also found to potentiate the release of acetylcholine at neuromuscular junctions (Re et al., 2006). PrP^{C} has well known neuroprotective role against Bax induced apoptosis (van Delft et al., 2006;Yuan and Yankner, 2000) but this neuroprotective role of PrP is impaired upon its conversion into PrP^{SC} (Westergard et al., 2007a). There is no evidence about the direct involvement of PrP^{C} in mediating any neurotoxicity so far but synthetic peptide PrP106-126 is found to mimic the toxic effects of PrP^{SC} (Selvaggini et al., 1993) but in the presence of PrP^{C} (Brown et al., 1994;Forloni et al., 1993). PrP^{C} can bind up to four Cu^{+2} ions in its octa-peptide repeat region (Walter et al., 2006) showing role of PrP in Cu metabolism and traffickling at synapses (Brown, 2001;Walter et al., 2006). Copper serves as an important co-factor for a number of enzymes catalyzing redox cellular reactions (Westergard et al., 2007b). Any impairment in the uptake or transport of highly reactive Copper ions (Puig and Thiele, 2002) can lead to several neurodegenerative diseases (Waggoner et al., 1999).

3.2.4 The concept of Prion pathology

Physiological functions of PrP^{C} as mentioned above are impaired once it comes in contact with PrP^{SC} leading to prion pathology. But it is still unexplored how PrP^{SC} impairs the normal physiological functions of PrP^{C}.

3.2.4.1 Conversion of PrP^{C} into PrP^{SC}

Prion pathology arises due to misfolding of the cellular form of prion protein (PrP^{C}) which is transformed into its pathogenic form known as scrapie form of prion protein (PrP^{SC}) (Klemm et al., 2012). Cellular form of prion protein is encoded by *PRNP* gene and is expressed highly in CNS (Bolton et al., 1984;Prusiner et al., 1984). Both cellular form and scrapie forms of prion protein share the same amino acid sequence and are encoded by a same gene (Basler et al., 1986;Oesch et al., 1985). PrP^{C} is detergent soluble and sensitive to PK digestion and is involved in lots of physiological functions of the cell. But after conversion of PrP^{C} into PrP^{SC}, all the

protective functions of PrP^{C} are lost and toxic functions are gained by its pathological form (PrP^{SC}). Schematic representation of prion replication is illustrated in figure 3.3.

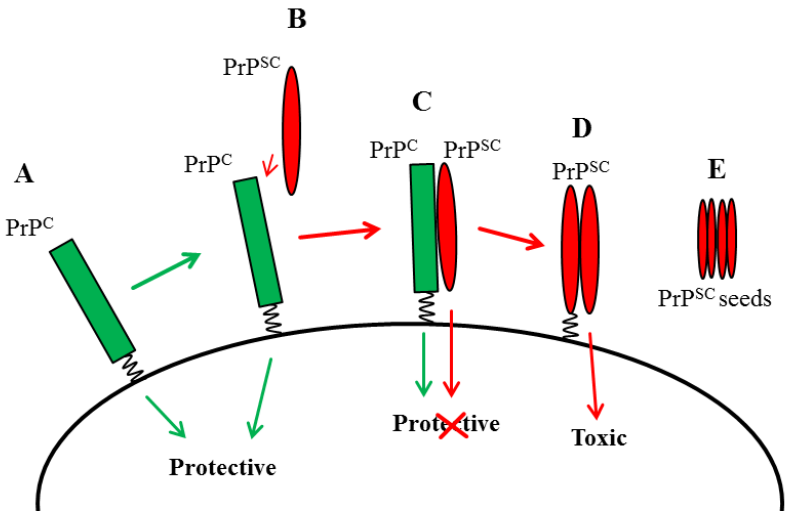

Figure 3-3: Schematic representation of Prion replication (Conversion of PrP^{C} into PrP^{SC})
Localization of normal cellular prion protein at cell surface anchored into lipid rafts with the help of GPI anchor and implicated variety of neuroprotective functions **(A)**. PrP^{SC} appears to contact PrP^{C} **(B)**. PrP^{SC} comes in contact to PrP^{C} and neuroprotective functions of PrP^{C} are impaired (loss of functions) **(C)**. PrP^{C} is also converted to PrP^{SC} due to some unknown reasons after contact with PrP^{SC} and PrP^{SC} then implicates neurotoxic function (gain of toxic functions) **(D)**. Newly formed PrP^{SC} is released into extra-cellular spaces and serves as seeds for further prion replication **(E)**.

3.2.4.2 Conformational shift

Pathogenic form of the prion protein; PrP^{SC}, which is predominantly beta sheet rich structure containing up to 45% beta sheet contents and 30% alpha helical structures results by conversion from alpha helical rich structure PrP^{C} containing up to 40% alpha helical structure and 3% beta sheet contents (Pan et al., 1993;Prusiner et al., 1998) as demonstrated in figure 3.4.

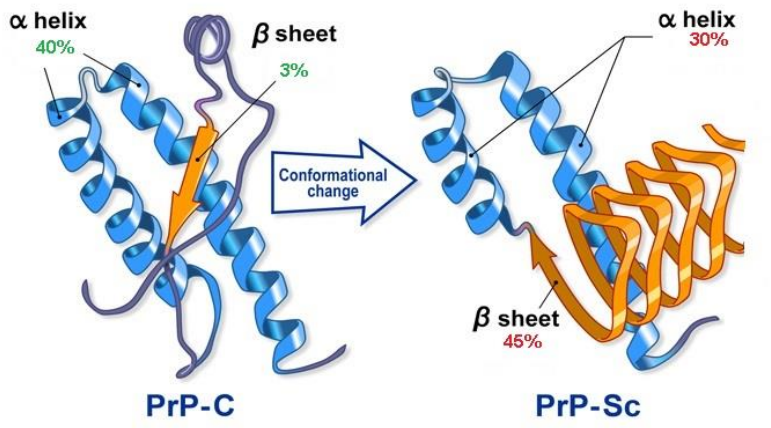

Figure 3-4: Conformational shift during conversion of PrP^{C} into PrP^{SC}
Alpha helical rich conformer; PrP^{C} is converted to β sheet rich conformer; PrP^{SC}. Source modified: (Eghiaian et al., 2004)

3.2.4.3 Properties of PrP^{SC}

Resultant PrP^{SC} is resistant to proteolytic digestion and has the tendency to form PK resistant aggregates that in turn accumulate in the brain (Ross and Poirier, 2004) which is considered to be the main pathological event resulting in neurodegeneration. The scrapie form of prion protein (PrP^{SC}) is insoluble in detergents and resists radiation (Bellinger-Kawahara et al., 1987a) which can easily inactivate both bacteria and viruses (Alper, 1985). The sensitivity of scrapie form of prion protein to various chemicals differs widely suggesting that infectivity of the scrapie form of prion protein is not determined by nucleic acid (Bellinger-Kawahara et al., 1987b).

3.2.4.4 Prion pathology

Hallmark histopathological features of prion diseases include sponges formation/ vacuole formation throughout the cerebral grey matter (Figure 3a), astrogliosis and microgliosis (Figure 3b), formation and deposition of amyloid plaques accompanied by neuronal loss, (Figure 3c). Spongiformation is the most consistent histopathological characteristic found in CNS of patients with prion diseases, hence term "spongiform encephalopathy" is attributed to describe this group of diseases. Spongiformation is characterised by a fine vacuole-like morphology of varying sizes approximately 2-200μm in diameter (Figure 3.5). These vacuoles may be present in any layer of the cerebral cortex, transforming gradually into large irregular cavities within the neuropil. Spongiformation mainly occurs within neuronal processes (mainly neurites) and cell bodies

accompanied by additional frequent expression in the basal ganglia and thalamus. Presence, severity and distribution of spongiformation is more variable in cerebellar region of the brain.

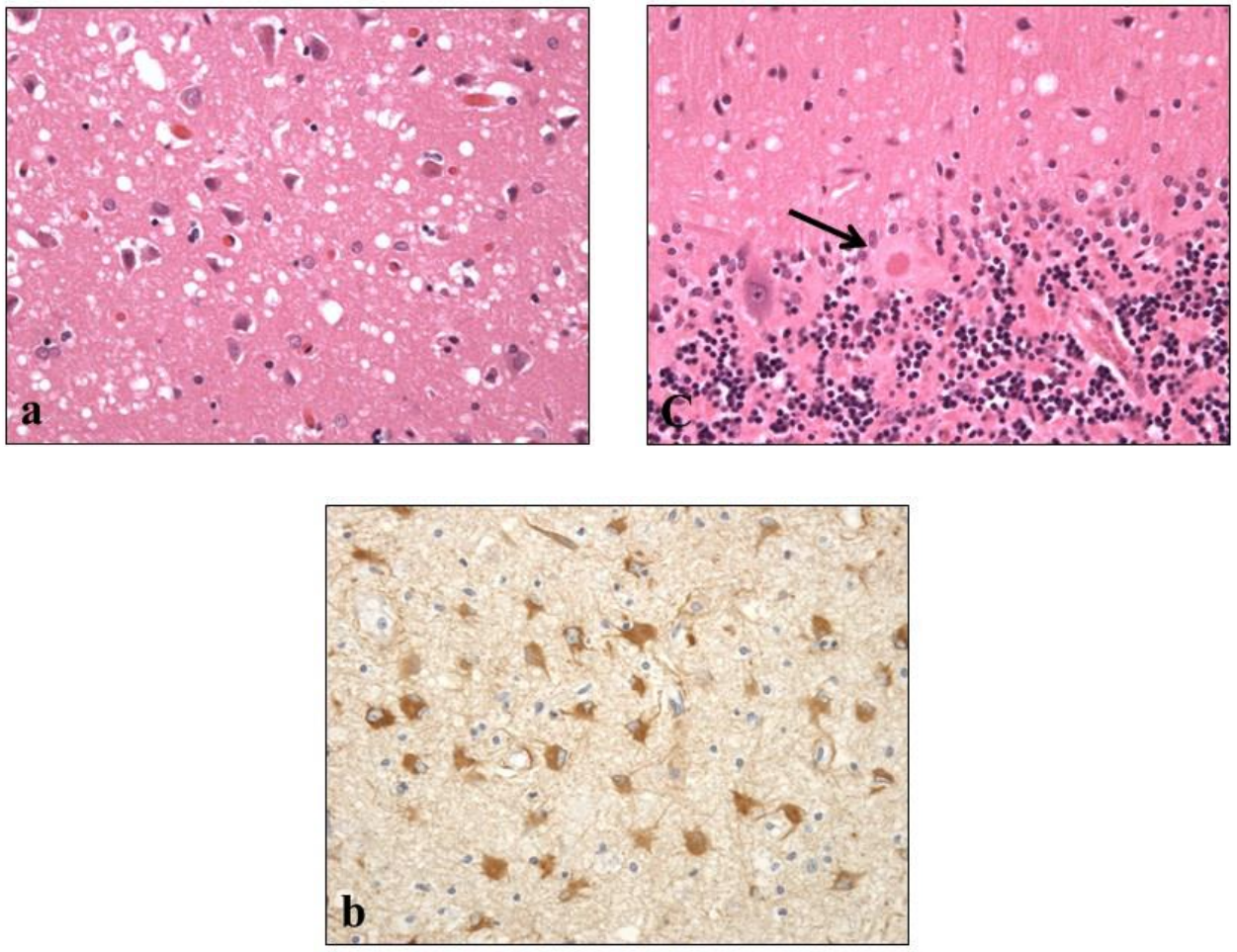

Figure 3-5: Pathological changes in human prion disease
Micro-vacuolar degeneration in the frontal cortex in sporadic CJD (haematoxylin and eosin stain) **(a)**. Astrocytes immunolabelled for glial fibrillary acidic protein in the thalamus of a variant CJD case **(b)**. A kuru plaque (arrow) within the granular layer of the cerebellum in sporadic CJD **(c)**. (Source: http://www.cjd.ed.ac.uk/documents/neuropath.pdf)

3.2.5 Spread of prion in the body

3.2.5.1 Transmission

Other than sporadic and familial prion diseases, prions can be efficiently transmitted experimentally through infected brain tissue, blood or blood derivatives, skin (Carp, 1982;Glaysher and Mabbott, 2007;Mohan et al., 2004) and aerosols (Denkers et al., 2013;Haybaeck et al., 2011;Nichols et al., 2013). After entry, prions can invade peripheral

immune cells, reside in immune cells and impair their functions and replicate in peripheral lymph nodes before gaining access to the CNS. M cells are unique epithelium cells which help the TSE agent to reach the Follicular dendritic cells (FDCs) in Gut associated lymphoid tissues (GALT) by transcytosis through intestinal epithelium which usually limits the entry of pathogens (Heppner et al., 2001). Prions can tolerate digestive enzymes and are very less vulnerable to gastric acidity in case of oral prion challenge (Kimberlin and Walker, 1989). In aerosol transmission, M cells and epithelial cells of the nasal mucosa play a role in the transport of prion (Kincaid et al., 2012). Relevance of transmission by blood, skin and oral routes to naturally occurring TSEs remains to be established.

3.2.5.2 Peripheral Replication

In many TSEs, prions accumulate and replicate within secondary lymphoid organs (SLOs: spleen, lymph nodes, tonsils, appendix and Peyer's patches) before neuroinvasion occurs. Dendritic cells (DCs) reside in vicinity of peripheral lymphoid tissues including GALT and are destined for antigen presentation to and priming of B cells and T cells (Huang et al., 2002a). PrP^{C} is expressed at moderate levels in circulating lymphocytes, including in B cells. However, PrP^{C} expression in B cells is not required for prion neuroinvasion (Klein et al., 1998), and PrP^{C} expression solely in B cells is not sufficient for prion replication (Montrasio et al., 2001). FDCs express high levels of PrP^{C} and are considered to be the site of PrP^{SC} accumulation and replication in the lymphoid tissues of prion-infected mice (Kitamoto et al., 1991). Complement receptors CD21 and/or CD35 of FDCs help trap and retain opsonized antigens within SLOs. Ablation of CD21 and/ or CD35 complement receptors increases resistance to intraperitoneal prion inoculation (Zabel et al., 2007) showing importance of opsonizing complement components in prion pathogenesis.

3.2.5.3 Neuroinvasion of Prions

The innervation pattern of SLOs is primarily sympathetic, and experimental models show that prion agents spread from SLOs to the CNS through the autonomic nervous system (Clarke and Kimberlin, 1984;Cole and Kimberlin, 1985;Heggebo et al., 2003;McBride and Beekes, 1999) Chemical or immunological sympathectomy prevented or significantly delayed peripheral prion pathogenesis (Glatzel et al., 2001). Different scenarios have been envisaged, including direct cell to cell contact, vesicle associated infectivity for example, prion transmission through exosomes

(Fevrier et al., 2004), tunnelling nanotubes (Gousset et al., 2009) and free-floating infectious particles (Silveira et al., 2005).

3.2.6 Classification of prion strains in human prion diseases

There are different forms of prion diseases in human, each with distinct clinical manifestations associated with characteristic neuropathological events (Bruce, 2003). So prion diseases encompass a wide spectrum of histopathological phenotypes (Gambetti et al., 2003). Sporadic Creutzfeldt-Jakob disease (sCJD) is the most prevalent (85%) prion disease in humans (Peden and Ironside, 2004). On contrary to familial form of CJD (which invariably results from mutations in the *PRNP* gene) and acquired forms of CJD, (including iatrogenic CJD and variant CJD) the etiology of sCJD is unknown. The transmissibility of prion diseases depends upon the misfolding of the cellular prion protein (PrP^{C}) and its conversion into its pathogenic form; scrapie form of prion protein (PrP^{SC}) (Klemm et al., 2012). Heterogeneity of disease pathology correlates to different forms of PrP^{SC} (can also be called as prion strains), which can be differentiated on the basis of their characteristic physiochemical properties which are helpful in the molecular identification of various prion strains (Bessen and Marsh, 1994;Telling et al., 1996).

3.2.6.1 Codon 129 genotype of PrP

Codon 129 of the prion protein gene (*PRNP*) is the site of a common methionine (M)/valine (V) polymorphism. *PRNP* gene can be either homozygous at codon 129 for M/M or V/V or can also be heterozygous for M/V. It is observed that the pathological phenotype of the prion diseases, whether sporadic, familial or acquired by infection, often is different depending on the genotype at codon 129 of *PRNP* gene of the affected individual (Gambetti et al., 2003). There is marked codon 129 based genetic susceptibility in sporadic CJD showing more prevalence in homozygotes at codon 129 of *PRNP*, where either methionine or valine may be encoded. Heterozygotes appear significantly protected against developing sporadic CJD (Collinge et al., 1991;Palmer et al., 1991;Windl et al., 1996). Therefore, genotype at codon 129 of *PRNP* gene appears to be a modifier of the disease pathology in human prion diseases (Gambetti et al., 2003).

3.2.6.2 Type of PrP^{SC}

Human prion diseases are characterized by two types of scrapie prion protein (PrP^{SC}) that are easily recognized by their electrophoretic mobility on western blot based on the molecular weight of the PrP^{SC} after digestion by the proteolytic enzyme proteinase K (PK). In PrP^{SC} type 1 the PK-resistant PrP^{SC} has electrophoretic mobility on gel to 21 kDa with its N-terminus starting at residue 82. In PrP^{SC} type 2, the corresponding PK-resistant PrP^{SC} migrates on gel to approximately 19 kDa with its N-terminus starting at residue 97 (Parchi et al., 2000). It is reported that the disease phenotypes of the patients with prion diseases associated with PrP^{SC} type 1 often are distinct from the phenotypes associated with PrP^{SC} type 2. This suggests that, the PrP^{SC} type is another modifier in human prion diseases. However, the disease-modifying role of the genotype at codon 129 and of the PrP^{SC} type is not totally independent. Approximately 95% of the patients with sCJD having MM genotype at codon 129 have PrP^{SC} type 1 whereas 86% of the sCJD patients having VV or MV genotype at codon 129 have PrP^{SC} type 2 (Parchi et al., 1996;Parchi et al., 1999). Therefore, the MM homozygosity favors the formation of PrP^{SC} type 1 and the presence of one or two V at codon 129 favours the formation of PrP^{SC} type 2.

So both modifiers; genotype of PrP at codon 129 and type of PrP^{SC}: type 1 or 2 determine the fate of the disease. So sporadic CJD can be classified into six groups based on the presence of one of the three (MM, MV, VV) genotypes at codon 129 and either type 1 or type 2 PrP^{SC}. Sometimes type 1 PrP^{SC} and type 2 PrP^{SC} can co-exist as well either in together in the same region of brain or separately in different regions hence leading further to the complexity of diseases. The presence of the both types of PrP^{SC} together is not independent but associated with codon 129 genotype. More than 95% of the patients of this type of prion disease are homozygous for methionine at codon 129, whereas heterozygous codon 129 MV patients are rare.

3.2.7 Pathophysiological events in sCJD

Main etiological events triggering the spontaneous onset of sCJD are still unknown. But there are multiple pathological events which lead to the progression of the disease. Two well studied of them include neuroinflammation and oxidative stress.

3.2.7.1 Neuroinflammation in sCJD

Neuroinflammation is one of the key pathological features of sCJD. sCJD is characterized by subtype dependent clinico-pathological manifestations with each subtype depicting a characteristic clinical and neuropathological features (Parchi et al., 2012). Prime neuropathological lesions include sponges formation, neuronal loss, astrogliosis, microgliosis, and PrP^{SC} aggregation (Liberski and Ironside, 2004). Increased expression of pro- and anti-inflammatory cytokines in CNS and mediators of immune response in the CSF of CJD patients evident inflammation in CNS during CJD (Sharief et al., 1999;Stoeck et al., 2006).

The accumulation of PrP^{SC} containing neurotoxic peptide region 106- 126 in the central nervous system is considered to be responsible for neuronal degeneration (Forloni et al., 1993) preceded by activation of glial cells and neuronal loss (Budka, 2003;Jendroska et al., 1991). Neuronal loss in CJD is mainly caused by apoptosis (Giese et al., 1995;Gray et al., 1999a;Gray et al., 1999b). It has been proposed that apoptotic cell death is related to the influence of cytokines, which are produced by activated astrocytes and microglia (Sawada et al., 1999). A significant increase in the CD68 positive microglia in the deeper layers and GFAP positive astrocytes in superficial layers of cortex is observed in sCJD patients. Correlation between the severity of neuropathological lesions and the number of activated astrocytes or microglia indicate that the PrP^{SC} deposition in CJD may be involved in triggering the inflammatory response (Van et al., 2002).

3.2.7.1.1 Cytokines induced during prion infection

Pro-inflammatory cytokines like IL-1α, IL-1β, TNF, IL-6 and IL-17 have higher expression in patients with TSEs (Sharief et al., 1999;Van et al., 2002). IL-1β is supposed to be produced by activated microglia. Furthermore, anti-inflammatory cytokines like transforming growth factor-β (TGFβ) in mice infected with prions (Baker et al., 1999a), IL-4 and IL-10 in the cerebrospinal fluid of CJD patients are also increased in their levels (Stoeck et al., 2005).

3.2.7.1.2 Chemokines induced by prion infection

Levels of CC-chemokine ligand 2 (CCL2; also known as MCP1) are also increased in ME7-infected C57BL/6 mice but its ablation had no effect on survival time, microglial cell activation or neuronal damage following prion infection (Felton et al., 2005). Similarly, levels of

CCL5 (also known as RANTES) and its receptors CCR1, CCR3 and CCR5 are also increased in mouse prion models (Baker et al., 1999b). CXCL9 and CXCL10, which signal through CXC-chemokine receptor 3 (CXCR3) (Riemer et al., 2000;Schultz et al., 2004) and CXCL13 (also known as BLC) (Baker et al., 2002;Riemer et al., 2000) are also increased in prion diseases. Reduced production of pro-inflammatory cytokines and prolonged incubation time in prion diseases are attributed to the absence of CXCR3.

3.2.7.2 Oxidative stress in sCJD

Oxidative stress is one of the key features in the pathophysiology of prion diseases (Yun et al., 2006). The PrP^{SC} amyloid plaques found in brain tissues of patients with prion diseases are surrounded by reactive microglia (Block and Hong, 2005;Kim and de, 2005) which result in local inflammatory response and production of reactive oxygen (ROS) and nitrogen species (RNS) along with the release of various proinflammatory cytokines, chemokines, complement proteins and acute phase proteins, that can be harmful for the neurons in the vicinity. This suggests that microglia mediated neuroinflammation, can be either a cause or a consequence of chronic oxidative stress and mitochondrial damage (Agostinho et al., 2008) as illustrated in figure 3.6.

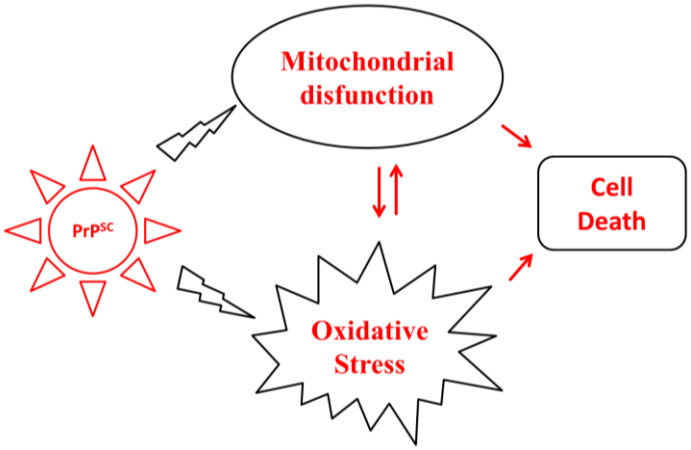

Figure 3-6: PrP^{SC} aggregates and amyloids can directly induce mitochondrial disfunction and microglial mediated oxidative stress
Mitochondria can be a source and a target of ROS. The excessive production of ROS by mitochondria and/or by reactive glial cells triggers mitochondrial dysfunction and oxidative stress leading to cell death. Mitochondria dysfunction and the oxidative stress associated with an active immune response are prominent events in prion pathologies. Modified: (Agostinho P. and Oliveira C.R.)

3.2.7.2.1 Reactive oxygen and nitrogen species

A correlation exists between amyloid deposition, glial activation, and oxidative stress in the brains of CJD patients (van et al., 2004). Chronic activation of microglia leads to the release of nitric oxide (NO), ROS, and thus mitochondrial dysfunction (Colton et al., 2001;Mhatre et al., 2004). Inducible nitric oxide synthase (iNOS), which is absent in the healthy brain cells, but is expressed by proinflammatory cytokines induced by activated microglia and astrocytes (Brown and Bal-Price, 2003) is responsible for inducing the production of RNS. The stimulated expression of iNOS can cause prolonged production of NO in higher amounts. Nitric oxide (NO) can act as a cytotoxic molecule, killing both pathogenic as well as healthy host neurons.

Activated microglia and astrocytes can produce nascent $O2^-$ by NADPH oxidase catalyzed reaction (Abramov et al., 2005;Mhatre et al., 2004) by utilizing electrons from NADPH to reduce O_2 to O_2^-. This nascent O_2^- can readily form hydrogen peroxide (H_2O_2) by a reaction catalyzed by superoxide dismutase (SOD) followed by generation of highly toxic hydroxyl radicals (HO^-) in the presence of redox-active iron. As a consequence, antioxidative capacity of cells is overwhelmed by ROS leading to oxidative stress (Dringen et al., 2005).

Under the effect of oxidation and/or nitration of proteins, ROS and RNS can stimulate the formation of mitochondria permeability transition pore (MPTP). MPTP opening is a normal cellular process and does not damage the cell, but prolonged opening of MPTP can lead not only to apoptosis or necrosis of the cell but also the release of cytochrome C and other apoptogenic proteins including apoptosis inducing factor (AIF) and SMAC/Diablo which can potentiate apoptosis by activation of Bid/Bax/Bad pathway (Eckert et al., 2003;Moreira et al., 2005;Pereira et al., 2004).

Conversion of PrP^C into PrP^{SC} leading to PrP^C deficiency in the brain cells is another aspect leading to oxidative stress in prion diseases. Since PrP^C also possesses a SOD-like function, so it also results in a reduced antioxidant capacity of brain cells leading to oxidative stress (Brown et al., 1997;Klamt et al., 2001).

Pathological events occurring during the pathophysiology of sCJD are still not completely explored. Identification and characterization of full spectrum of sCJD variants is important for epidemiological surveillance of the disease. Proteome wide studies are required for mapping the

whole proteome to uncover the underlying etiological factors in prion diseases. Use of high throughput proteomic approaches can be helpful in identification of regulated proteins, protein abundance, and variations in the expression of proteins, their post translational modifications and interaction of proteins with other proteins and networks which can be helpful in understanding the underlying cellular processes during the pathophysiology of the disease. Use of differential proteomics is also tempting in identifying early disease biomarkers, differential diagnosis and prompt therapeutics of various diseases (Zhang et al., 2008). This study provides the first comprehensive analysis of differential proteomic regulations of the two most prevalent subtypes of sCJD (MM1 and VV2) and underlying molecular mechanisms which are regulated during the course of the diseases which may have implication in the disease pathophysiology. This study can be helpful in identifying the potential disease modifying agents, therapeutic partners and diagnostic biomarkers.

3.3 Objectives of the study

Role of cerebellum part of brain in regulating important physiological functions like voluntary movements of the body, memory and vision implicate its relation to clinical symptoms shown in sCJD which include dementia, cognitive impairment, myoclonus, pyramidal/extrapyramidal signs and visual disturbances. This makes cerebellum an important part of the brain to look for the whole proteomic alterations occurring during the pathophysiology of sCJD which are not explored till to date. So this study was planned to explore the whole proteomic regulations in the two most prevalent subtypes of sCJD (MM1 and VV2) in the cerebellum region of brain which controls many of the important body functions and these functions are impaired during the course of disease in sCJD.

Main objectives of this study were:

1- Identification and characterization of proteomic alterations in cerebellum of brain from MM1 and VV2 subtypes of sporadic Creutzfeldt-Jakob disease (sCJD) by using 2-Dimensional gel electrophoresis and Mass-spectrometry
2- To explore the identified regulated cellular mechanisms/ functions and their key molecular players
3- To validate the identified regulated proteomic regulations at transcriptional and translational level
4- To explore the role of identified key players during the pathophysiology of disease for their diagnostic or therapeutic potential.

4 Materials and Methods

4.1 Materials

4.1.1 Chemicals

Chemicals used in this study were bought from Roche (Basel, Switzerland), Biochrome (Cambridge, UK), Sigma-Aldrich (Deisenhofen, Germany), Merck (Haar, Germany), Roth (Karlsruhe, Germany) and Bio-Rad (München, Germany).

4.1.2 Antibodies

Primary and secondary **a**ntibodies which were used either for western blot (WB) or immunofluorescence (IF) are listed below in Table 4.1 and Table 4.2 respectively.

Table 4-1: List of Primary antibodies with their application in current study

Primary Antibody	Origin	Company	Cat. No.	Dilution (WB)	Dilution (IF)
SAF70	Mouse	SP Bio	A03206	1:1000	NA
GFAP	Mouse	Dako	M 0761	1:2000	NA
SOD1	Mouse	Novocastra	NCL-SOD1	1:1000	NA
LDH	Goat	Abcam	Ab2101	1:500	NA
DJ-1	Goat	Santa Cruz	sc-27006	1:500	1:200
HSP27	Rabbit	Novus	AF1580	1:1000	NA
SUCLA2	Rabbit	GeneTex	GTX109728	1:2500	NA
PRDX6	Rabbit	Abcam	ab59543	1:2000	NA
TALDO1	Rabbit	GeneTex	GTX102076	1:2000	NA
TDP43	Mouse	Abcam	Ab57105	1:1000	NA
CKB	Rabbit	GeneTex	GTX101760	1:1000	NA
SEPT6	Rabbit	Santa Cruz	sc-20180	1:1000	NA
PKM2	Mouse	Abcam	ab55602	1:500	NA
Nrf2	Rabbit	Abcam	ab62352	1:500	NA
Phosp-Nrf2	Rabbit	Abcam	ab76026	1:500	NA

Table 4-2: List of secondary antibodies with their application in current study

Secondary Antibody	Origin	Company	Cat. No.	Dilution (WB)	Dilution (IF)
Mouse-HRP	Goat	JacksonIR Lab	115-035-062	1:5000	NA
Rabbit-HRP	Goat	JacksonIR Lab	111-035-144	1:5000	NA
Goat-HRP	Donkey	JacksonIR Lab	705-035-003	1:5000	NA
Mouse-CY3	Goat	Sigma	C2181	NA	1:200
Rabbit 488	Goat	Invitrogen	A11008	NA	1:200

4.1.3 Proteins standards and sample loading buffer

Table 4-3: List of protein standard and sample loading buffer

Standard	Company	Cat. No.	Volume Used (WB)
Precision Plus Dual Color Protein Standard	Bio-Rad	161-0374	5µL
Roti-Load (4X)	Roth	K929.1	¼ of sample volume

4.1.4 Oligonucleotides

Information about the probes used in this study for RT-qPCRs is listed below in the Table 4.4.

Table 4-4: List of probes used for RT-qPCR for mRNA expressional analysis

Number	Gene name	Serial No.	Company	Cat. No.
1	SOD1	Hs00533490_m1	Life Technologies	4453320
2	LDHB	Hs00929956_m1	Life Technologies	4453320
3	HSPB1	Hs00356629_g1	Life Technologies	4453320
4	PARK7	Hs00994896_g1	Life Technologies	4448892
5	SUCLA2	Hs00605838_g1	Life Technologies	4448892
6	PRDX6	Hs00705355_s1	Life Technologies	4453320
7	SEPT6	Hs00248408_m1	Life Technologies	4448892
8	TALDO1	Hs00997203_m1	Life Technologies	4448892
9	TARDBP	Hs00606522_m1	Life Technologies	4453320
10	CKB	Hs00176484_m1	Life Technologies	4448892
11	PKM2	Hs00761782_s1	Life Technologies	4448892
12	Nrf2	Hs00975961_g1	Life Technologies	4448892

13	HMO1	Hs01110250_m1	Life Technologies	4453320
14	GSTM2	Hs00265266_g1	Life Technologies	4448892
15	PRDX3	Hs00428953_g1	Life Technologies	4453320

4.1.5 Kits and commercial buffers

Kits and commercial buffers used in this study are listed below in the Table 4.5.

Table 4-5: List of Kits and Commercial buffers used

Kit/ Buffer	Company	Cat. No.
mirVana miRNA isolation kit	Life Technologies	Ambion AM1560
RNase-free DNase- kit	Life Technologies	Ambion AM1907
High Capacity cDNA Archive kit	Applied BioSystems	4368814
Taq Man Universal Master Mix	Applied BioSystems	4324018

4.1.6 Laboratory equipment and other material

Various instruments/ equipments used in this study are listed in the Table 4.6.

Table 4-6: List of the laboratory equipment and other material used

Equipment	Company
Homogenization Pestle and Tube	B. Braun
Centrifuge 5415 C	Eppendorf
SmartSpec Plus Spectrophotometer	Bio-Rad
Rehydration and IEF trays	Bio-Rad
Protean i12 IEF Cell	Bio-Rad
The PROTEAN II XL electrophoresis chamber	Bio-Rad
Water bath	GFL
Mini Protean Tetra System	Bio-Rad
Power Pac Basic	Bio-Rad
Trans-Blot Turbo Transfer System	Bio-Rad
CanoScan	Cannon
Shaker	Heidolph Duomax1030
Chemi Doc XRS+ (Molecular Imager)	Bio-Rad
IPG Strips	Bio Rad

C1000 Touch Thermal Cycler	Bio Rad
LighterCycler480 II	Roche

4.1.7 Softwares

Different bio-informatics softwares used in this study are listed below in the Table 4.7.

Table 4-7: List of Bio-informatic softwares used

Software/ Program	Application	References
DECODON Delta2D	Analysis of 2-DE gel	DECODON GmbH, Greifswald Germany
Lab Image 2.7.1	Densitomatric analysis	GraphPad Software, Inc. California, USA
Image J	Densitomatric analysis	National institutes of Health, USA
Graphpad Prism 5	Statistical analysis	La Jolla, San Diego, CA, USA
IPA	Pathway analysis of data	Redwood City, CA, USA
Scaffold 4	Analysis of proteomic data	Portland, Oregon US

4.1.8 Stock Solutions

Running buffer 10x (1L)

144 g Glycin

30 g Tris

10 g SDS

ddH_2O

Transfer buffer 10x (1L)

48 mM TRIS (58.2 g)

39 mM Glycin (29.3 g)

1 mM SDS (0.375 g)

ddH_2O

OKANO 10x (1L)

3 mM Tris pH=8

2 mM NaCl

0.05 % Triton X 100

0.1 mM EDTA

0.002 % SDS

0.1 % BSA

10 x TBST

50 mM TRIS (60.57 g)

150 mM NaCl (87.66 g)

0.05 % Tween 20 (5 ml)

pH 7.6

4.2 Methods

4.2.1 Sample Collection and processing

Cerebellum tissue samples from the brains of pathologically confirmed sCJD patients were received from the Brain bank of Institute of Neuropathology HUB-ICO-IDIBELL and Clinic Hospital-IDIBAPS Biobank according to the Spanish legislation on the collection and transport of biological samples and also after the approval from local ethics committee. The time lapse between the death of the patient and its postmortem was between 1 h and 45 min to 24 h and 30 min. Whole brains from CJD cases were cut into two parts. Half part of frontal pole and cerebellum hemisphere were fixed with 4% buffered formalin followed by treatment with formic acid. After the process of fixation and decontamination, these parts were stored at -80 °C until further used in immunohistochemical experiments. Other fresh half parts of the brain from frontal lobe and cerebellum were snap frozen and stored at –80 °C until further use. For controls brain samples, one hemisphere was cut immediately in 1 cm thick coronal sections, and selected areas of the encephalon were quickly dissected, frozen and stored at –80 °C until further use. The other hemisphere was fixed with 4% buffered formalin for 3 weeks for morphological studies. Four samples each from MM1 and VV2 subtypes along with their age matched non-demented controls were used for proteomic study. Mean age of the samples from age matched non-demented controls, MM1 and VV2 subtypes along with their standard deviations were 63 ± 12.19, 70 ± 8.83 and 72 ± 3.74 respectively. All the samples used for this study were female patients to exclude the possibility of gender based differences.

4.2.2 Preparation of tissue lysates and isolation of proteins from tissue lysates

Frozen cerebellum tissue samples weighing up to 30-40 mg were taken in 10% w/v of lysis buffer (7M Urea, 2M Thio-urea, 4 % CHAPS, 20 µl/ml Ampholytes, 10mg/ml DTT, protease and phosphatase inhibitors) and homogenized with the help of tissue homogenizer at 200 cycles/ minute at room temperature for 3 min. Tissue lysates were further incubated at 4°C for overnight. On next day, tissue lysates were centrifuged at the speed of 14000 rounds per minute (RPM) for 20 min. Supernatants having the soluble proteins were carefully collected leaving behind the pellets.

4.2.3 Determination of protein concentration

The concentrations of proteins in tissue lysates of cerebellum were determined by using Bradford assay (Bio-Rad). Working solution of Bradford was prepared by diluting Bradford with ddH_20 with a ratio of 1:5. Different concentrations of protein standard (BSA) ranging from 0.0-1.0 mg/ ml in ddH_20 were prepared. Protein samples with unknown concentrations were diluted 1:20. 20 µl of different concentrations of protein standard and diluted samples (20 µl) were mixed with 980 ml of working solution of Bradford and incubated for 10 min. at room temperature (RT). The optical density (OD) of the samples was measured at wavelength of 595 nm. Protein concentrations were further calculated with the help of OD values by using Microsoft Office 2007 Excel software.

4.2.4 Sample Characterization

4.2.4.1 Proteinase K Digestion

200µg of proteins from sporadic CJD brain (10% w/v) homogenates (both MM1 and VV2 subtypes along with age matched non-demented controls) were digested with 2.5µg/ml and 5µg/ml of proteinase K for 1 h at 37 °C and the reaction was stopped by heating the samples later at 65°C for 15 min for deactivating the enzymatic activity. Then samples were boiled at 95°C for 5 min after mixing them with 4X Roti-Load (sample loading buffer). Samples were cooled down and were used further for SDS-PAGE and Western immunoblotting.

4.2.5 Protein Electrophoresis (SDS-PAGE)

For separation of proteins by SDS-PAGE, 4% stacking and 12.5% resolving gels were used for stacking and separating the proteins respectively according to their molecular weight. Recipe used for preparation of the gels is as follows:

Components	Bottom Gel (Volume for 2 Gels)	Upper Gel (Volume for 2 Gels)
Buffer	3.7 ml	1.05 ml
40% Acrylamide	4.4 ml	0.84 ml
Destilled H_2O	6.8 ml	2.6 ml
APS 10%	150 µl	45 µl
TEMED	6 µl	5 µl

Buffers used in preparation of the upper gel and bottom gel are listed below:

Bottom gel buffer (450 ml)

2 parts 1.5 M Tris base (54.513 mg/300 ml)

1 part 1.5 M Tris HCl (35.468 mg/150 ml)

1.8 g SDS pH 8.8

Upper gel buffer (500 ml)

30 g Tris

0.2 g SDS

50 µg of proteins were mixed with an equal volume of 2X sample loading buffer and heated at 95ºC for 5 min. and loaded into the gel. Molecular weight of the desired proteins was determined by running the Protein dual color standard in parallel. SDS-PAGE was run at constant voltage of 100 at RT until tracking dye (bromophenol blue) reached to the bottom of separating gel. Recipe for SDS running buffer used for electrophoresis is as follows:

SDS-running buffer (Electrophoresis buffer)

192 mM glycine

0.1% SDS

25 mM Tris-base pH 8.3

4.2.6 Western blot

After the completion of protein electrophoresis, the separating gel was removed from between the glass plates and placed in a transfer buffer for 1 min. Polyvinylidene fluoride Membrane (PVDF) of the size of the gel was taken and equilibrated by placing in methanol for 1 min. Then PVDF membrane was placed in transfer buffer for 1 min. Two thick blot filter paper of the size of gel were also soaked in transfer buffer for 1 min. Recipe for the transfer buffer used is given below:

Transfer buffer 1x (1L)

100 ml 10x Transferbuffer

200 ml Methanol

700 ml water

The gel placed above the membrane was sandwiched between the two thick blot filter papers. This blotting setup was placed in the trans-blotter and run at constant voltage of 14 for 60 min. After the completion of transfer, the membrane was blocked with blocking buffer for 60 min. with gentle shaking. Blocking buffer was prepared using Not-fat dry milk powder in a wash solution. Recipes for wash solution and blocking buffer are as follows:

Wash solution (PBS-T)

PBS and 0.1% of Tween-20

Blocking Buffer

5% Non-Fat Dry Milk Powder in wash solution (PBS-T)

Then membrane was incubated with the primary antibody prepared in the same blocking buffer for overnight at 4ºC with gentle shaking. Next day, membrane was washed with wash buffer (2X for 5 min and 3X for 15 min. each) followed by incubation of the membrane with corresponding HRP conjugated secondary antibody (Table 2) for 1 h. Membrane was again washed with wash buffer (2X for 5 min and 3X for 15 min. each).

4.2.7 Imaging of Western blotted membrane

The immunoreactivity was detected by incubating the membrane with enhanced chemiluminescence (ECL) solution for 1 min. and scanning with Chemi-Doc (Bio-Rad) by exposing from 200 to 800 sec. Recipe for the ECL solution used is as follows:

Enhanced Chemiluminescence Solution (ECL)

Solution 1 (10 ml):

100 µl 250 mM Luminol (0.44 g/10 ml DMSO)

44 µl 90 mM p-Coumaric acid

1 ml 1 M Tris/HCl pH 8.5

8.85 ml H_2O

Solution 2 (10 ml):

6 µl 30% H_2O_2

1 ml 1 M Tris/HCL pH 8.5

9 ml H_2O

Mix both solutions 1:1

Densitometric analysis of the results was performed with Image Lab whereas statistical analysis was performed with Graph Pad Prism 5. Regulations in the results were considered significant when the *p*-value was lower than 0.05 in student's t test.

4.2.8 Stripping of membrane

Same membrane was stripped for reusing it further for examining the expression of more proteins. Protocol of use of different stripping buffers for this purpose and their recipes are as follows:

Strong Stripping Buffer*:* Membrane was incubated with stripping buffer for 15 min. on gentle shaking followed by 2X washing with dd H_20 each for 5 min. Then membrane was ready again for reuse from the step of blocking. Recipe for this stripping buffer is

0.2 M NaOH

(0.2 M / 5 M) * 250 ml = 10 ml of 5 M NaOH + 240 ml water

Mild Stripping Buffer: Membrane was incubated with stripping buffer for 5-10 min for two times and using fresh stripping buffer each time on gentle shaking followed by 2X washing with PBS (1x) each for 10 min. Then membrane was further washed two times with TBST (1X) each for 5 min. Then membrane was ready for reuse from the step of blocking. Recipe for this stripping buffer is:

15 g glycine

1 g SDS

10 ml Tween 20

Adjust pH to 2.2

Distilled water up to 1 L

4.2.9 Two Dimensional Electrophoresis (2-DE)

In two-dimensional electrophoresis proteins are separated in two dimensions: based on isoelectric focusing (IEF) in first dimension and SDS-PAGE in second dimension.

4.2.9.1 First dimensional electrophoresis

In first dimension proteins were separated horizontally on an IPG strip by isoelectric focusing (IEF); separation of proteins on the basis of their *pI* values. Seventeen centimeter pre-cast immobilized non-linear (IPG) strips with a pH range of 3-10 (ReadyStrip IPG: 3-10NL, Bio Rad) were used.

4.2.9.1.1 Rehydration

The protein sample was prepared by diluting 150 µg of proteins from the sample with rehydration buffer up to the total volume of 325 µl for 17cm IPG strips. Recipe for rehydration buffer is as follows:

Rehydration buffer

7 M urea

2M thio-urea

4% CHAPS

15 mM DTT and 0.2% ampholytes

IPG strips were rehydrated with already prepared 325 µl of sample by loading the sample carefully into the track of the IEF cassette (Bio-Rad) and placing the IPG strip (with gel side down) over the sample without air bubbles (after removing its protective film). After 1 h of incubation at RT, mineral oil (Bio-Rad) was loaded above the IPG strips to prevent the evaporation of the sample during next 12 h of incubation for active rehydration at 50 Volts. After completion of active rehydration, following set of different voltages were used for IEF:

1- 500V for 1 hour (Slow)
2- 1000V for 1 hour (Gradual)
3- 8000V for 60000 Vh (Rapid)

4.2.9.2 Equilibration

After the completion of IEF, already separated proteins on IPG strips were equilibrated in equilibration buffer with DTT to reduce and IAA to alkylate the cysteines respectively. This helps to prevent vertical streaking after staining of second dimension gels. Equilibration was achieved by incubating the IPG strips with equilibration buffer 1 followed by incubation with equilibration buffer 2 each for 20 min on a slow shaking. Recipes for equilibration buffer 1 and 2 are as follows:

Equilibration buffer I

6 M urea
2% SDS
30% glycerin
0.375 M Tris pH 8.8, 2% (w/v) Dithiothreitol (DTT)

Equlibration buffer II

6 M urea
2% SDS
30% glycerin
0.375 M Tris pH 8.8, 2.5% (w/v) Iodoacetamide (IAA), Bromophenol blue (BPB) in traces

4.2.9.3 Second dimension electrophoresis by SDS-PAGE

During the second dimension, already equilibrated strips were placed on top of vertical 12% SDS polyacrylamide gels. A protein marker was also loaded into the gel for the identification of molecular weights of proteins. SDS-PAGE for second dimension was run at a constant voltage of 100 at RT until tracking dye (bromophenol blue) reached to the bottom of gel. After completion of second dimension gels were removed and stained further with silver stain for visualization of whole proteome.

4.2.9.4 Visualization for whole proteome and imaging of the gels

Gels were stained with silver stain for the visualization of the protein spots on the gels. Different steps in the protocol of silver staining include:

I. **Fixation:** Fixative (50% Methanol + 12% Acetic Acid + ddH_2O) was used to fix the proteins in the gel by using for 1hr on shaker.

II. **Washing:** Gel was washed with 50% and 30% Ethanol respectively each for 20 min on shaker.

III. **Sensitization:** Sensitization of gel was done with freshly prepared solution of 0.02% (0.8mM $Na_2S_2O_3$) by incubating the gel for 60 seconds.

IV. **Washing:** Gel was washed with ddH_2O three times each for 20 sec. to remove loosely bound sensitization solution for having better background.

V. **Silver staining:** Gel was silver stained with freshly prepared solution of (0.2% $AgNO_3$+0.026% Formaldehyde) and incubating the gel for 20 min.

VI. **Washing:** Gel was washed with ddH_2O three times each for 20 sec. to remove loosely bound silver staining solution for having better background.

VII. **Developing:** Protein spots on the gel were developed by using the freshly prepared solution of (6% Na_2CO_3+0.0185% Formaldehyde+16µM $Na_2S_2O_3$) for 3-6 min until the bands appeared on the gel.

VIII. **Stopping:** Developing of the gel was stopped by using the solution of fixative (50% Methanol+12% Acetic Acid+ ddH_2O) for 10 min and then incubating the gel in ddH_2O for 10 min.

IX. **Scanning:** Gel was scanned by using the CanoScan Scanner and saving the images in Tiff format.

X. **Storage:** Gel was stored for longer time as a record by drying the gel using the dryer or for shorter time by using the solution of 5% Acetic Acid for overnight.

Gels obtained after staining with silver stain are shown in figure 4.1.

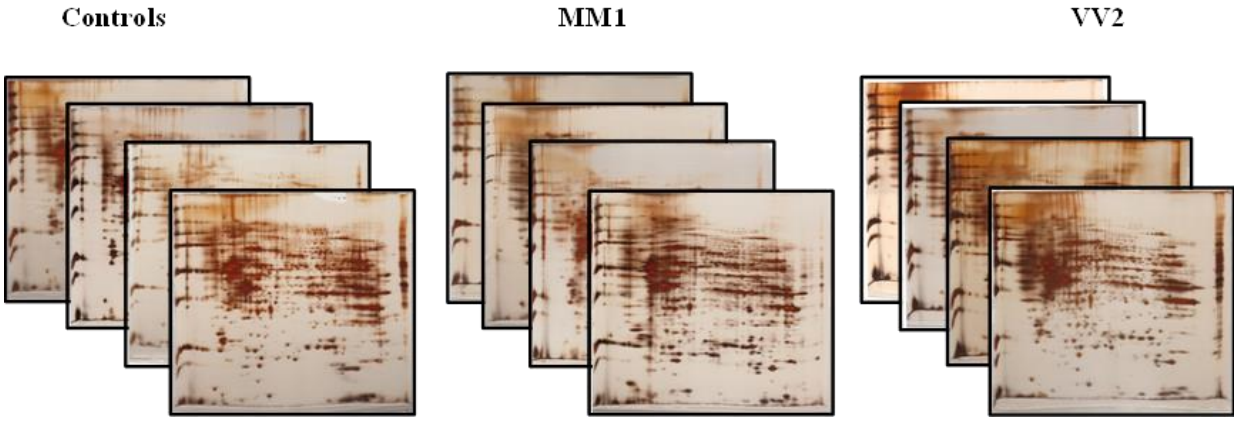

Figure 4-1: Gels stained with silver stain
Four *2DE* gels corresponding to four samples in each biological group were prepared and stained with silver stain for visualization of whole proteome on the gels from each sample.

4.2.9.5 Analysis of protein spots with DECODON Delta2D software

All 12 gel images from three biological groups (Control, MM1 and VV2) were further processed in DECODON Delta2D software for the analysis of protein/ spot abundances of all protein spots on 2DE gels. The differences in spot abundance of each spot on the gels between different groups were detected by Delta2D in terms of the intensity of each spot. Densitometry analysis of all protein spots was done by using unpaired Student's t-test for statistical significance. Means and standard deviations were calculated from four sets of experiments. Differential regulation of protein spots between different groups was also calculated by using a 1.5 cut off value of fold change. A protein spot was considered as differentially regulated when its densitometric analysis

showed at least 1.5 fold change in abundance and when the *p*-value was <0.05 in unpaired Student's t-test.

4.2.10 Identification of protein/ peptide sequences by LC/MS-MS

4.2.10.1 In-gel digestion, preparation of proteins and proteolytic fragments

4.2.10.1.1 Excision and destaining of protein spots

Regulated protein spots were excised from silver stained 2DE gel into small slices with the help of a scalpel and transferred to microcentrifuge tubes. Destaining of the protein spots is important as silver stain interferes during mass spectrometry. Silver stained protein spots were destained by oxidation of metallic silver bound to the proteins by using 15 mM potassium ferricyanide/50 mM sodium thiosulfate (Aldrich/Sigma-Aldrich, Steinheim, Germany). Sodium thiosulfate is used to make complex with the released silver ions. Complete destaining was achieved by using 50 mM ammonium bicarbonate/50% acetonitrile (ACN) (Sigma-Aldrich). After completion of destaining, samples were dried with the help of SpeedVac SVC100 (Savant Instruments, Farmingdale, NY) for 15 min.

4.2.10.1.2 Reduction of disulfide bonds and alkylation of free cysteines

After destaining of the proteins, the disulfide bonds between the amino acids of proteins should be broken irreversibly along with unfolding of tertiary structures of proteins. This was achieved by treating the dried protein spots with 10 mM dithiothreitol /100 mM ammonium bicarbonate for 45 min. at 56°C followed by incubation with 55 mM iodoacetamide/ 100 mM ammonium bicarbonate for 30 min. at room temperature in the dark. Then protein spots were washed with 100 mM ammonium bicarbonate followed by incubation with 1:1 solution of 100 mM ammonium bicarbonate with ACN for 15 min.

4.2.10.1.3 Enzymatic digestion

For cutting the proteins into the shorter fragments (peptides), dried samples were enzymatically digested with 10−20 µL of trypsin digestion (0.1 µg/µl) solution (Promega, Madison, WI) on ice for 45 min. followed by an overnight incubation at 37°C in digestion solution without trypsin.

4.2.10.1.4 Extraction of peptides

For extraction of digested fragments from gel matrix samples were treated with 0.1% trifluoracetic acid (TFA) for 30 min. in a sonicating water bath Transsonic 310/H (Elma, Pforzheim, Germany) followed by extraction with 30% ACN in 0.1% TFA and 60% ACN in 0.1% TFA. The eluate was collected in Eppendorf tubes and dried with the SpeedVac. The extracted peptides were dissolved in 0.1% formic acid (FA) for MALDI-TOF-MS/MS.

4.2.10.2 Identification of protein/peptide sequence analysis

Peptides digested with trypsin were separated with the help of liquid chromatography and analyzed on MALDI-TOF mass spectrometer. Data acquisition was performed using Raw2MSM v1.17 software (Max Planck Institute for Biochemistry, Martinsried, Germany). All processed data were analyzed using Mascot (Matrix Science, London, UK; version 2.4.1) set up to search the UniProt/SwissProt database (release 02/14 filtered for *Homo sapiens*, 16665 entries) using a peptide mass tolerance of 5 ppm for precursors and 0.02 Da for fragments, respectively. The search criteria were set to a maximum of two missed cleavages allowed by trypsin and protein modifications set to methionine oxidation and carbamidomethylcysteine when appropriate.

4.2.10.3 Criteria for validation of mass spectrometry data

Raw files in the scaffold software format were further screened to remove false positively identified results based on following criteria:

1. **Score/peptide count** – peptide count is the number which represents the number of times peptide form the protein sequence has been detected by the mass spectrometer. Minimum of two confident peptide counts were considered for the further functional analysis.

2. **Molecular mass** – As each protein has its unique molecular mass, therefore identified protein was confirmed, if it was from the excised spot by comparing the theoretical molecular mass of protein with experimental molecular mass on the gel map with help of marker sequence.

3. **Isoelectric pH (*pI*)** – As each protein has its unique isoelectric pH, so theoretical *pI* was compared with experimental pI on the gel map.

4.2.11 mRNA expression of identified proteins for validation

Fifteen controls as well as MM1 samples along with ten VV2 samples were used for studying the mRNA expression of proteins for validation. Samples each for MM1 and VV2 subtype from cerebellum part of brain tissue from pathologically confirmed sCJD cases and their age matched controls were used for mRNA extraction and further RT-qPCRs. Mean age of the samples from age matched non-demented controls, MM1 and VV2 subtypes along with their standard deviations were 62.13 ± 12.06, 65.93 ± 14.55 and 63 ± 12.09 respectively.

4.2.11.1 RNA isolation and purification

Extraction of RNA from cerebellum of CJD and age-matched controls was performed by using mirVana miRNA isolation kit (Ambion AM1560) according to the instructions in the manual provided by the manufacturer. Brief description of the protocol is as given below:

1- The sample was first disrupted in 10% w/v of denaturating lysis buffer (Ambion Lysis Binding buffer for frozen tissue) provided along with the kit which also stabilized RNA and inactivated RNases.
2- The lysate was then extracted with an equal volume of Acid-Phenol: Chloroform for removing most of the other cellular components including most of the DNA leaving a semi-pure RNA sample. Tubes were vortexed for 30–60 sec to mix followed by centrifugation for 5 min at maximum speed (10000x g) at room temperature to separate the aqueous and organic phases.
3- Organic phase was further purified by adding 1.25 volumes of 100% Ethanol to samples, which were passed through a filter column containing a glass fiber filter which immobilizes the RNA. The filter was then washed for three times, and finally the RNA is eluted with low ionic pre-heated (95 °C) nuclease-free water.

After extraction of total RNA, samples were treated with RNase-free DNase- kit (Ambion AM1907) to remove contaminating DNA for preventing subsequent amplification later on. This was performed according to the instructions in the manual provided by the manufacturer. Brief description of the protocol is as given below:

1- 0.1 volume of 10× TURBO DNase Buffer and 1 µL TURBO DNase to the RNA, and was mixed gently followed by incubation at 37°C for 20–30 min.
2- 0.1 volume of resuspended DNase inactivation Reagent was added and mixed well followed by incubation for 5 min at room temperature along with occasional mixing.
3- Columns were centrifuged at 10000× g for 1.5 min and RNA was transferred to fresh RNase free tube.

After purification of RNA, the concentration of RNA in every sample was measured at 260/280 by using Nanodrop 2000 spectrophotometer (ThermoScientific, USA). Quality of the extracted RNA was evaluated in terms of RNA integrity number (RIN) with Agilent 2100 BioAnalyzer (Agilent, US). Only samples with RIN value equal or more than 6 were selected for further use.

4.2.11.2 Retro-transcription reaction

The retro-transcription reaction of the extracted purified RNA from cerebellum tissue samples was done by using the C1000 Touch Thermal Cycler (Bio Rad) with the High Capacity cDNA Archive kit (Applied Biosystems) according to the instructions in the manual provided by the manufacturer. A parallel reaction for a RNA sample was run without reverse transcriptase to assess the contamination with genomic DNA. Brief description of the protocol is as given below.

Recipe for Reverse transcription

Reagents (1 µg mRNA)	**Volume**
10x RT Buffer	2µl
25 x dNTPs	0.8 µl
10x Random Primer	2 µl
Reverse Transcriptase	1 µl
mQ H_20	4.2 µl
Total Master Mix	**= 10 µl**
RNA	10 µl
Total volume	**= 20 µl**

Program:

Step 1: 25 °C for 10 min

Step 2: 37 °C for 2 hrs

Step 3: 85 °C for 5 min

Step 4: 4 °C for storage

(Temperature of lid should remain at 37 °C)

4.2.11.3 RT-qPCR

cDNA samples obtained from the retro-transcription reaction were diluted 1:15 with RNase free water. Duplicate reactions of each cDNA sample was used for performing PCR reaction in 384-well optical plates (Roche) utilizing Light cycler 480 II (Roche). Parallel amplification reactions for each sample were performed using 20× TaqMan Gene Expression Assays (Applied Biosystems) and 2× TaqMan Universal PCR Master Mix (Applied Biosystems). β-glucuronidase (GUSβ) was used as housekeeping gene for internal control for normalization. The steps of PCR reaction are as follows:

Recipe for RT-qPCR:

Reagents	**Volume**
Probe	0.5 µl
Master Mix	5 µl
cDNA	4.5 µl
Total volume	**= 10 µl**

Program:

Step 1: 50 °C for 2 min

Step 2: Denaturation at 95 °C for 10 min

40 cycles for anealing

Step 3: 95 °C for 15 second

Step 4: 60 °C for 1 min.

TaqMan PCR data were retrieved using the Sequence Detector Software (SDS version 2.1, Roche). Subsequently, CT data for each sample were analyzed with the double delta CT (ΔΔCT)

method. Delta CT (ΔCT) values represent the normalized levels of each target gene in correlation with housekeeping gene (GUSβ), whereas ΔΔCT values were calculated as the ΔCT of each sample minus the mean ΔCT of the population of control samples (calibrator samples). The fold change was determined using the equation 2ΔΔCT.

4.2.12 Mice models of sCJD (sCJD MM1 and VV2 transgenic mice models)

Double transgenic (129Met-Tg340) or (129Val-Tg361) mice were used to develop humanized CJD as previously described by (Padilla et al., 2011;Zafar et al., 2015;Zafar et al., 2016). Briefly, Tg340 mice used for this purpose were PrP knock out and were expressing 4 fold higher expression of human PrP^C having methionine at codon 129 (Met129) of PrP for developing MM1 mice model of sCJD. 10% (w/v) of tissue homogenate from sCJD MM1 brain tissue was used as inoculum for inducing CJD in mice. Mice with 6-10 weeks of age were anaesthetized and 2 mg of inoculum was injected in the right parietal lobe with the help of a 25-gauge disposable hypodermic needle (6 mice for each group and time point were used). Mice were observed daily and neurological assessment was done weekly for the development of any clinical signs. Collection of samples (Brains) of the inoculated mice along with their age matched healthy controls was done post inoculation at day 60 and 120 for pre-clinical stage, at day 160 for clinical stage and at day 183 for late clinical. Sacrifice of mice was done by euthanizing the animal followed by necropsy of whole animal. Half part of the brain sample was fixed in 10% buffered formalin for quantification of spongiform degeneration and performing immune-histological experiments. The other half of the brain sample was frozen at −80°C for other biochemical or molecular biological experiments. Similar methodology was adopted for developing VV2 mice model of sCJD by using PrP KO Tg361 mice expressing 4 fold higher expression of human PrP^C having valine at codon 129 (Val129) of PrP followed by injection of 10% (w/v) of tissue homogenate from sCJD VV2 brain tissue as inoculum. In case of VV2 mice model of CJD, collection of samples (Brains) of the inoculated mice along with their age matched healthy controls was done post inoculation at day 120 for early-clinical stage, at day 160 for clinical stage and at day 180 for late clinical to terminal stage. This difference in the disease stages between two mice models is due to the early development of disease in mice with VV genotype at codon 129 of humanized PrP. Graphical presentation of preparation of mice models of sCJD is shown in figure 4.2.

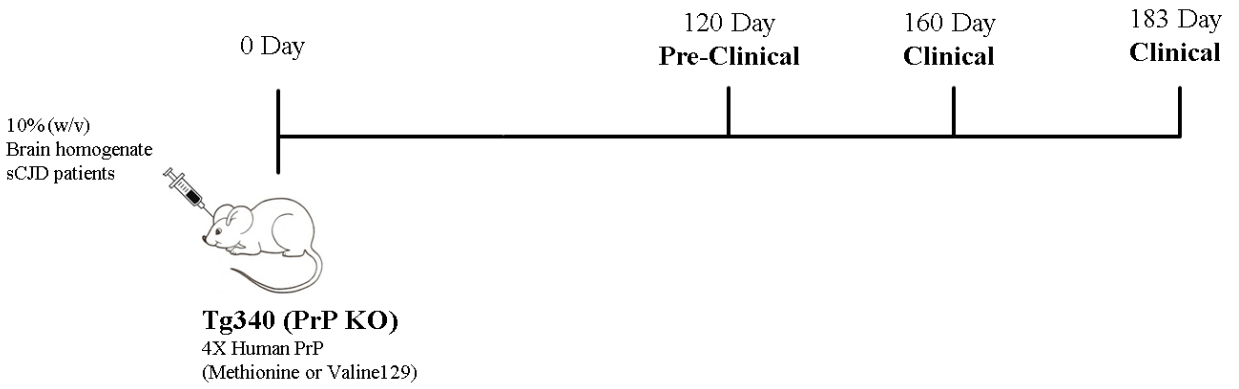

Figure 4-2: Graphical presentation of preparation of mice models of sCJD
Double transgenic mice Tg340 knock out for PrP and expressing four fold expression of humanized PrP with either Methionine or Valine at codon 129 of PrP were used. 10% brain homogenate from sCJD patient either from MM1 or VV2 subtype was injected into the right parietal lobe of the Tg340 mice brain to develop MM1 and VV2 mice models of sCJD respectively. Samples were collected for pre-symptomatic, early-symptomatic and late-symptomatic stages of disease at corresponding time points of 120, 160 and 183 dpi respectively.

4.2.13 Electrochemiluminescence-based Enzyme-linked immunosorbent assay (ELISA)

Electrochemiluminescence (ECL) based ELISA was performed to see the expression of DJ-1 in CSF samples from CJD patients. ECL based ELISA is a sensitive technique having ability to detect even very low expression of proteins by using smaller possible volumes of various biological samples. As compared with conventional ELISA, ECL based ELISA requires the use of special plates with Carbon ink electrodes embedded into the plates which serve as (1) capture phase for antibodies or other biomolecules and (2) provide electrochemical energy required to induce the emission of a luminescence, which is quantified as read out. The principle of ECL based ELISA is based on electrochemical stimulation of a SULFO-TAG label (ruthenium II tris-bipyridine-(4-methylsulfonate) NHS ester) tagged to the detection antibodies leading to the induction of a redox-reaction resulting in the emission of light at 620 nm which is detected with the help of high resolving CCD camera in the MSD Sector Imagers.

4.2.13.1 Protocol of Electrochemiluminescence-based ELISA

Carbon ink electrodes embedded microtitre plate was coated with 30 µl of 0.15 µg/ml of capture antibody (in PBS without tween) in each well and was incubated for overnight at 4 °C. All the wells coated with capture antibody were washed for three times on the next day with 150 µl of

PBS-T (PBS+0.05%Tween) as a wash buffer followed by blocking with 150 µl of 1% BSA for 1 h at room temperature with shaking at 300 rpm. Then all the blocked wells were washed for three times with 150 µl of PBS-T. For preparation of standard curve, recombinant DJ-1 was diluted to 2500 pg/ml. Serial dilution was performed by adding 100 µl from diluted single use standard to 300 µl of 1% BSA for seven times. 25 µl of serial dilutions of recombinant DJ-1 and CSF samples diluted at a ratio of 1:4 with 1% BSA (15 µl CSF + 45 µl 1% BSA) in duplicates were loaded into the wells on the plate.

	Calibrator	**Human DJ-1**	**Dilution factor**
Dilution of DJ1 standard: 20 µl stock + 180 µl 1% BSA	Stock Calibrator		10
100 µl + 300 µl 1% BSA	Calibrator 1	25000	4
100 µl + 300 µl 1% BSA	Calibrator 2	6250	4
100 µl + 300 µl 1% BSA	Calibrator 3	1562.5	4
100 µl + 300 µl 1% BSA	Calibrator 4	391.6	4
100 µl + 300 µl 1% BSA	Calibrator 5	97.6	4
100 µl + 300 µl 1% BSA	Calibrator 6	24.4	4
100 µl + 300 µl 1% BSA	Calibrator 7	6.1	4
Only 400 µl 1% BSA	Calibrator 8	0	n/a

Plate was incubated for 1 h at room temperature with shaking at 700 rpm. Followed by washing of all the wells for three times with 150 µl of PBS-T each time. Then 25 µl of SULFO-TAG labelled anti DJ-1 detection antibody with a concentration of 0.1 µg/ml was applied in every well and plate was again incubated for 1 h at room temperature with shaking at 300 rpm. After one hour, all the wells were washed for three times with 150 µl of PBS-T followed by application of 150 µl of 2X read buffer in each well. Then plate was read with the help of a Meso Scale Discovery Sector Imager.

4.2.14 Immunofluorescence

Formic acid treated frozen tissue samples from cerebellum region of brain from CJD (MM1) and age matched non demented control cases, were paraffin embedded and fixed with paraformaldehyde. Tissue samples were cut into sections of 4 µm thickness with the help of

cryostat at -20°C. These sections were mounted on histological glass slides and further treated with 2% of hydrogen peroxide and 10% methanol for 30 min at room temperature to reduce the internal activity of peroxidases in tissue sections. Slides were washed with PBS two times each for 5 min. Antigenic site on tissue sections was exposed by permeabilization by using PBS supplemented with 0.2 % Triton X-100 for 10 min. followed by washing with PBS for three times each for 5 min. Unwanted proteins were blocked by using 5% normal serum with PBS for 2 h. After the completion of blocking, sections were incubated with primary antibody (pAb) for overnight at 4°C with appropriate dilution of pAb diluted (Table 1) in 5% serum with PBS. On next day, sections on the slides were washed with PBS for three times each for 5 min. followed by incubation with appropriate corresponding horseradish peroxidase (HRP) labelled secondary antibody for 2h at RT. Then slides were washed again with PBS for three times each for 5 min. followed by incubation with DAPI (0.1 μg/ml of PBS) for 10 min. for staining nucleus. At the end of nuclear staining, slides were washed again with PBS for two times each for 5 min. Then slides were air dried and mounted with cover slip by using anti fade mounting medium. Slides were visualized using a fluorescence microscope.

4.2.15 Statistical Analysis

The data were analyzed with the help of GraphPad Prism 5 software (San Diego, USA). All experimental errors are shown as SEM. Statistical significance was calculated by nonparametric unpaired Student´s t test and nonparametric one way ANOVA followed by Turkey's multiple comparison test. Results were accepted as significant when $*p < 0.05$, $**p < 0.01$ and $***p < 0.001$.

4.2.16 Ethics statement

Human samples used in this study were obtained from Brain Bank and Biobank of Hospital Clinic-IDIBAPS of the Institute of Neuropathology, HUB-ICO-IDIBELL, Spain after accomplishing all the rules and laws of Spanish legislation (Ley de la Investigación Biomédica 2013 and Real DecretoBiobancos, 2014) and also with agreement of the local ethics committees.

All experiments with mice models of sCJD were conducted in agreement with the ethical regulations of Regierungspräsidium Tübingen (Regional Council) Experimental No. FLI 231/07 file reference number 35/9185.81-2 and also by following the rules and laws of institutional and

French national guidelines, in conjuction with the European Community Council Directive 86/609/EEC. The experimental protocol was approved by the ethics committee of INRA Toulouse/ENVT.

5 Results

5.1 Characterization of samples from MM1 and VV2 subtypes of sCJD

5.1.1 Strain specific alteration of total PrP expression

PrP is present in three isoforms (Di-glyco, Mono-glyco and Un-glycosylated) in the brain. Total PrP expression in cerebellum part of brain tissue from sCJD remains unchanged in MM1 subtype but significantly increased in VV2 subtype as compared to age matched controls (Llorens et al., 2013). In this study, western blot results demonstrated typical PrP three bands pattern corresponding to di-glyco, mono-glyco and un-glycosylated forms of PrP. Interestingly, VV2 subtype showed a significant increase in total PrP protein expression in cerebellum of brain as compared to age matched non-demented controls as well as MM1 subtype. However, MM1 subtype showed slight but not a significant increase in total PrP protein expression as compared to controls (Fig. 5.1).

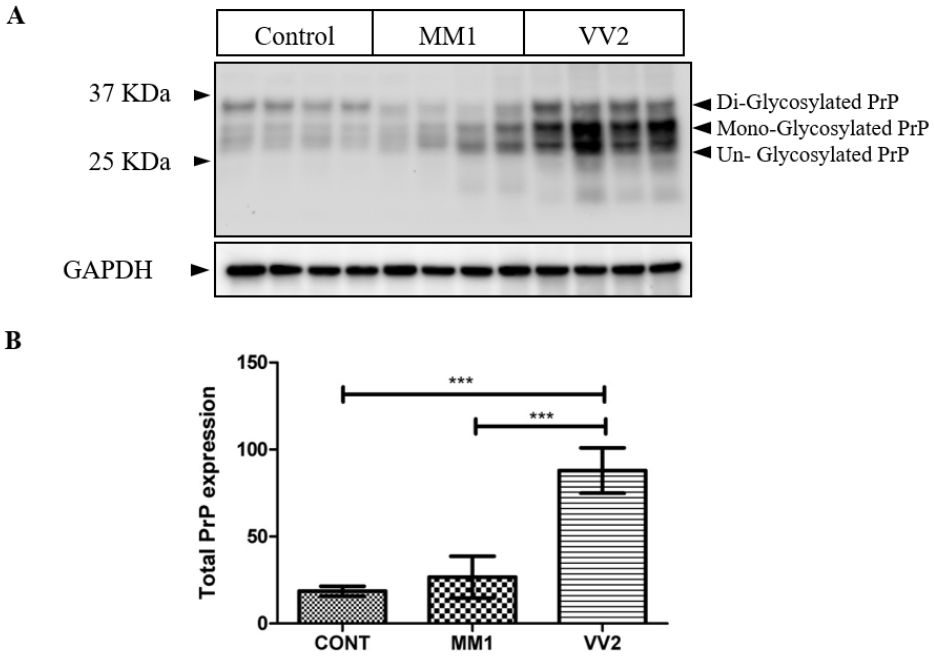

Figure 5-1: Analysis of total PrP protein expression in cerebellum from MM1 and VV2 subtypes of sCJD

Western blotting of samples from MM1 (n=4) and VV2 (n=4) subtypes of sCJD along with their age matched non-demented controls (n=4) from cerebellum of brain with anti-PrP (SAF70) antibody **(A)**.

Densitometeric analysis showed significant upregulation of total PrP levels only in VV2 subtype **(B)**. GAPDH was used as a loading control. The statistical significance was calculated with one way ANOVA followed by Turkey post test to compare all pairs of columns. *$p < 0.05$, **$p < 0.005$, ***$p < 0.001$.

5.1.2 Presence of proteinase K (PK) resistant pathogenic PrP

During the progression of disease, normal cellular prion protein (PrP^{C}) is converted to its pathogenic form known as PrP^{SC}, which is resistant to proteolytic digestion called as PrP^{res}. Western blot experiment showed significantly increased level of PK resistant PrP^{res} bands in sCJD (VV2 subtype) samples as compared to sCJD (MM1 subtype) samples from cerebellum. However, control samples from cerebellum of brain from age matched non-demented patients showed complete digestion of proteins indicating the presence of no PrP^{res}. Type 2 PrP^{SC} present in VV2 subtype showed more electrophoretic mobility on SDS-PAGE gel as compared to type 1 PrP^{SC} in MM1 subtype (Fig. 5.2). Presence of more PrP^{res} in VV2 subtype indicates the role of genotype of PrP (at codon 129) in determining cerebellum region of brain being more affected in VV2 subtype as compared to MM1 subtype (Polymenidou et al., 2005).

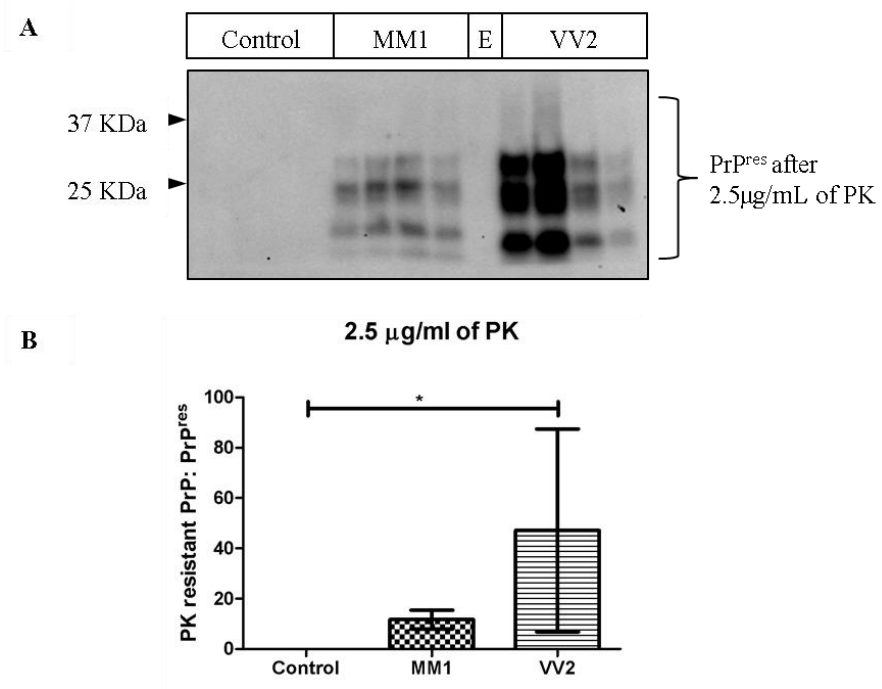

Figure 5-2: Analysis of proteinase K (PK) resistant pathogenic PrP^{SC} from cerebellum in MM1 and VV2 subtypes of sCJD

PK digestion of samples from MM1 (n=4) and VV2 (n=4) subtypes of sCJD along with age matched non-demented controls (n=4) from cerebellum of brain with 2.5 µg/ml of PK was followed by separation on SDS-PAGE gel. Western blotting was performed by using anti-PrP (SAF70) antibody **(A)**.

Densitometeric analysis showed the presence of PK resistant PrP: PrP^{SC} levels both in MM1 and VV2 subtypes as compared to age matched non-demented controls **(B)**. "E" is for empty well which was kept intentionally empty to avoid an overflow of sample between two adjacent wells. The statistical significance was calculated with one way ANOVA followed by Turkey post test to compare all pairs of columns. *$p < 0.05$, **$p < 0.005$, ***$p < 0.001$.

5.2 Identification of differentially regulated protein spots by Delta2D software

Visualization of spots on 2DE gels by using silver stain was followed by matching of spots on all gels from all three experimental groups. Total of 688 protein spots on all 2DE gels (four gels from each of four samples from each of three experimental groups) from four independent experiments of MM1 and VV2 subtypes and from age matched non-demented controls were detected by using 100% spot matching approach in Delta2D software. Densitometery analysis revealed twenty five differentially regulated protein spots (Fig. 5.3) which were selected for further identification by using mass spectrometry.

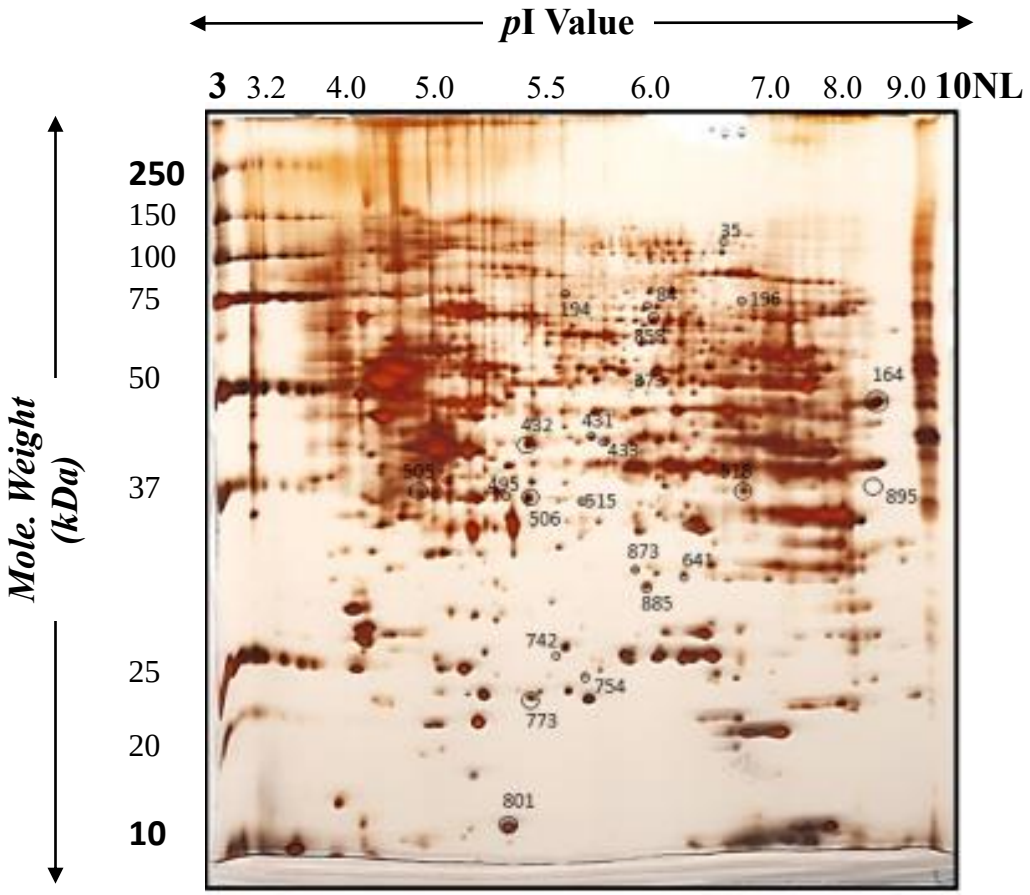

Figure 5-3: 2DE map of the total tissue lysate of human cerebellum proteome
2DE map showing the localization (*pI* values by horizontal bar and molecular weights (*kDa*) by vertical bar) of 25 differentially regulated proteins spots both in MM1 and VV2 subtypes of sCJD. Unpaired Student's T-test was used for statistical analysis of the protein spots. *p*-value was considered significant when *p < 0.05.

5.3 Identification of differentially regulated proteins by MALDI-TOF MS/MS

Identification with MS/MS MALDI-TOF revealed 366 proteins in both subtypes. Screening by matching the *pI* value and molecular weight of each identified protein to its corresponding spot unveiled 83 regulated proteins in both subtypes. The discrepancy between the number of protein spots and number of proteins can be explained by the coexistence of different isoforms of the same proteins or coexistence of different proteins of same similar *pI* values and molecular weights in the same spot. Total of forty differentially regulated proteins were identified in MM1 subtype whereas forty three proteins were identified to be differentially regulated in VV2 subtype. Twelve of these proteins were common between two subtypes (Fig. 5.4). In MM1

subtype, 18 proteins were upregulated and 22 were down regulated. On the other hand, 27 proteins were upregulated in VV2 subtype and 18 were down regulated in VV2 subtype as compared to age matched non-demented controls (Fig. 5.5).

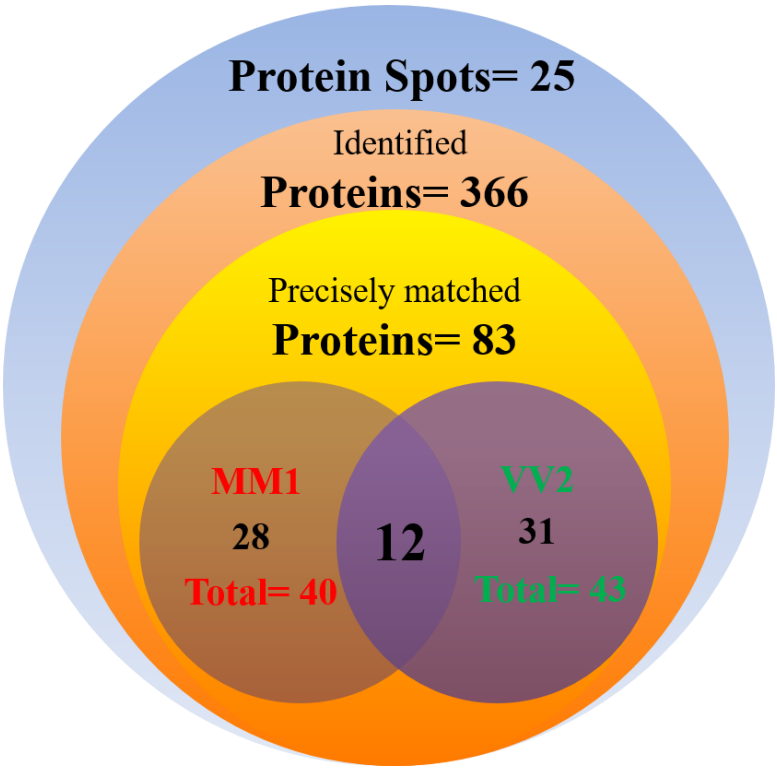

Figure 5-4: Number of proteins identified by MS/MS MALDI-TOF in MM1 and VV2 subtypes of sCJD

Twenty five differentially regulated protein spots revealed 366 regulated proteins in cerebellum of MM1 and VV2 subtypes of sCJD. Only 110 proteins of total identified proteins qualified further screening criteria of *pI* and molecular weight match with their corresponding spots and minimal peptide count of 2. Forty and forty three proteins were regulated in MM1 and VV2 subtype each respectively with twelve proteins common between two subtypes in cerebellum.

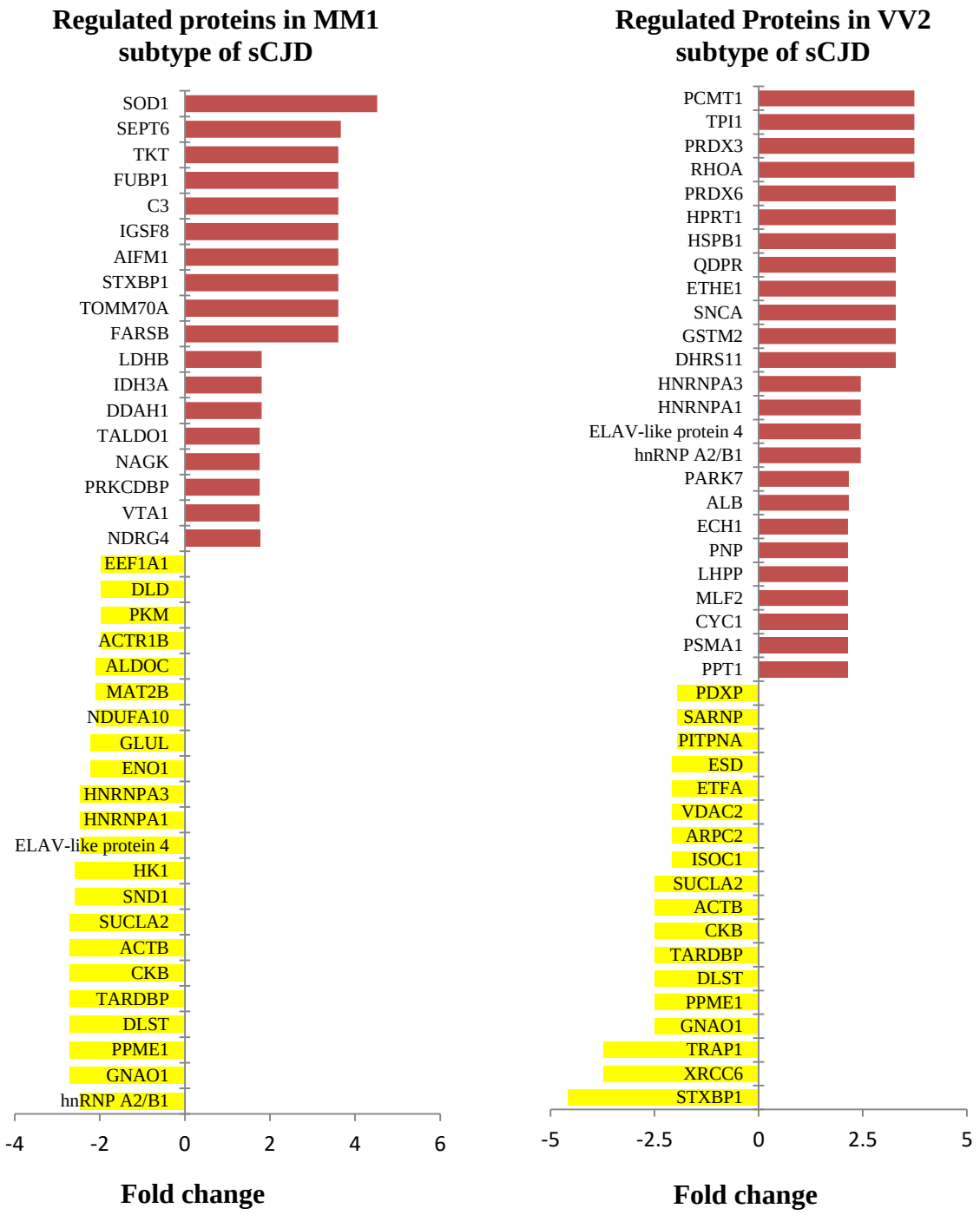

Figure 5-5: Fold changes of the proteins regulated in MM1 and VV2 subtypes (represented by their gene names from Uni Prot)

18 proteins were upregulated and 22 were down regulated in MM1 subtype **(A)** and 27 proteins were upregulated and 18 were down regulated in VV2 subtype **(B)** of sCJD cases. Upregulated proteins are shown by red bars and down regulated proteins are shown by yellow bars in the figure.

5.4 Common differentially regulated proteins

sCJD related proteins in both subtypes showed almost similar trend of expressional regulation between MM1 and VV2 subtypes. A common differential expression in both subtypes was found for twelve proteins while seven of them showed a similar expressional regulation in both subtypes. These seven proteins were down-regulated in both subtypes and were including Guanine nucleotide-binding protein G(o) subunit alpha, Protein phosphatase methylesterase 1, Dihydrolipoyllysine-residue succinyltransferase component of 2-oxoglutarate dehydrogenase complex, TAR DNA-binding protein 43, Creatine kinase B-type, Actin, cytoplasmic 1 and Succinyl-CoA ligase [ADP-forming] subunit beta. Rest five of the twelve common proteins showed subtype specific expressional regulation. Syntaxin-binding protein 1 was upregulated in MM1 subtype but down-regulated in VV2 subtype as compared to their age matched non-demented controls. Dihydrolipoyl dehydrogenase, Heterogeneous nuclear ribonucleoproteins A2/B1, ELAV-like protein 4, Heterogeneous nuclear ribonucleoprotein A3 and Heterogeneous nuclear ribonucleoprotein A1 were upregulated in VV2 subtype in comparison to MM1 subtype and vice versa in MM1 subtype in comparison to VV2 subtype.

All identified differentially regulated proteins from both subtypes (shown in Table 5.1) were grouped on the basis of their molecular functions into eight groups which include i)- cell cycle; gene expression and cell death, ii)- cellular stress response/ oxidative stress, iii)- signal transduction and synaptic functions, iv)- carbohydrate metabolism, v)- energy metabolism, vi)- cell growth, proliferation and differentiation, and vii)- intracellular transport and cytoskeleton related functions. There were also few proteins which could not be classified into any of the above-mentioned groups and were classified under other functions.

Table 5-1: List of differentially regulated proteins in MM1 and VV2 subtypes of cerebellum of brain from sCJD patients

Only significantly differentially regulated proteins were included which were having more than 1.5 fold change in abundance along with *p*-value < 0.05 (analyzed by unpaired Student's *t*-test). Furthermore, all the differentially regulated proteins were classified into eight groups on the basis of their molecular functions including i)- cell cycle; gene expression and cell death, ii)- cellular stress response/ oxidative stress, iii)- signal transduction and synaptic functions, iv)- carbohydrate metabolism, v)- energy metabolism, vi)- cell growth, proliferation and differentiation, vii)- intracellular transport and cytoskeleton related functions and other functions. *p*I stands for Isoelectric point, "Seq. Cov." stands for Sequence coverage, "Reg." stands for Regulation, "↓" stands for downregulated, "↑" stands for Upregulated, "↔" stands for not identified and "Fold" denotes fold of regulation/ change.

Spot ID	Protein Name	MM1 subtype			VV2 subtype			Access. UniProt	MW (kDa)	*pI*	Peptide count	Seq. Cov. (%)
		Reg.	Fold	*P*-value	Reg.	Fold	*P*-value					
1- Cell cycle, gene expression and cell death												
35	Staphylococcal nuclease domain-containing protein 1	↓	-2.57	0.045	↔	↔	↔	Q7KZF4	101.99	6.7	3	3.19
164	Elongation factor 1-alpha 1	↓	-1.97	0.013	↔	↔	↔	P68104	50.14	9.1	3	26.00
196	Phenylalanine--tRNA ligase beta subunit	↑	3.60	0.009	↔	↔	↔	Q9NSD9	66.11	6.3	3	4.75
196	Apoptosis-inducing factor1 (Fragment of a.a. 102-613)	↑	3.60	0.009	↔	↔	↔	O95831	55.81	6.8	6	11.10
196	Far upstream element-binding protein 1	↑	3.60	0.009	↔	↔	↔	Q96AE4	67.56	7.1	12	24.40
432	TAR DNA-binding protein 43	↓	-2.70	0.0051	↓	-2.49	0.0055	Q13148	44.73	5.8	4	11.60
518	NADH dehydrogenase [ubiquinone] 1 alpha subcomplex subunit 10 (Fragment of a.a. 36-355)	↓	-2.09	0.028	↔	↔	↔	O95299	37.14	6.8	2	5.35
895	Heterogeneous nuclear ribonucleoproteins A2/B1	↓	-2.45	0.020	↑	2.45	0.020	P22626	37.43	8.9	3	9.63
895	ELAV-like protein 4	↓	-2.45	0.020	↑	2.45	0.020	P26378	41.77	9.4	3	9.74
895	Heterogeneous nuclear ribonucleoprotein A1	↓	-2.45	0.020	↑	2.45	0.020	P09651	38.74	9.1	3	12.10
895	Heterogeneous nuclear ribonucleoprotein A3	↓	-2.45	0.020	↑	2.45	0.020	P51991	39.59	9.1	13	32.50
742	Alpha-synuclein	↔	↔	↔	↑	3.29	0.022	P37840	14.45	4.6	3	27.1
742	Heat shock protein beta-1	↔	↔	↔	↑	3.29	0.022	P04792	22.782	5.9	4	26.30
773	Serum albumin (Fragment of a.a. 19-210)	↔	↔	↔	↑	2.16	0.0003	P02768	22.26	5.6	6	9.03
873	SAP domain-containing ribonucleoprotein	↔	↔	↔	↓	-1.95	0.026	P82979	23.67	6.1	6	32.90
885	Proteasome subunit alpha type-1	↔	↔	↔	↑	2.14	0.046	P25786	29.55	6.1	3	12.90

885	Cytochrome c1 (Fragment of a.a. 85-325)	↔	↔	↔	↑	2.14	0.046	P08574	27.35	6.4	3	13.50
885	Myeloid leukemia factor 2	↔	↔	↔	↑	2.14	0.046	Q15773	28.14	6.4	4	15.30
2- Cellular stress response/ Oxidative stress												
164	Dihydrolipoyl dehydrogenase	↓	-1.97	0.013	↔	↔	↔	P09622	54.17	7.9	2	8.64
196	Apoptosis-inducing factor 1 (Fragment of a.a. 102-613)	↑	3.60	0.009	↔	↔	↔	O95831	55.81	6.8	6	11.10
196	Complement C3 (Fragment of a.a. 23-667)	↑	3.60	0.009	↔	↔	↔	P01024	71.31	6.8	12	8.24
433	Glutamine synthetase	↓	-2.21	0.002	↔	↔	↔	P15104	42.06	6.4	6	17.40
495	N(G),N(G)dimethylarginine-dimethylaminohydrolase1	↑	1.8	0.029	↔	↔	↔	O94760	31.12	5.5	2	8.07
495	Isocitrate dehydrogenase [NAD] subunit alpha (Fragment of a.a. 28-366)	↑	1.8	0.029	↔	↔	↔	P50213	36.64	5.7	7	19.40
495	L-lactate dehydrogenase B chain	↑	1.8	0.029	↔	↔	↔	P07195	36.63	5.7	10	34.10
506	Protein NDRG4	↑	1.75	0.049	↔	↔	↔	Q9ULP0	38.45	5.7	2	6.82
518	Fructose-bisphosphate aldolase C	↓	-2.09	0.028	↔	↔	↔	P09972	39.45	6.4	3	9.62
801	Superoxide dismutase [Cu-Zn]	↑	4.52	0.002	↔	↔	↔	P00441	15.93	5.7	11	69.50
84	X-ray repair cross-complementing protein 6	↔	↔	↔	↓	-3.73	0.006	P12956	69.84	6.2	2	4.60
84	Heat shock protein 75 kDa (Fragment of a.a. 60-704)	↔	↔	↔	↓	-3.73	0.006	Q12931	73.54	6.1	2	4.97
641	Electron transfer flavoprotein subunit alpha (Fragment of a.a. 20-333)	↔	↔	↔	↓	-2.06	0.036	P13804	32.96	7.1	5	19.20
742	Dehydrogenase/reductase SDR family member 11 (Fragment of a.a. 31-260)	↔	↔	↔	↑	3.29	0.022	Q6UWP2	25.22	5.6	2	9.62
742	Glutathione S-transferase Mu 2	↔	↔	↔	↑	3.29	0.022	P28161	25.74	5.9	2	10.10
742	Persulfide dioxygenase ETHE1	↔	↔	↔	↑	3.29	0.022	O95571	27.87	6.3	4	18.10
742	Dihydropteridine reductase	↔	↔	↔	↑	3.29	0.022	P09417	25.78	6.9	4	20.10
742	Heat shock protein beta-1	↔	↔	↔	↑	3.29	0.022	P04792	22.78	5.9	4	26.30
742	Peroxiredoxin-6	↔	↔	↔	↑	3.29	0.022	P30041	25.03	6.0	12	41.10
754	Thioredoxin-dependent peroxide reductase (Fragment of a.a. 63-256)	↔	↔	↔	↑	3.73	0.032	P30048	21.46	5.7	6	33.60
773	Protein DJ-1	↔	↔	↔	↑	2.16	0.0003	Q99497	19.89	6.3	12	59.30
3- Signal transduction and synaptic functions												
196	Syntaxin-binding protein 1	↑	3.60	0.009	↔	↔	↔	P61764	67.57	6.5	4	6.90
858	Syntaxin-binding protein 1	↔	↔	↔	↓	-4.57	0.0075	P61764	67.57	6.5	13	19.50
196	Complement C3 (Fragment of a.a. 23-667)	↑	3.60	0.009	↔	↔	↔	P01024	71.31	6.8	12	8.24

431	Beta-centractin	↓	-1.97	0.030	↔	↔	↔	P42025	42.29	5.9	3	9.57
432	Guanine nucleotide-binding protein G(o) subunit alpha	↓	-2.70	0.005	↔	↔	↔	P09471	40.05	5,3	2	6.50
432	Protein phosphatase methylesterase 1	↓	-2.70	0.005	↔	↔	↔	Q9Y570	42.31	5.6	3	11.10
432	Guanine nucleotide-binding protein G(o) subunit alpha	↔	↔	↔	↓	-2.49	0.0055	P09471	40.05	5,3	2	9.60
432	Protein phosphatase methylesterase 1	↔	↔	↔	↓	-2.49	0.0055	Q9Y570	42.31	5.6	3	11.10
433	Glutamine synthetase	↓	-2.21	0.0022	↔	↔	↔	P15104	42.06	6.4	6	17.40
506	Protein kinase C delta-binding protein	↑	1.75	0.049	↔	↔	↔	Q969G5	27.70	6.0	3	13.80
641	Voltage-dependent anion-selective channel protein 2	↔	↔	↔	↓	-2.06	0.36	P45880	31.56	7.5	4	17.0
742	Hypoxanthine-guanine phosphoribosyltransferase	↔	↔	↔	↑	3.29	0.022	P00492	24.58	6.2	5	30.70
754	Transforming protein RhoA	↔	↔	↔	↑	3.73	0.032	P61586	21.76	5.8	3	20.70
873	Phosphatidylinositol transfer protein alpha isoform	↔	↔	↔	↓	-1.95	0.026	Q00169	31.80	6.1	6	21.10
885	Purine nucleoside phosphorylase	↔	↔	↔	↑	2.14	0.046	P00491	32.11	6.4	7	29.10
4- Carbohydrate metabolism												
35	Hexokinase-1	↓	-2.57	0.045	↔	↔	↔	P19367	102.48	6.3	7	7.42
164	Pyruvate kinase PKM	↓	-1.97	0.013	↔	↔	↔	P14618	57.93	7.9	2	6.03
433	Alpha-enolase	↓	-2.21	0.002	↔	↔	↔	P06733	47.17	7.0	4	12.40
506	Transaldolase	↑	1.75	0.049	↔	↔	↔	P37837	37.54	6.3	24	53.10
518	Fructose-bisphosphate aldolase C	↓	-2.09	0.028	↔	↔	↔	P09972	39.45	6.4	3	9.62
754	Triosephosphate isomerase	↔	↔	↔	↑	3.73	0.032	P60174	30.79	5.6	14	54.20
5- Energy metabolism												
432	Dihydrolipoyllysine-residue succinyltransferase component of 2-oxoglutarate dehydrogenase complex	↓	-2.70	0.005	↔	↔	↔	P36957	41.38	5.9	4	10.20
432	Creatine kinase B-type	↓	-2.70	0.005	↔	↔	↔	P12277	42.64	5.3	4	13.10
432	Succinyl-CoA ligase [ADP-forming] subunit beta	↓	-2.70	0.005	↔	↔	↔	Q9P2R7	44.58	5.6	31	40.00
432	Dihydrolipoyllysine-residue succinyltransferase component of 2-oxoglutarate dehydrogenase complex	↔	↔	↔	↓	-2.49	0.005	P36957	41.38	5.9	4	10.20
432	Creatine kinase B-type	↔	↔	↔	↓	-2.49	0.005	P12277	42.64	5.3	4	13.10
432	Succinyl-CoA ligase [ADP-forming] subunit beta	↔	↔	↔	↓	-2.49	0.005	Q9P2R7	44.58	5.6	32	41.70
495	L-lactate dehydrogenase B chain	↑	1.80	0.029	↔	↔	↔	P07195	36.63	5.7	10	34.10
6- Cell growth, proliferation and differentiation												

196	Immunoglobulin superfamily member 8	↑	3.60	0.009	↔	↔	↔	Q969P0	65.03	8.2	9	19.60
196	Transketolase	↑	3.60	0.009	↔	↔	↔	P29401	67.87	7.5	22	33.50
506	Protein NDRG4	↑	1.75	0.049	↔	↔	↔	Q9ULP0	38.45	5.7	2	6.82
754	Protein L-isoaspartate(D-aspartate)O-methyltransferase	↔	↔	↔	↑	3.73	0.032	P22061	24.63	6.7	15	59.00
885	Palmitoyl-protein thioesterase 1	↔	↔	↔	↑	2.15	0.046	P50897	34.19	6.0	2	7.84
7- Intracellular transport and cytoskeleton												
196	Mitochondrial import receptor subunit TOM70	↑	3.60	0.009	↔	↔	↔	O94826	67.45	6.7	4	6.58
373	Septin-6	↑	3.66	0.005	↔	↔	↔	Q14141	49.71	6.2	9	22.40
432	Actin, cytoplasmic 1	↓	-2.70	0.005	↓	-2.49	0.005	P60709	41.73	5.2	7	30.70
506	Vacuolar protein sorting-assoc. protein VTA1 homolog	↑	1.75	0.049	↔	↔	↔	Q9NP79	33.88	5.8	3	12.40
641	Actin-related protein 2/3 complex subunit 2	↔	↔	↔	↓	-2.06	0.036	O15144	34.33	6.84	4	13.00
873	Pyridoxal phosphate phosphatase	↔	↔	↔	↓	-1.95	0.026	Q96GD0	31.69	6.11	7	26.40
8- Other functions												
506	N-acetyl-D-glucosamine kinase	↑	1.75	0.049	↔	↔	↔	Q9UJ70	37.37	5.8	6	21.20
518	Methionine adenosyltransferase 2 subunit beta	↓	-2.09	0.028	↔	↔	↔	Q9NZL9	37.55	6.9	3	8.68
641	Isochorismatase domain-containing protein 1	↔	↔	↔	↓	-2.06	0.036	Q96CN7	32.23	6.9	3	13.80
641	S-formylglutathione hydrolase	↔	↔	↔	↓	-2.06	0.036	P10768	31.46	6.5	15	42.20
885	Phospholysine phosphohistidine inorganic pyrophosphate phosphatase	↔	↔	↔	↑	2.14	0.046	Q9H008	29.16	5.8	7	28.50
885	Delta(3,5)-Delta(2,4)-dienoyl-CoA isomerase (Fragment of a.a. 34-328)	↔	↔	↔	↑	2.14	0.046	Q13011	32.20	5.9	15	38.10

5.5 Regulation of identified cellular molecular mechanisms

Classification of all the identified proteins in both MM1 and VV2 subtypes in to different functional groups revealed that almost all the cellular functions are regulated during the course of the disease (Figure. 5.6). Cell cycle: gene expression and cell death related cellular molecular functions were the most highly regulated (24% in MM1 and 27% in VV2 subtype), cellular stress response/ oxidative stress related cellular functions were the second most highly regulated (22% in MM1 and 25% in VV2 subtype) and signal transduction and synaptic functions were the third most highly regulated (15% in MM1 and 18% in VV2 subtype) molecular functions in both subtypes each based on the number of regulated proteins to the corresponding molecular function.

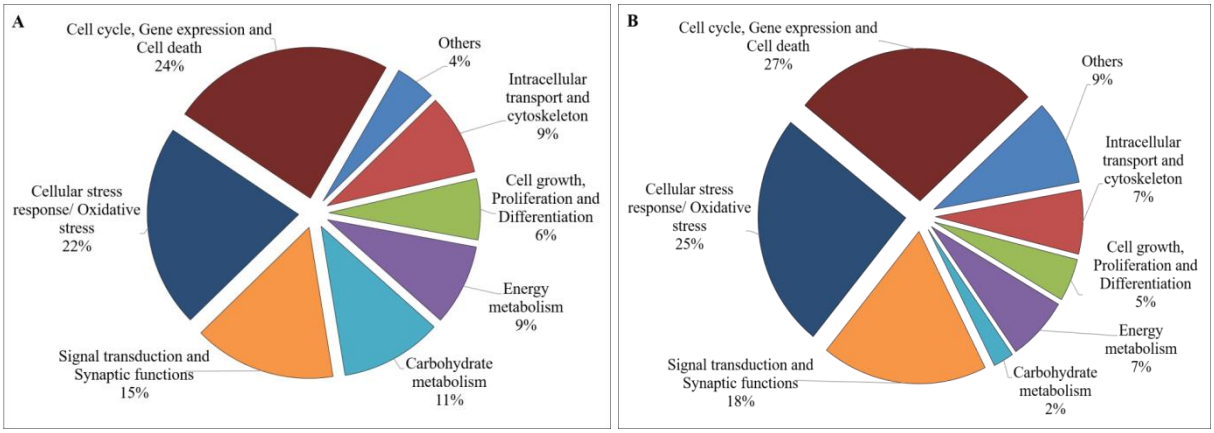

Figure 5-6: Regulation of identified cellular molecular mechanisms in MM1 (A) and VV2 (B) subtypes

All identified regulated proteins from MM1 **(A)** and VV2 **(B)** subtypes were classified into different functional groups based on their molecular functions. The molecular functions were assigned as in UniProt protein database.

Most of the proteins involved in cellular stress response/ oxidative stress related functions in both subtypes were related to oxidative stress. Similarly other molecular functions including carbohydrate metabolism were 11% in MM1 and 2% in VV2 subtype, energy metabolism were 9% in MM1 and 7% in VV2 subtype, cell growth, proliferation and differentiation related cellular molecular functions were 6% in MM1 and 5% in VV2 subtype, and intracellular transport and cytoskeleton related molecular functions were regulated 9% in MM1 and 7% in VV2 subtype. 4% and 9% of proteins from MM1 and VV2 subtypes respectively were not able to be assigned any function so they were sub-classified under “other” functions.

5.6 Comparative analysis of functional classification

Comparison of the regulated cellular functions between two subtypes based on proteomics data revealed that i)- cell cycle; gene expression and cell death, ii)- cellular stress response/ oxidative stress, and iii)- signal transduction and synaptic functions were top three regulated cellular functions in both subtypes in the same order and each of these function was deregulated more in VV2 subtype as compared to MM1 subtype. Whereas metabolism related molecular functions (carbohydrate metabolism and energy metabolism) and cell growth, proliferation and differentiation related molecular functions were deregulated more in MM1 subtype as compared to VV2 subtype (Figure. 5.7). Cellular stress response/ oxidative stress related cellular mechanisms comprised mainly of cellular mechanisms related to oxidative stress related cellular responses in both subtypes indicating oxidative stress as one of the major contributing factors adding to the disease pathology.

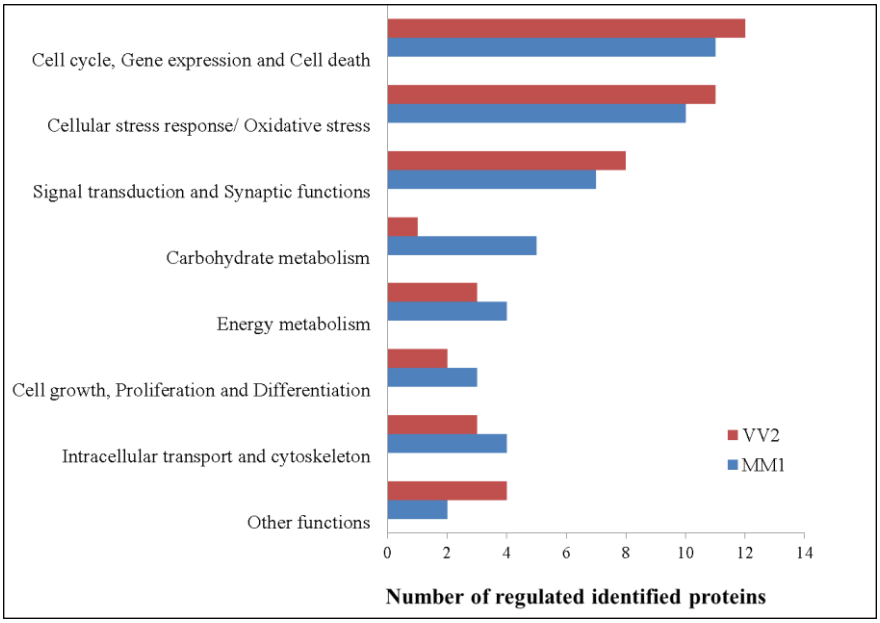

Figure 5-7: Comparison of functional classification of MM1 and VV2 subtypes of cerebellum of brain from sCJD patients

5.7 Validation of MS/ MS Data

5.7.1 Validation at mRNA level by RT-qPCR

Eleven proteins from the whole proteomic data set identified by MS/ MS were selected throughout the data equally from both subtypes, based on low and high peptide counts, sequence coverage and fold change, both down regulated as well as upregulated ones (Table 5.2) for further validation of identified regulated proteomic data to elucidate the expressional

regulations at mRNA level by using RT-qPCR. Regulation of the corresponding protein spots selected for validation of proteomic findings after mass-spectrometery is shown in annexure.

Table 5-2: List of selected proteins from sCJD (MM1 and VV2 subtypes) for further validation at transcriptional and translational level.
Eleven proteins were selected throughout the whole data to validate the identified regulated proteomic data. Proteins were selected which were identified individually in each subtype, commonly identified in both subtypes, having low and high peptide count, sequence coverage, fold change and both down regulated (represented by ↓) as well as upregulated (represented by ↑) ones, "Reg." denotes "Regulation".

Spot	Protein selected for further validation	MM1 subtype		VV2 subtype	
		Reg.	Fold change	Reg.	Fold change
164	Pyruvate kinase PKM1/2	↓	-1.97	--	--
373	Septin-6	↑	3.66	--	--
495	L-lactate dehydrogenase B	↑	1.80	--	--
506	Transaldolase	↑	1.75	--	--
801	Superoxide dismutase [Cu-Zn]	↑	4.52	--	--
742	Heat shock protein beta-1	--	--	↑	3.29
742	Peroxiredoxin-6	--	--	↑	3.29
773	Protein DJ-1	--	--	↑	2.16
432	TAR DNA-binding protein 43	↓	-2.70	↓	-2.49
432	Creatine kinase B-type	↓	-2.70	↓	-2.49
432	Succinyl-CoA ligase subunit β	↓	-2.70	↓	-2.49

Pyruvate kinase M2 (Q9UKK4) and Transaldolase (P37837) were selected for their role in carbohydrate metabolism whereas Succinyl-CoA ligase [ADP-forming] subunit beta (Q9P2R7) and Creatine kinase B-type (P12277) were selected for their role in energy metabolism. Septin-6 (Q14141) was selected for its role in intracellular transport and cytoskeleton related molecular functions. TAR DNA-binding protein 43 (P12277) was selected for its role in cell cycle: gene expression and cell death related functions. Five proteins including L-lactate dehydrogenase B chain (P07195), heat shock protein beta-1 (P04792), peroxiredoxin-6 (P30041), protein DJ-1 (Q99497) and superoxide dismutase 1 (P00441) were selected for their role in oxidative stress.

Pyruvate Kinase M2 showed upregulation in its mRNA expression in both subtypes (Fig. 5.8 A). The mRNA expression for Septin-6 was upregulated while it was un-altered for TDBP (Gene name for TAR DNA-binding protein 43), down regulated for CK-B (Gene name for Creatine kinase B-type) and unchanged for SUCLA2 (Gene name for Succinyl-CoA ligase [ADP-forming] subunit beta) as well (Fig. 5.8 B-E). The mRNA expression was also un-altered for LDH-B (gene name for L-lactate dehydrogenase B) (Fig. 5.8 F) but upregulated for TALDO-1 (Gene name for transaldolase), HSPB1 (gene name for heat shock protein beta-1),

PRDX6 (gene name for peroxiredoxin-6), PARK7 (gene name for protein DJ-1) and SOD1 (gene name for Superoxide dismutase [Cu-Zn]) (Fig. 5.8 G-K). Altogether, these results show that mRNA expression of mostly validated proteins showed similar trend to their corresponding regulated protein spots analyzed by Delta2D-Decodon and proteins in those spots identified later by MS/ MS except unchanged for LDH-B, SUCLA2 and TDP while upregulated for PKM2. Protein expression is more stable than mRNA expression and can be independent of its mRNA expression as protein expression is also influenced by various post translational modifications.

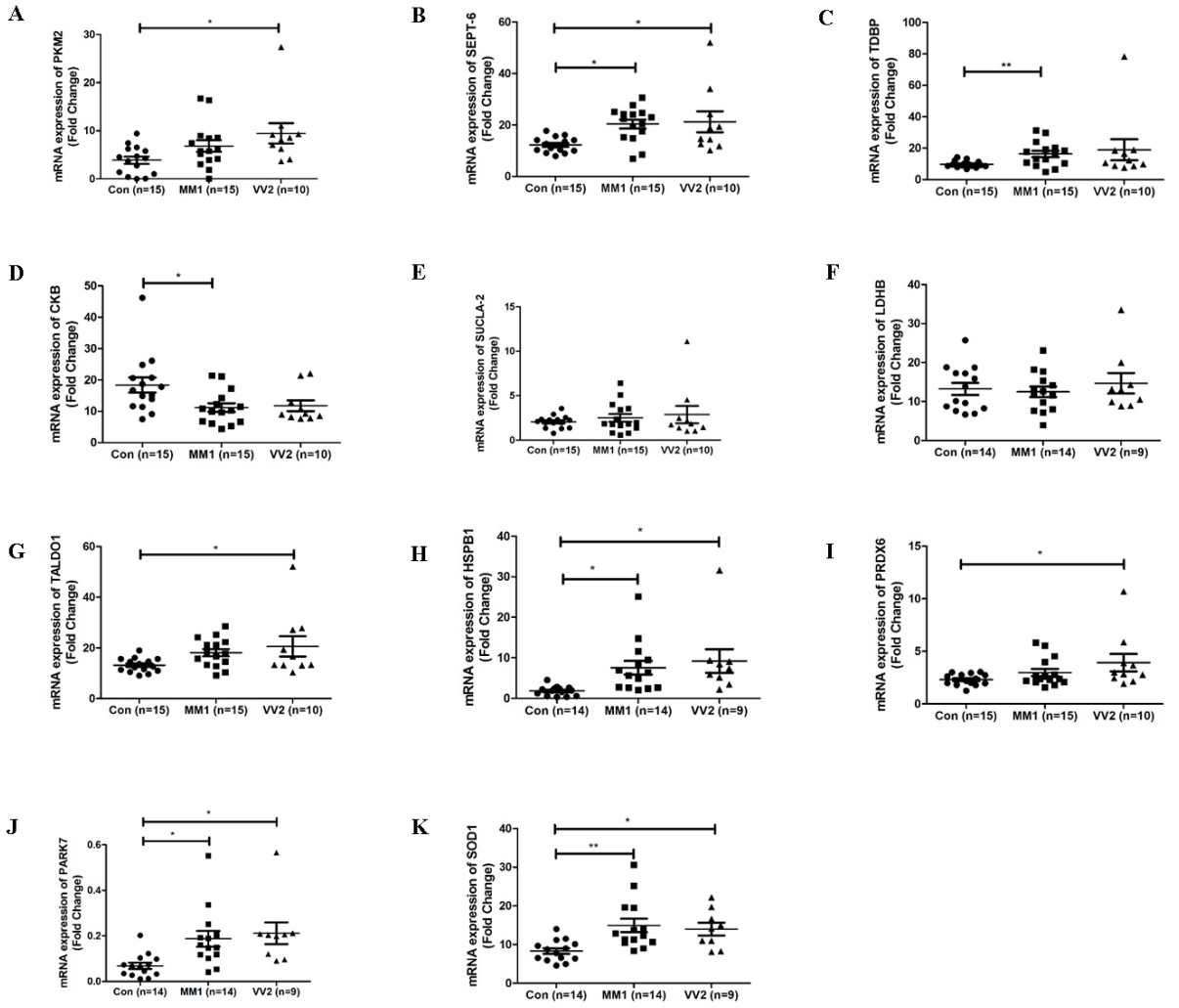

Figure 5-8: mRNA expression profile of selected eleven proteins for validation.
RT-qPCR analysis of PKM2 **(A)**, SEPT-6 **(B)**, TDBP **(C)**, CKB **(D)**, SUCLA-2 **(E)**, LDH-B **(F)**, TALDO-1 **(J)**, HSPB1 **(H)**, PRDX6 **(I)**, PARK7 **(J)** and SOD1 **(K)** in control ($n = 14\pm15$), sCJD MM1 ($n = 14\pm15$) and sCJD VV2 ($n = 9\pm10$) samples is shown. Values are normalized using GUS-b as internal control. The statistical significance was calculated with one way ANOVA followed by Turkey post test to compare all pairs of columns. Data are represented as the mean SEM. *p <0.05, **p <0.01, ***p <0.001.

5.7.2 Validation at Protein level

Already validated proteins at their mRNA level, were further validated at protein level for expressional regulations by using western blot. PKM2, TDP43, CKB and SUCL2 were found downregulated, septin-6, LDH, HSP27, Prdx6, DJ-1 and SOD1 were upregulated and TALDO1 did not show any detectable regulation (Fig. 5.9).

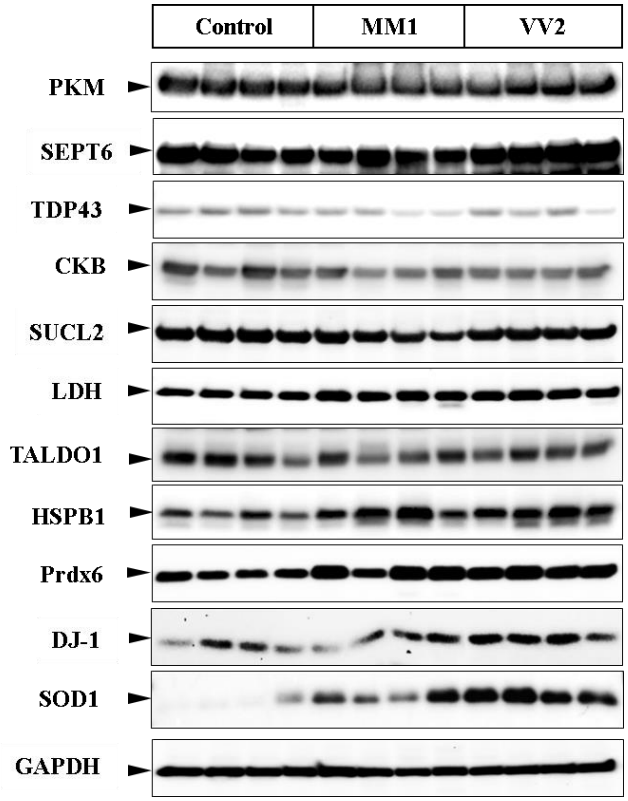

Figure 5-9: Protein expression of selected proteins for validation
Western blot analysis of PKM, Sept-6, TDP43, CKB, SUCL2, LDH, TALDO1, HSPB1, Prdx6, DJ-1 and SOD1. in control ($n = 4$), sCJD MM1 ($n = 4$) and sCJD VV2 ($n = 4$) samples is shown. GAPDH was used as a loading control.

Densitometric analysis revealed a significant increase in the expression of LDH, HSPB1, Prdx6 and SOD1 in both MM1 and VV2 samples whereas septin-6 and DJ-1 showed upregulation only in VV2 samples. DJ-1 although showed the trend of an increase in their expression in MM1 subtype yet results were not statistically significant. CKB showed a significant decrease in the protein expression both in MM1 and VV2 subtypes, PKM, TDP43, and SUCL-2 expressions were found to be downregulated in MM1 subtype only. Although TDBP showed the trend of a decrease in its expression in VV2 subtype as well yet results were not statistically significant. No significant regulation in TALDO1 protein expression was detected (Fig. 5.10 A-K). Altogether, these results show that protein expression of all the

validated proteins also showed a similar trend to their corresponding regulated protein spots analyzed by Delta2D-Decodon and proteins in those spots identified later by MS/ MS.

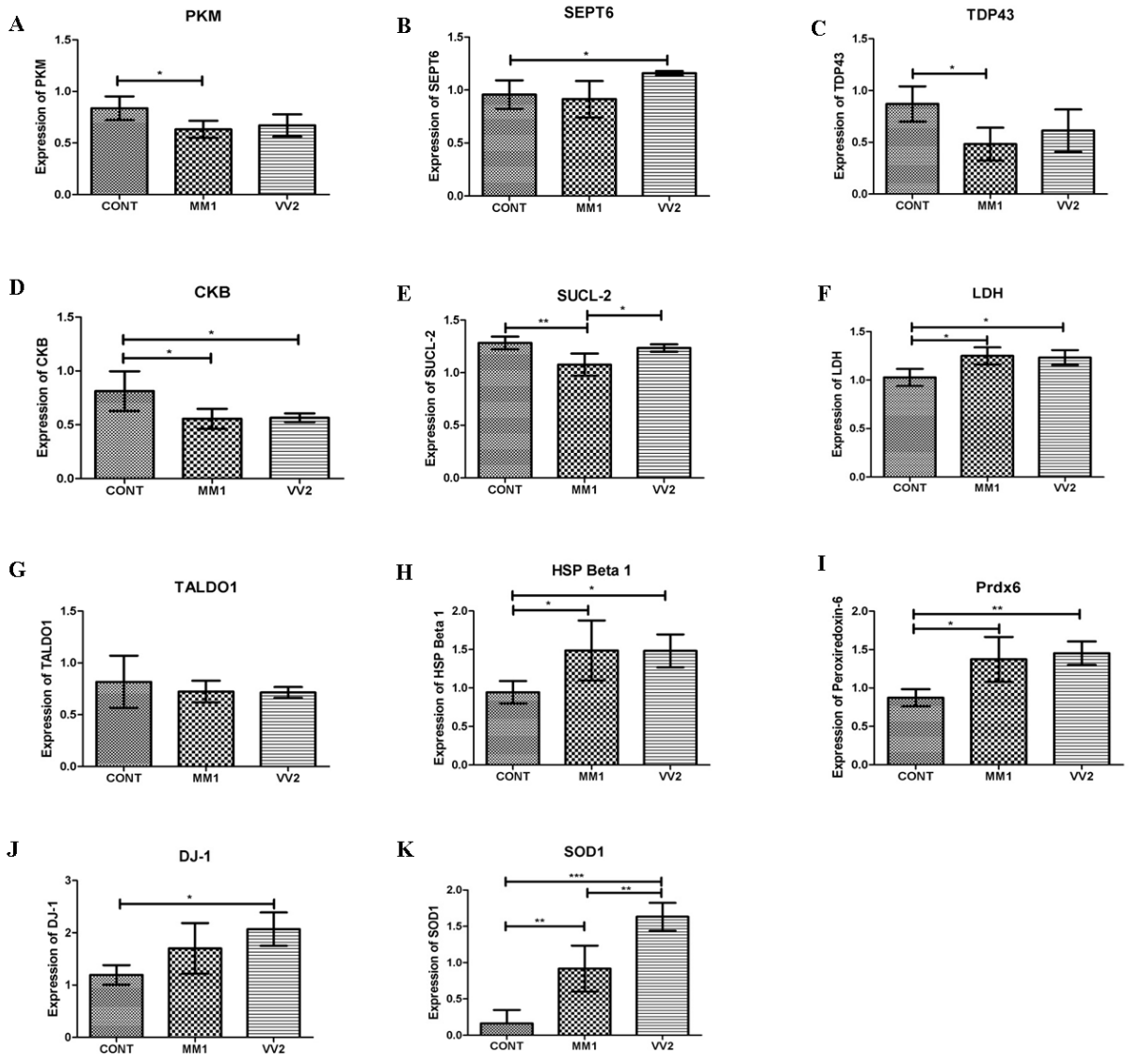

Figure 5-10: Densitometeric analysis of selected nine proteins for validation
Densitometeric analysis of PKM **(A)**, SEPT-6 **(B)**, TDBP **(C)**, CKB **(D)**, SUCL-2 **(E)**, LDH-B **(F)**, TALDO-1 **(J)**, HSPB1 **(H)**, PRDX6 **(I)**, PARK7 **(J)** and SOD1 **(K)** with control ($n = 4$), sCJD MM1 ($n = 4$) and sCJD VV2 ($n = 4$) samples is shown. The statistical significance was calculated with one way ANOVA followed by Turkey post test to compare all pairs of columns. Data are represented as the mean SEM. *$p < 0.05$, **$p < 0.005$, ***$p < 0.001$.

5.8 Identification of key players during the pathophysiology of sCJD

Proteins having highest fold changes, peptide counts, sequence coverages in our data set belonged mainly to either metabolic pathways or oxidative stress related functions. Oxidative stress related cellular activities comprised of one of the major regulated cellular mechanisms based on our proteomic findings in both subtypes (MM1 and VV2). Along with many other proteins in this functional category of oxidative stress related cellular mechanism, DJ-1 exclusively got more of our attention due to its high peptide count (12) and the highest sequence coverage (59.3%) in our data. DJ-1 is known for its role in oxidative stress and familial form of Parkinson's disease which makes it even more interesting candidate to be analysed more in sCJD. Identification of regulated expression of DJ-1 urged us to further explore the implication of DJ-1 in particular in MM1 and VV2 subtypes of sCJD. Furthermore, oxidative stress can be one cause of the deregulations of many cellular activities including cellular metabolic pathways, signal transduction mechanisms, misfolding of proteins, mitochondrial damage and also leading to the activation of apoptotic pathways causing cell death. So, further downstream experiments were performed to elucidate the implication of DJ-1 and oxidative stress during the pathophysiology of the disease in sCJD.

5.9 Implication of oxidative stress and DJ-1 during pathophysiology of the disease in sCJD

Oxidative stress is one of the major contributors in various neurodegenerative diseases but it is less previledged during the pathophysiology of the sCJD so far. Here, we could identify oxidative stress as one of the major regulated mechanisms based on our proteomic results from MM1 and VV2 subtypes of sCJD. This implies that oxidative stress can have a major role in gearing up the pathophysiological events during the course of the disease in sCJD.

Amongst many other oxidative stress related identified proteins, DJ-1 has the highest peptide count and sequence coverage indicating its very low false discovery rate (FDR) and very high confidence of its true identifaction. DJ-1 is known for its role in protection against oxidative stress and as a sensor of oxidative stress. So we performed further experiments to elucidate the implication of DJ-1 during the pathophysiology of the disease in sCJD and its potential use as biomarker of oxidative stress.

5.9.1 Expressional regulation of DJ-1 in cerebellum of sCJD is due to oxidative stress

Immunofluorescent experiments were performed to highlight if expressional regulation of DJ-1 is due to oxidative stress specifically in cerebellum of sCJD. DJ-1 is mainly localized in the

cytosol of the cell but it is localized to mitochondrial matrix (Blackinton, J.; Lakshminarasimhan, M.; 2009) and nucleus (Su-Jeong Kim, Yun-Jong Park 2012) during oxidative stress to perform its antioxidative functions directly. Its nuclear translocalization is important for its protective function by acting as a transcriptional regulator. Immunofluorescent experiment results showed an upregulation in the expression of DJ-1 in sCJD (MM1) as compared to age matched non-demented controls. Furthermore, DJ-1 was translocalized to the nuclear region in human sCJD (MM1) (Fig. 5.11). Nuclear translocalization of DJ-1 is important for its direct protective function against oxidative stress by regulating the transcription of antioxidative genes in the nucleus. These results suggest that expressional regulation of DJ-1 in sCJD is due to the effect of oxidative stress.

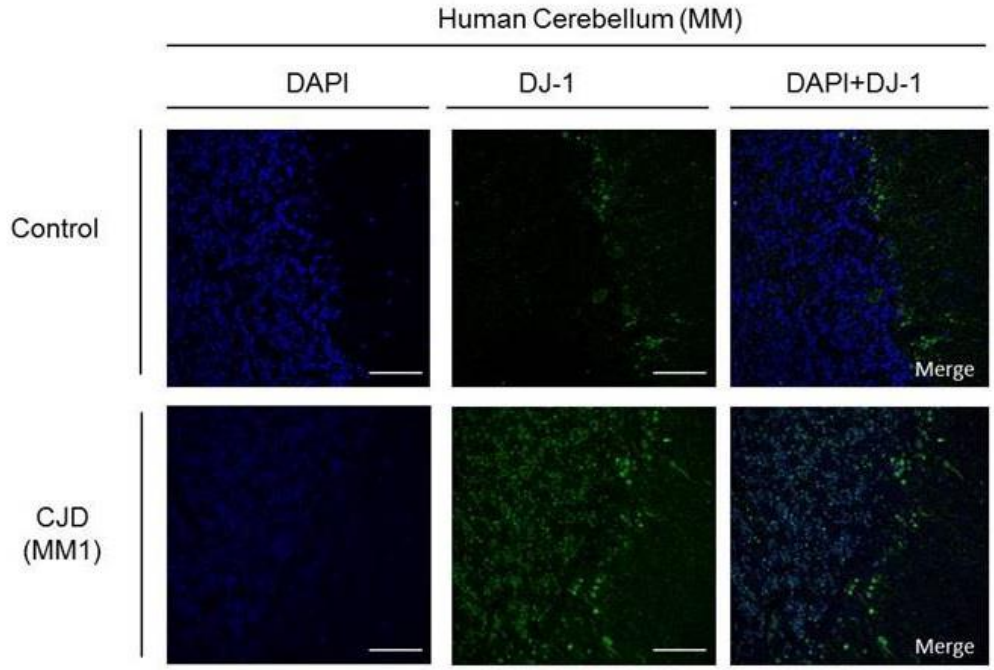

Figure 5-11: Expressional regulation and localization of DJ-1 in cerebellum of sCJD (MM1)
Immunoflourescence experiment results show upregulation of the expression of DJ-1 and its oxidative stress mediated translocalization into nucleus in cerebellum of human sCJD MM1 as compared to age matched non-demented controls using anti DJ-1 primary antibody.

5.9.2 Mechanism of action of DJ-1 in neuroprotection against oxidative stress: by regulating Nrf2/ARE pathways

One proposed mechanism of action of DJ-1 in regulating the oxidative stress is by regulation of nuclear factor erythroid derived 2 like 2 (Nrf2) signalling pathway. This regulation of Nrf2 functions by DJ-1 during oxidative stress is already reported in vitro (Cailing Liu and Yuming Chen et al., 2014), in AD brains (Stéphanie Baulac and Hope Lu et al., 2009) and in mice models of PD (Nirit Lev and Yael Barhum et al., 2015). So further experiments were performed to explore the regulation of Nrf2/ARE pathway in sCJD (MM1 and VV2 subtypes) which is reported to be mediated by DJ-1 and has an implication in protecting the cells against oxidative stress. Nrf2 is a transcription factor encoded by the *NFE2L2* gene in human (Moi et al., 1994) and is involved in regulating the expression of anti-oxidative proteins for protection against oxidative stress implied by ROS or inflammation (Itoh et al., 1997). Nrf2 is localized in cytoplasm under normal conditions in its inactive form with Keap1 which continuously degrades Nrf2 by directing Nrf2 to ubiquination. Many *in vitro* studies have shown that under the effect of oxidative stress, DJ-1 deactives Keap1 activity and Nrf2 is released from Keap1. After its release, Nrf2 is further phosphorylated which is necessary for its translocalization to nucleus for performing its downstream functions by transcriptionally activating anti-oxidative response elements (ARE) which lead to the expression of glutathione peroxidase, glutathione S transferase, heme oxygenase 1 and peroxiredoxins to protect the cell from oxidative damage.

5.9.3 Expressional analysis of Nrf2: the downstream regulator of DJ-1 during oxidative stress

Nrf2 which is reported to be a downstream regulator of DJ-1 (Clements et al., 2006a) showed a significant upregulation in its mRNA expression both in MM1 and VV2 subtypes of sCJD cases as shown in fig. 5.12 (A) indicating high cellular demand for Nrf2 to protect the cell (Clements et al., 2006a) from oxidative damage. Under normal physiological conditions, Nrf2 is continuously ubiquitinated in the cytoplasm for degradation by proteasomes as its controlling mechanism. We observed a significant decrease in the expression of ubiquitinated Nrf2 in MM1 and VV2 subtypes of sCJD as compared to age matched non-demented controls indicating that Nrf2 is not ubiquinated more in sCJD cases due to its release from Keap1 and its need by the cell under oxidative stress (Figure. 5.12 B and C).

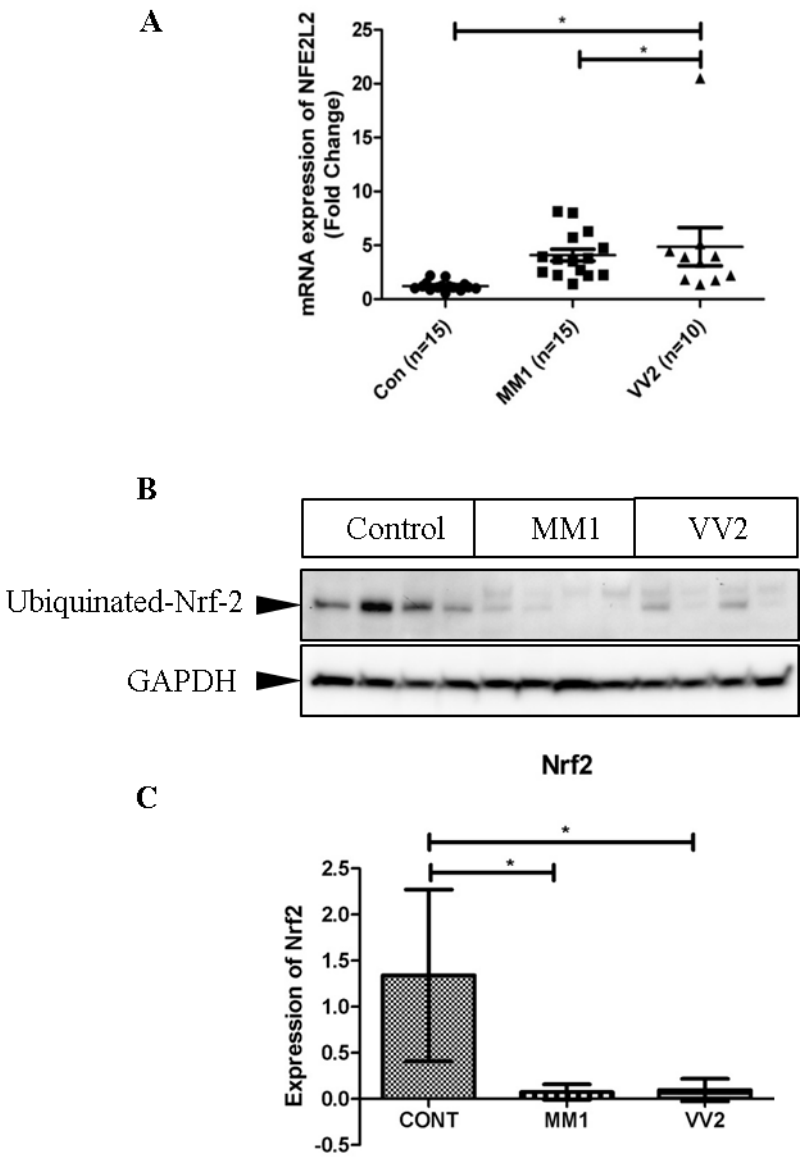

Figure 5-12: Expressional analysis of Nrf2: the downstream regulator of DJ-1 during oxidative stress in cerebellum from MM1 and VV2 subtypes of sCJD

mRNA expression of NFE2L2 using RT-qPCR in control ($n = 15$), sCJD MM1 ($n = 15$) and sCJD VV2 ($n = 10$) samples is shown. Values are normalized using GUS-b as internal control **(A)**. Western blotting of samples from MM1 (n=4) and VV2 (n=4) subtypes of sCJD along with age matched non-demented controls (n=4) from cerebellum of brain with anti Nrf2 antibody **(B)**. GAPDH was used as a loading control. Densitometeric analysis of western blot results with Nrf2 showed significant downregulation of Nrf2 expression in both MM1 and VV2 subtypes **(C)**. The statistical significance was calculated with one way ANOVA followed by Turkey post test to compare all pairs of columns. Data are represented as the mean SEM. $*p < 0.05$, $**p < 0.005$, $***p < 0.001$.

5.9.4 Phosphorylation of Nrf2 in cerebellum from MM1 and VV2 subtypes of sCJD

After release of Nrf2 from Keap1, it is phosphorylated by variety of enzymes which is necessary for its activation as well as for its nuclear translocalization (Apopa et al., 2008;Huang et al., 2002b) to perform its down stream function: which is the activation of

antioxidative genes. So further experiments were conducted to observe the expressional regulation of phosphorylated Nrf2 in MM1 and VV2 subtypes of sCJD. An increase in the expression of phosphorylated Nrf2 was observed in both MM1 and VV2 subtypes of sCJD as compared to age matched non-demented controls but its expression was significantly increased only in VV2 subtype indicating that phospho-Nrf2 is expressed more in VV2 subtype as well as in MM1 to protect the cell against oxidative stress by activating its target genes (Figure. 5.13).

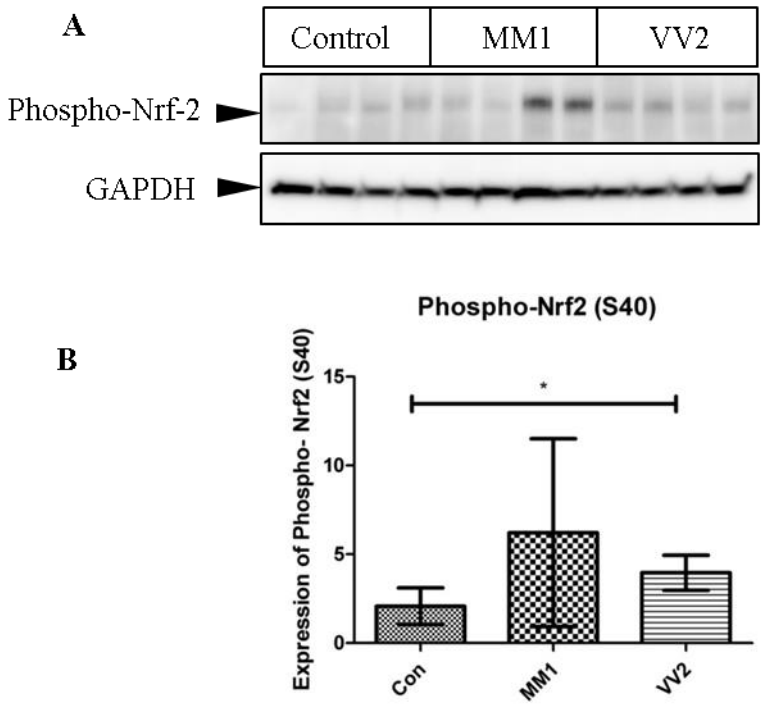

Figure 5-13: Expressional analysis of Phospho-Nrf2: the activated form of Nrf2 during oxidative stress in cerebellum from MM1 and VV2 subtypes of sCJD

Western blotting of samples from MM1 (n=4) and VV2 (n=4) subtypes of sCJD along with age matched non-demented controls (n=4) from cerebellum part of the brain with anti phospho-Nrf2 antibody. GAPDH was used as a loading control **(A)**. Densitometeric analysis of western blot with phospho-Nrf2 showed significant upregulation of Nrf2 expression in VV2 subtype **(B)**. The statistical significance was calculated with one way ANOVA followed by Turkey post test to compare all pairs of columns. Data are represented as the mean SEM. *$p < 0.05$, **$p < 0.005$, ***$p < 0.001$.

5.9.5 Activation of Anti-oxidation response elements (ARE) (the downstream regulators of Nrf2 pathway during oxidative stress)

After trans-localization into nucleus, phosphorylated Nrf2 is reported to induce the transcription of ARE in nucleus. So, we examined the expressional profile of ARE in MM1 and VV2 cases of sCJD. ARE include glutathione S transferase Mu2 (GSTM2), Glutamate Cysteine Ligase C (GCLC), heme oxygenase 1 (HO-1) and thioredoxin-dependent peroxide

reductase (Prdx3). We could also observe upregulation of glutathione S transferase Mu2 (GSTM2) and thioredoxin-dependent peroxide reductase (Prdx3) at translational level, in our proteomic data set identified with the help of MALDI-TOF MS/MS. Furthermore we examined the mRNA and protein expression of heme oxygenase 1 (HO-1), thioredoxin-dependent peroxide reductase (Prdx3) and glutathione S transferase Mu 2 (GSTM2) in MM1 and VV2 cases of sCJD. Significant upregulation for HMOX1 both at mRNA and protein level only in VV2 subtype, for PRDX3 only in VV2 subtype at mRNA level but in both subtypes (MM1 and VV2) at proetin level and for GSTM2 in both subtypes (MM1 and VV2) at mRNA level was observed. These results all together indicated the activation of ARE machinery most likely mediated by DJ-1 through Nrf2 (on the basis of previous studies as already mentioned) in response to oxidative stress in order to protect the cells against oxidative damage (Figure. 5.14 (A-C)).

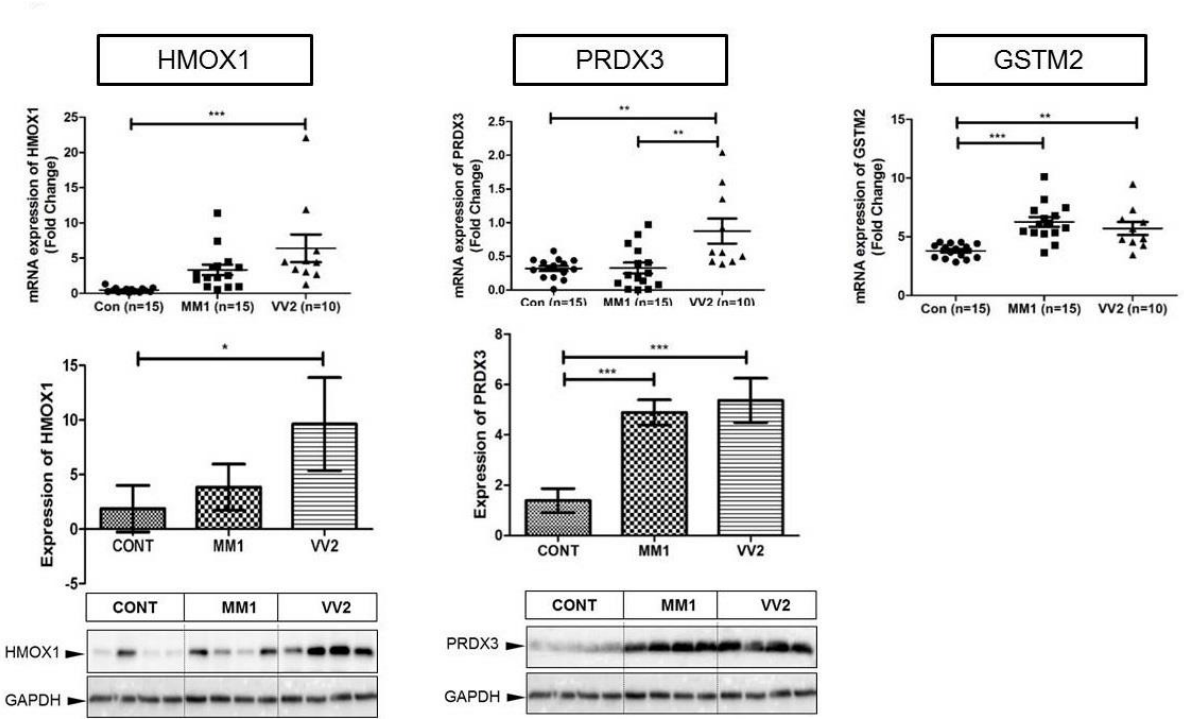

Figure 5-14: mRNA expression of Anti-oxidation response element (ARE): Heme oxygenase 1 (HO-1), Glutathione S transferase Mu 2 (GSTM2) and Thioredoxin-dependent peroxide reductase (Prdx3) the downstream regulator of Nrf2 pathway

RT-qPCR analysis of HMOX1 **(A)** GSTM2 **(B)** and PRDX3 **(C)** in control ($n = 15$), sCJD MM1 ($n = 15$) and sCJD VV2 ($n = 10$) samples is shown. Values are normalized using GUS-b as internal controls. The statistical significance was calculated with one way ANOVA followed by Turkey post test to compare all pairs of columns. Data are represented as the mean SEM. *p <0.05, **p <0.01, ***p <0.001.

5.9.6 Expressional regulation of DJ-1 in cerebellum of mice model of CJD

Immunofluorescent experiments with cerebellum of mice model of CJD (MM1) along with its age matched controls were performed to highlight expressional regulation of DJ-1 in cerebellum of mice model of CJD. Immunofluorescent experiment results showed an upregulation in the expression of DJ-1 in cerebellum of mice model of CJD (MM1) as compared to age matched controls like in human cerebellum of sCJD (MM1) cases. Furthermore, DJ-1 was more localized in the nuclear region (Fig. 5.15) similarly to human cerebellum of sCJD (MM1) cases. Nuclear translocalization of DJ-1 is important for its direct protective function against oxidative stress by regulating the transcription of antioxidative genes in the nucleus. These results suggest that expressional regulation of DJ-1 in cerebellum of mice model of CJD (MM1) is due to the effect of oxidative stress and is similar to that of human cerebellum of sCJD (MM1) cases.

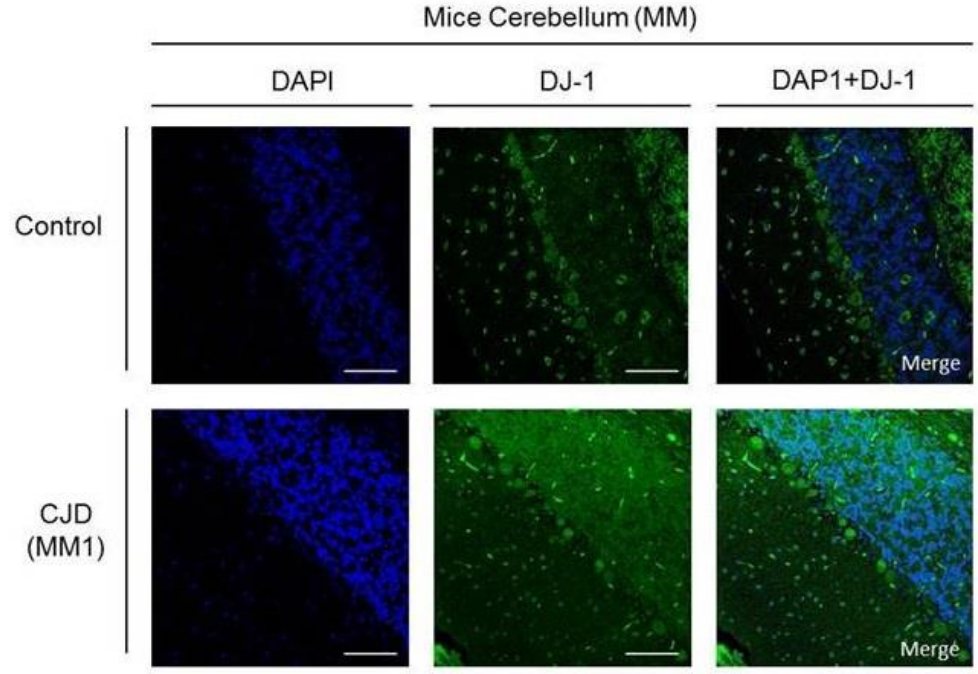

Figure 5-15: Expressional regulation and localization of DJ-1 in cerebellum of mice model of CJD (MM1)
Immunoflourescence experiment results show upregulation of the expression of DJ-1 and its oxidative stress mediated translocalization into nucleus in cerebellum of mice CJD (MM1) at 183 dpi as compared to age matched controls using anti DJ-1 primary antibody.

5.10 DJ-1 as a sensor of oxidative stress during early progression of sCJD

DJ-1 is also known as sensor of oxidative stress (Ariga et al., 2013). To elucidate its role as a sensor of oxidative stress in sCJD specifically, further experiments were performed to examine the expression of DJ-1 at pre-symptomatic, symptomatic and late symptomatic stages of disease in mice models of sCJD.

5.10.1 Expression of DJ-1 at presymptomatic and symptomatic stage in sCJD MM1 and VV2 mice models

In order to evaluate the expressional regulation of DJ-1 during the progression of disease, mice models of sCJD both with MM1 and VV2 genotype (at codon 129 of *PRNP* gene) were used. Western blot results showed a significant upregulation in the expression of DJ-1 in the cerebellum of sCJD MM1 mice at pre-symptomatic stage as compared to age matched healthy controls. DJ-1 expression was decreased during early-symptomatic stage but again started to rise during late-symptomatic stage in MM1 subtype as compared to its expression at pre-symptomatic stage (Fig. 5.16 A). But expression of DJ-1 remains higher at all stages of the disease right from the beginning of disease progression as compared to the corresponding healthy controls. Similarly, DJ-1 expression in the cerebellum of sCJD VV2 mice was also significantly upregulated during early-symptomatic stage as compared to healthy controls whereas DJ-1 expression was decreased during both symptomatic and late-symptomatic to terminal stages as compared to its expression at pre-symptomatic stage (Fig. 5.16 B). But expression of DJ-1 remained significantly higher at all stages of the disease right from the pre-symptomatic stage, during the progression of disease as well as at late pre-symptomatic stage as compared to the corresponding healthy controls.

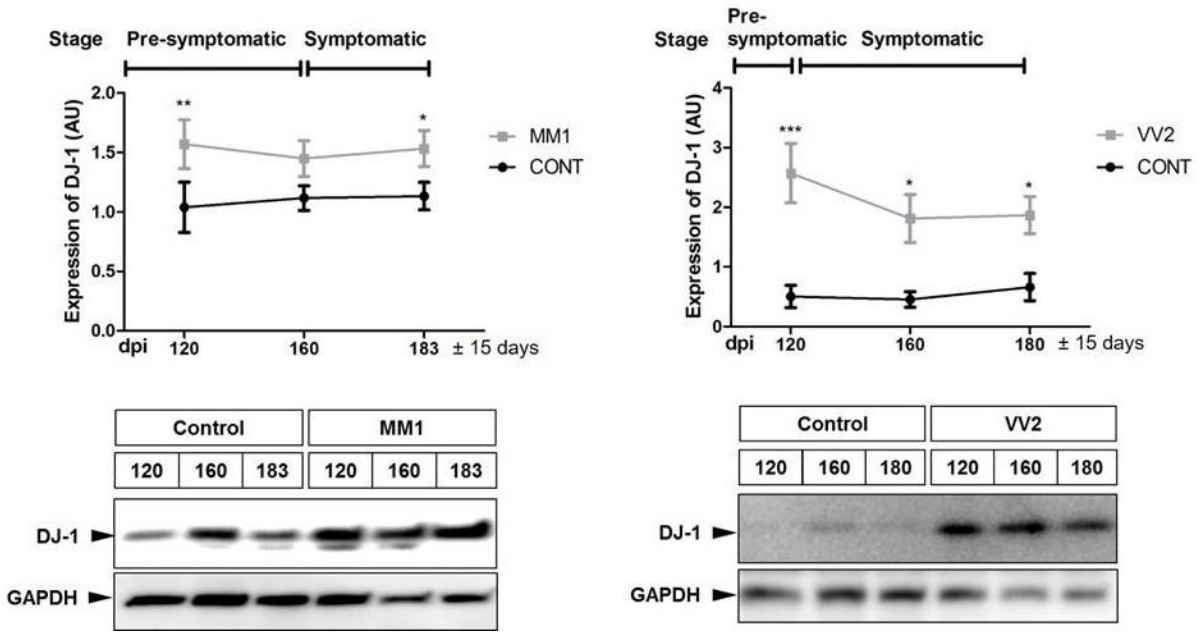

Figure 5-16: Expression of DJ-1 at pre-symptomatic and symptomatic stage in sCJD MM1 and VV2 mice models

Double transgenic mice Tg340/ Tg361 PrP knock out and expressing 4 fold expression of humanized PrP with either methionine or valine at codon 129 of PrP were inoculated with 10% brain homogenate from sCJD patient either from MM1 or VV2 subtype to develop MM1 and VV2 mice models of sCJD respectively. Mice were sacrificed and brain samples were collected at 120 days post inoculation (dpi)

for pre-symptomatic stage, at 160 dpi for early symptomatic stage and at 183 dpi for late symptomatic stage (in case of MM1 mice model) and at 120 dpi for early-symptomatic, at 160 dpi for symptomatic and at 180 dpi for late symptomatic to terminal stage (in case of VV2 mice model) due to early development of disease in VV2 mice model. DJ-1 expression in cerebellum of sCJD-MM1 mice model with controls (n=3) and MM1 (n=3) for each time point **(A)** and sCJD-VV2 mice model with controls (n=4) and VV2 (n=4) for each time point **(B)** was observed by Western blot analysis using DJ-1 antibody and densitometry analysis from three (for MM1 mice model of sCJD) and from four (for VV2 mice model of sCJD) independent (±SD) western blotting experiments. GAPDH was used as a loading control. The statistical significance was calculated with two way ANOVA. Data are represented as the mean SEM. $*p < 0.05$, $**p < 0.005$, $***p < 0.001$.

5.10.2 Expression of DJ-1 during clinical phase of sCJD in CSF samples of sCJD patients

Production of toxins, misfolded and over-expressed proteins in various parts of brain in different neurodegenerative diseases is cleared from the brain by Glymphatic system resulting in the secretion of these toxins, misfolded and overexpressed proteins in Cerebrospinal fluid (CSF). So CSF can be very important for diagnostic point of view in that it can reflect pathophysiological events going on inside the brain during the clinical phase of any neurodegenerative disease.

To highlight the role of DJ-1 as a sensor of oxidative stress during the clinical phase of the disease in human sCJD cases, protein expression of DJ-1 was examined in clinical CSF samples of MM1 and VV2 subtypes of sCJD patients. Western blot experiments with clinical CSF samples showed high protein expression of DJ-1 during the clinical phase of sCJD in MM1 and VV2 subtypes. Expression of DJ-1 was significantly increased in CSF samples of VV2 subtype of sCJD as compared to age matched non-demented controls. No significant upregulation was observed in case of MM1 subtype of sCJD cases indicating the secretion of overexpressed DJ-1 from cerebellum of only VV2 subtype into CSF as well (Fig. 5.17). Due to the less number of samples and low sensitivity of western blot, no significant differences could be found in MM1 subtype.

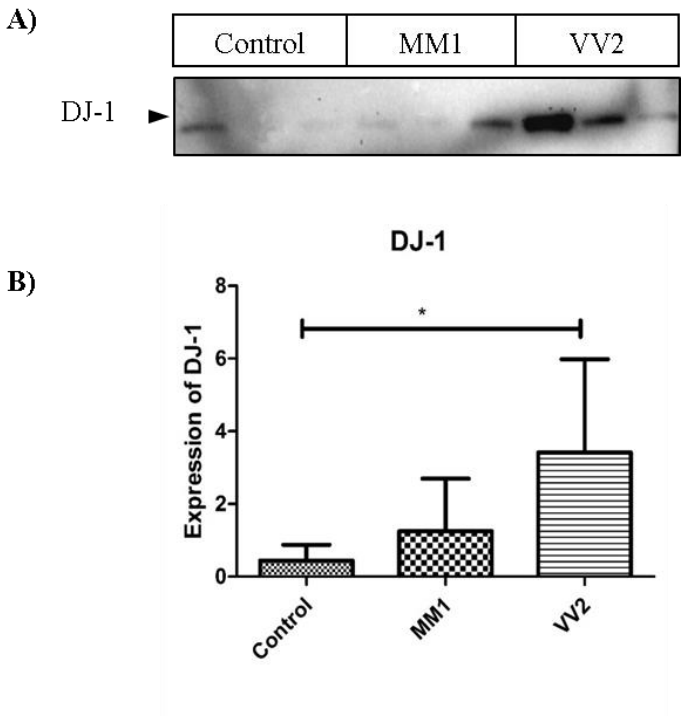

Figure 5-17: Western blot results showing protein expression of DJ-1 in clinical samples of CSF from MM1 and VV2 subtypes of sCJD patients

Western blot analysis of DJ-1 in control ($n = 3$), sCJD MM1 ($n = 3$) and sCJD VV2 ($n = 3$) shows upregulation of DJ-1 in CSF samples of VV2 subtype as compared to the CSF samples from age matched non-demented controls **(A)**. Densitometeric analysis of DJ-1 western blot in CSF samples of MM1 and VV2 subtype shows a significant increase in the expression of DJ-1 in VV2 subtype of sCJD **(B)**. Statistical significance was calculated by unpaired Student's T test. $*p < 0.05$, $**p < 0.005$, $***p < 0.001$.

Higher expression of DJ-1 during the clinical phase of sCJD revealed the presence of oxidative stress during the clinical stage of the disease and its expression in CSF flares up the idea of its use as a biomarker of oxidative stress and hence relevance to the disease progression in sCJD. For elucidation of this idea, a highly sensitive electrochemiluminescence (ECL) based ELISA was performed which can detect even very low expression of DJ-1. To see the variation in the expression of DJ-1 between MM1 and VV2 subtypes in a broader range, study cohort of clinical CSF samples from sCJD patients (MM1 and VV2 subtypes) was increased up to eighteen. Similar results were observed with ECL based ELISA showing significant upregulation of DJ-1 in both MM1 and VV2 subtypes of sCJD cases as compared to age matched non-demented individuals (Fig. 5.18).

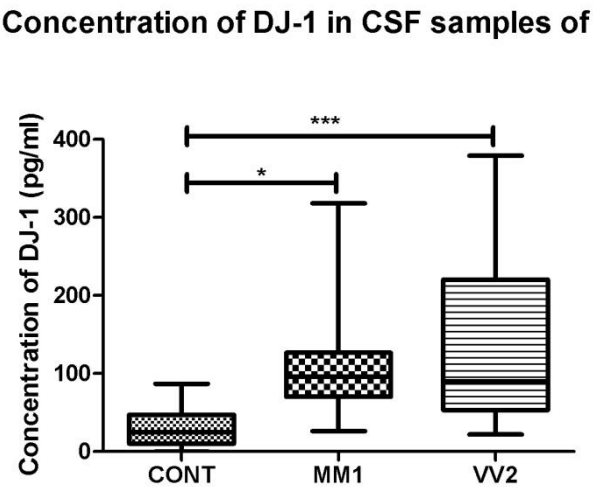

Figure 5-18: ELISA results showing protein expression of DJ-1 in clinical samples of CSF from MM1 and VV2 subtypes of sCJD patients

Analysis of DJ-1 expression with the help of highly sensitive ECL-based ELISA in control ($n = 18$), sCJD MM1 ($n = 18$) and sCJD VV2 ($n = 18$) shows significant upregulation of DJ-1 in CSF samples of VV2 subtype as compared to the CSF samples from age matched non-demented controls. Densitometeric analysis of DJ-1 concentration in CSF samples of MM1 and VV2 subtype shows a significant increase in the expression of DJ-1 in both MM1 and VV2 subtypes of sCJD. The statistical significance was calculated with one way ANOVA followed by Turkey post test to compare all pairs of columns. $*p < 0.05$, $**p < 0.005$, $***p < 0.001$.

5.10.2.1 Regulation of oxidative stress mediated DJ-1 expression in clinical CSF samples from sCJD (MM1 and VV2 subtypes) patients is not age dependent

Our various experimental results showed that pronounced oxidative stress is involved in regulating DJ-1 expression in cerebellum of brain from sCJD (MM1 and VV2 subtypes) patients. Oxidative stress can arise due to multiple factors. One of these can be aging, which also leads to the development of oxidative stress in brain (Romano et al., 2014). In order to find if oxidative stress mediated expressional regulation of DJ-1 in sCJD (MM1 and VV2) patients is correlated with the age of patients, an analysis was performed to find out if there is any correlation between clinical CSF DJ-1 expression and age of patients. Correlation analysis indicated a weak positive relationship between clinical CSF DJ-1 expression and age of patients. This indicates that regulation in the DJ-1 expression in sCJD (MM1 and VV2) patients is not merely due to the effect of age but it is more as a result of pathophysiological process in sCJD (Fig. 5.19).

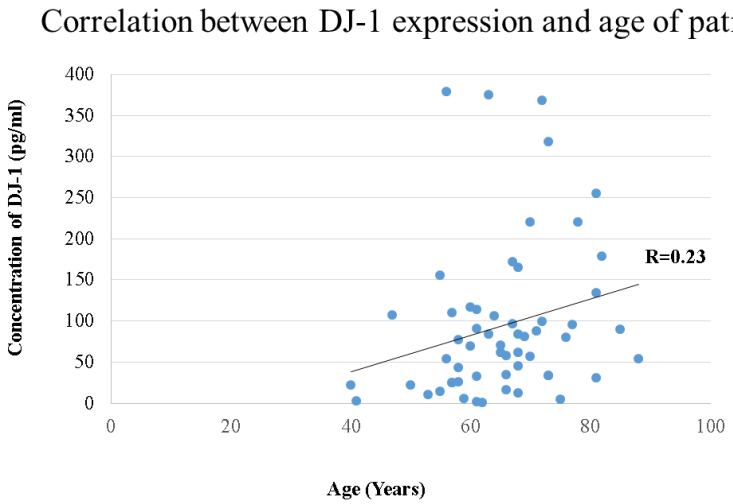

Figure 5-19: Correlation analysis between DJ-1 expression in clinical CSF samples of sCJD (MM1 and VV2) patients and age of the patients

Correlation analysis between DJ-1 expression in clinical CSF samples from sCJD (MM1 and VV2 subtypes) patients with age of the patients indicated a weak correlation between two parameters (as value of correlation coefficient was (R) = 0.23 which represents a weak positive correlation between two parameters under investigation). This weak correlation defines that oxidative stress mediated expression regulation of DJ-1 in clinical CSF samples from sCJD (MM1 and VV2) patients is not merely due to the phenomenon of aging but due to pathophysiological events going on in the brain.

All of these downstream experiments based on regulated proteomic data show the global expression of anti-oxidative proteins during the progression of the disease in sCJD indicating the presence of pronounced oxidative stress in MM1 and VV2 subtypes of sCJD. This data also highlight that DJ-1 can be a good sensor of oxidative stress even during early stages of disease.

6 Discussion

After the discovery of prions by Stanley Benjamin Prusiner in 1982, there are lots of theories/ explanations published about the pathophysiology of prion diseases and misfolding of cellular prion protein resulting in the formation of scrapie form of prion protein; the pathogenic form (Linden et al., 2008). But many years after the discovery of the etiological agent, we are still not able to discover the disease initiating factors/ conditions leading to the misfolding of a salutary protein. Misfolding of PrP^{C} leads to loss of its large number of physiological functions and resulting in the gain of number of toxic functions by its detrimental form (Linden et al., 2008). In order to explore the underlying pathophysiological mechanisms, identification of proteome wide alterations during the course of disease can be helpful in adding more to the existing knowledge and understanding of the pathophysiology of disease, sCJD in this case.

This study was planned in order to find whole proteomic regulations in two most prevalent subtypes (MM1 and VV2) of sCJD. Identified proteins are assigned to particular functional groups based on their molecular or biological functions (based on the information from UniProt database). Proteomic findings in this project indicate that almost all the cellular molecular mechanisms are impaired during the course of the disease. Pathological events are found more severe in cerebellum part of brain in case of VV2 subtype as compared to MM1 subtype, giving a notion that codon 129 genotype of *PRNP* gene and PrP type determine the region of brain for pathological events to occur.

Here function of each identified regulated protein is discussed to carefully understand the mechanism of disease pathology.

6.1 Cell cycle, gene expression and cell death

Cell cycle: Gene expression and Cell death related functions include cellular activities regulating the expression of various genes and apoptotic pathways. This group of functions is the most regulated molecular mechanism based on number of regulated proteins related to this category of functions. 24% of identified proteins in MM1 subtype and 27% of identified proteins in VV2 subtype belong to Cell cycle: Gene expression and Cell death related functions.

This group includes Staphylococcal nuclease domain-containing protein 1 (SND1) which is an important part of RNA-induced silencing (RISC) complex (Tsuchiya et al., 2007) and has a vital role in the post-transcriptional expressional regulation of various genes by regulating the miRNA function. Elongation factor 1-alpha 1 has a role in ubiquitous expression of proteins by recruiting aminoacyl-tRNA to 80S ribosome (Becker et al., 2013) and also in translocalization of proteins into nucleus (Khacho et al., 2008). Both of these proteins are found downregulated in MM1 subtype.

Phenylalanine-tRNA ligase beta subunit is found upregulated in MM1 subtype. It is responsible for biosynthesis of aminoacyl-tRNA. This is known as charging of tRNA with amino acid. Once the tRNA is charged then ribosome can transfer the amino acid from tRNA to the growing peptide so it is important for translation process.

Apoptosis-inducing factor 1 leads to programmed cell death during cellular stress conditions by triggering chromatin condensation and fragmentation of DNA (Ye et al., 2002) and Far upstream element-binding protein 1 also has a role in regulating cell proliferation and apoptosis (Zhang and Chen, 2013). Both of these proteins are found upregulated in MM1 subtype.

NADH dehydrogenase (ubiquinone) 1 alpha sub complex subunit 10 which is an important enzyme of cellular respiration in mitochondria (Nakamaru-Ogiso et al., 2010), is downregulated in MM1 subtype.

Proteins related to the processing of pre-mRNA, its packing into heterogeneous nuclear RNA (hnRNA) and then transport to cytoplasm for its expression include Heterogeneous nuclear ribonucleoproteins A2/B1, Heterogeneous nuclear ribonucleoprotein A1 and Heterogeneous nuclear ribonucleoprotein A3 and are found downregulated commonly in both subtypes of MM1 and VV2. ELAV-like protein 4 and TAR DNA-binding protein 43 are two other proteins found commonly downregulated in both subtypes. ELAV-like protein 4 is important for brain development (Bolognani and Perrone-Bizzozero, 2008) and plays its role by binding to AU rich element of mRNA thus enhancing the half-life of the transcript (Perrone-Bizzozero and Bolognani, 2002) and TAR DNA-binding protein 43 has a role in the regulation of translational process due to its ability to bind both DNA and RNA and pre-mRNA splicing. Hyperphosphorylation, ubiquitination and cleavage of TDP-43 is reported to have a role in the pathological events in frontotemporal dementia (with positive ubiquitin and negative tau and

alpha synuclein expression) and also in Amyotrophic lateral sclerosis (ALS) (Neumann et al., 2006).

Alpha-synuclein has a role in maintaining spatial learning and memory. In its aggregated form, it is also found in lewy bodies which is characteristic feature of PD, Heat shock protein beta-1 has a chaperone activity, protects the cells from thermal shock thus inhibits apoptosis and regulates cellular development. Both of these proteins are found upregulated in VV2 subtype.

Serum albumin, has a role in maintaining oncotic pressure of plasma, transport of hormones, fatty acids and drugs (Ha and Bhagavan, 2013). CSF/serum ratio of serum albumin predicts the CSF-blood permeability used as marker of blood brain barrier integrity (Andersson et al., 1994). (Sokrab et al., 1989) have reported the extravasation of serum albumin into neurons in the rat models of epileptic seizers. Proteasome subunit alpha type-1 has a role in protein turn over. Both of these proteins are identified as upregulated in VV2 subtype.

SAP domain-containing ribonucleoprotein is implicated in transcriptional and translational activities of the cell by its affinity to bind single stranded as well as double stranded DNA and it is identified as down regulated in VV2 subtype of sCJD.

Cytochrome c1 is a member of electron transport chain in mitochondria and its translocalization to cytoplasm potentiate mitochondrial apoptosome thus activating caspases in mitochondria (Adrian et al., 2001) and Myeloid leukemia factor 2 has a role in transcriptional regulation (Martin-Lanneree et al., 2006) and interacts with many other proteins like 14-3-3 zeta. Both of these proteins are upregulated in VV2 subtype.

This group of functions unveils the candidate proteins which lead to dysregulation of gene expression in the pathophysiology of sCJD by variety of ways including dysregulation at the level of mRNA synthesis, maturation of mRNA, protein synthesis and silencing of gene expression by miRNAs, ubiquitination and phosphorylation. Furthermore candidate proteins which regulate gene expression by activation of apoptotic pathways resulting in fragmentation of DNA. Nuclear transfer of proteins can be also important for the expression of many genes in the nucleus which is also found dysregulated in the pathophysiology of sCJD.

6.2 Cellular stress response/ Oxidative stress

Cellular stress response/ Oxidative stress related functions are the second most regulated molecular functions based on number of regulated proteins related to this category of functions. 22% of identified proteins in MM1 subtype and 25% of identified proteins in VV2 subtype belong to cellular stress response/ Oxidative stress related functions. Most of the proteins identified in this group are involved in the regulation of oxidative stress related functions.

Dihydrolipoyl dehydrogenase which can lead to production of ROS in mitochondria (Tahara et al., 2007) and Glutamine synthetase which has a role in detoxifying brain ammonia in astrocytes (Tumani et al., 1999) are found downregulated in MM1 subtype.

Under the effect of oxidative damage, Apoptosis-inducing factor 1 induces caspase independent programmed cell death (Yuste et al., 2005) and Complement C3 leads to production of inflammatory cytokines (Heese et al., 1998;Sayah et al., 1999). Both of these proteins are found upregulated in MM1 subtype.

N(G)-dimethylarginine dimethylaminohydrolase 1 is found upregulated in MM1 subtype and has a role in modulating NO production and cell proliferation by metabolizing asymmetric dimethyl arginine (ADMA) which is an inhibitor of nitric oxide synthase (NOS). Higher levels of DDAH1 indicate not only presence of NO but also its efforts in eliminating cellular NO levels (Zhang et al., 2011;Zhang et al., 2013).

Isocitrate dehydrogenase [NAD] subunit alpha (IDH1) indirectly plays a protective role during oxidative stress by producing NADPH (Molenaar et al., 2014), L-lactate dehydrogenase B chain is highly expressed in response to many kinds of tissue damages, Protein NDRG4 provides protection against neuronal cell death implicated by cellular stress conditions like ischemic stress (Zhou et al., 2001), Fructose-bisphosphate aldolase C protects the cells by producing ATPs and triggering glycolytic pathways (Owen et al., 2008) and Superoxide dismutase 1 protects the cells against ROS. All of these proteins are found upregulated in MM1 subtype.

X-ray repair cross-complementing protein 6, which repairs the damage in DNA caused by ROS (Vidal et al., 2001), Heat shock protein 75 kDa which stabilizes the mitochondrial function under stress conditions, Electron transfer flavoprotein subunit alpha which is

responsible for mitochondrial energy metabolism under stress are found downregulated in VV2 subtype.

Whereas Dehydrogenase/reductase SDR family member 11 and Glutathione S-transferase Mu 2 which have role in detoxifying ROS, Persulfide dioxygenase ETHE1 which catalyses the oxidation of H_2S in mitochondria: a reactive sulphur specie which is toxic for the cell, Dihydropteridine reductase implicates its reducing nature to perform oxidoreductive functions, Heat shock protein beta-1 which prevents the misfolding of proteins in response to oxidative stress (Di et al., 2010), Peroxiredoxin-6 who serves as an antioxidative enzyme during oxidative stress (Power et al., 2008), Thioredoxin-dependent peroxide reductase which is known to protect the cell against oxidative stress (Silva-Adaya et al., 2014), and Protein DJ-1 which is a sensor of oxidative stress and protects the cell against oxidative stress (Baulac et al., 2009) are all upregulated in VV2 subtype of sCJD.

This group of molecular functions reveals the presence of reactive sulphur species along with ROS and RNS which lead to multiple toxic mechanisms in the brain. Presence of ammonia which comes due to the breakdown of amino acids can also be toxic for the other cells.

6.3 Signal transduction and synaptic functions

Signal transduction and synaptic functions include the cellular activities involved in relay of signals/ information between different types of cells or neurons in the brain. This group of functions is the third most regulated molecular mechanism based on number of regulated proteins related to this category of functions. 15% of identified proteins in MM1 subtype and 18% of identified proteins in VV2 subtype belong to signal transduction and synaptic functions.

This group includes, Complement C3; which leads to the activation of many cellular responses/signals (Moller et al., 1997) and synthesis of cytokines (Sayah et al., 1999) and Protein kinase C delta-binding protein belongs to the family of enzymes which is involved in the regulation of processes like signal transduction in the brain (Nishizuka, 1986). Both of these proteins are upregulated in MM1 subtype.

Beta-centractin is a macromolecule responsible for transport from endoplasmic reticulum to Golgi and also for lysosomal, endosomal, nuclear, chromosomal movement and formation of spindles. Glutamine synthetase is an enzyme involved in the synthesis of glutamine which is an important amino acid serving as a potent source of nitrogen as a source for biosynthesis of nucleic acid and proteins (Wedler and Horn, 1976). Excessive ammonia and glutamate in the

brain is neurotoxic for neurons. Astrocytes take up excessive ammonia and glutamate from brain tissue and protect neurons against potentially neurotoxic glutamate and ammonia by converting into glutamine with the help of glutamine synthetase. In the presence of high ammonia in the brain tissue, astrocytes swell up (Tumani et al., 1999;Tumani et al., 2000). Both of these proteins are downregulated in MM1 subtype.

Three proteins are found commonly regulated in both subtypes of MM1 and VV2 belonging to signal transduction and synaptic functions. These include i)- Guanine nucleotide-binding protein G(o) subunit alpha, which is a signal transducing protein transmitting signals from the exterior of cell to its interior (Eaton et al., 2012). ii)- Protein phosphatase methylesterase 1, inhibits the activity of Protein phosphatase 2A (PP2A) resulting in inhibition of cell proliferation and metastasis. PPME1 is considered to have a role in regulate the Wnt signaling as well (Wandzioch et al., 2014). Both of these proteins are downregulated in both subtypes. iii)- Syntaxin binding protein 1 is another commonly found protein but identified as upregulated in MM1 subtype and downregulated in VV2 subtype. It is implicated in fusion of synaptic vesicles due to its strong binding ability with syntaxin (Rizo and Sudhof, 2002).

Proteins related to signal transduction and synaptic function identified in VV2 subtype include Hypoxanthine-guanine phosphoribosyl transferase, which has a role in brain development by transferring phosphoribosyl to purines thus generating purine nucleotides, Transforming protein RhoA, which has a role in signal transduction by regulating the polymerization of actin filaments and Purine nucleoside phosphorylase, regulates nucleotide salvage pathway. All of these proteins are identified as upregulated in VV2 subtype.

Voltage-dependent anion-selective channel protein 2 has a role in transduction of signaling cascades leading to the mitochondrial death during oxidative stress (Shoshan-Barmatz et al., 2006) and Phosphatidylinositol transfer protein alpha isoform has a role in transportation of phosphoinositoles in different intracellular compartments for both trafficking and signaling purpose when needed (Hsuan and Cockcroft, 2001). Both of these proteins are identified as downregulated in VV2 subtype.

6.4 Metabolic Pathways

Proteins involved in various metabolic activities like mainly in carbohydrate metabolism and energy metabolism are regulated more in MM1 subtype based on the number of proteins related to this functional category as compared to VV2 subtype.

6.4.1 Carbohydrate metabolism

Hexokinase-1, Pyruvate kinase PKM (Pyruvate kinase is a glycolytic enzyme and catalyzes the interconversion of phosphoenolpyruvate to pyruvate which serves as a source of net energy), Alpha-enolase and Fructose-bisphosphate aldolase C are the enzymes of glycolysis process and all of these enzymes are found downregulated in MM1 subtype. Transaldolase is another important enzyme during carbohydrate metabolism is found upregulated in MM1 subtype.

Triosephosphate isomerase is the only enzyme related to carbohydrate metabolism found regulated in VV2 subtype. It is an enzyme of glycolysis process and is found upregulated in VV2 subtype.

6.4.2 Energy metabolism

Energy metabolism related proteins include upregulated L-lactate dehydrogenase B in MM1 subtype which is responsible for interconversion of pyruvate and lactate during low levels of oxygen and this process is implicated as source of energy.

Three proteins related to energy metabolism are identified to be downregulated commonly in both subtypes and they include Dihydrolipoyllysine-residue succinyltransferase component of 2-oxoglutarate dehydrogenase complex which is involved in the catabolism of Lysine to acetyl CoA with the help of saccharopine having implication in energy metabolism, Creatine kinase B-type which is responsible for the transfer of phosphate group between creatine and phospho-creatine for production ATPs during the periods of energy demand (Schmid et al., 2006) and Succinyl-CoA ligase [ADP-forming] subunit beta which is an important enzyme of tri-carboxylic acid cycle (TCA) in mitochondrial which is implicated in energy production in the form of ATPs, is found downregulated commonly in both subtypes of MM1 and VV2.

6.5 Cell growth, proliferation and differentiation

Cell growth, proliferation and differentiation related functions include 6% of identified proteins in MM1 subtype and 5% of identified proteins in VV2 subtype.

In this group of functions, Immunoglobulin superfamily member 8 which can have a role in regulating neurite outgrowth and neural network and Transketolase which is an important enzyme of pentose phosphate pathway having a role in producing nicotinamide adenine dinucleotide phosphate (NADPH) for biosynthesis of fatty acid, cholesterol, neurotransmitter,

nucleotides and pentose sugar, are found upregulated in MM1 subtype. Protein NDRG4 which has a role in neuronal differentiation (Nakada et al., 2002).

Palmitoyl-protein thioesterase 1 is an enzyme responsible for deacylation of proteins which are palmitoylated. PPT1 deficiency results in apoptosis of cortical neurons (Cho and Dawson, 2000). Protein L-isoaspartate(D-aspartate)O-methyltransferase has its role in methylation of proteins having its implication in the maintenance of CNS function and growth (Yamamoto et al., 1998). Both of these proteins are identified as upregulated in VV2 subtype.

6.6 Intracellular transport and cytoskeleton

Intracellular transport and cytoskeleton refers to complex network of tubules and filaments which not only maintains the integrity and shape of cell but also facilitates the intracellular trafficking. Proteins regulating intracellular transport and cytoskeleton include 9% of identified proteins in MM1 subtype and 7% of identified proteins in VV2 subtype.

Mitochondrial import receptor subunit TOM70 is involved in import of precursor proteins of mitochondria. Septin-6 belongs to the family of septins which are highly expressed in brain and are found involved in many nervous disorders like PD and AD (Ihara et al., 2007;Kinoshita et al., 1998a;Kinoshita et al., 1998b). Septins are important for their role in cell division (Surka et al., 2002a;Surka et al., 2002b), apoptotic pathways, vesicle trafficking, cytoskeletal arrangement and cell polarity (Kinoshita, 2006). Vacuolar protein sorting-assoc. protein VTA1 homolog has a role in degradation of membrane proteins in lysosomes. All of these proteins are found upregulated in MM1 subtype.

In this group of functions, Cytoplasmic Actin 1; a well-known cytoskeleton protein is commonly downregulated in both subtypes of MM1 and VV2.

Actin-related protein 2/3 complex subunit 2 is an important regulator of organization of actin filaments (Mathur et al., 2003), Pyridoxal phosphate phosphatase which has a cofilin dependent role in reorganization of actin cytoskeleton. Both of these proteins are downregulated in VV2 subtype.

6.7 Others

Some of the proteins which are not able to be assigned any specific molecular function remain unclassified and are placed in this group. This group contains upregulated N-acetyl-D-glucosamine kinase and downregulated Methionine adenosyltransferase 2 subunit beta identified in MM1 subtype.

Whereas Isochorismatase domain-containing protein 1 and S-formylglutathione hydrolase are found downregulated in VV2 subtype while Phospholysine phosphohistidine inorganic pyrophosphate phosphatase and Delta(3,5)-Delta(2,4)-dienoyl-CoA isomerase are identified as upregulated in VV2 subtype.

All these regulated proteins show a global dysregulation in the molecular cellular functions of the cells in sCJD which indicates a wide devastation in brain demanding for further addressing of each regulated molecular phenomenon. In this regard, we further discuss the oxidative stress related cellular activities which are found significantly regulated in sCJD in this study.

6.8 Implication of oxidative stress (OS) in sCJD (As one of the major regulated cellular mechanisms)

Oxidative stress refers to an imbalance of the equilibrium between the levels of ROS and cellular potential to detoxify these reactive intermediates, leading to perilous condition contributing to cellular and molecular damage. The presence of OS can be estimated in three ways: i)- directly by estimation of the ROS ii)- indirectly by estimating the damage caused by OS to biomolecules and iii)- indirectly by measuring the anti-oxidative response (level of anti-oxidants) in the cell. First way that is direct estimation of ROS is quite challenging due to higher instability of ROS. For this reason, last two ways are mostly followed in the research. We could also identify OS as one of the major regulated molecular mechanism during the pathophysiology of sCJD based on the presence of higher number of proteins related to oxidative stress related mechanism of the cell. Functional classification of proteomic data also indicated the presence of pronounced level of OS based on oxidative stress related molecular functions as one of the major regulated cellular mechanism. OS in a cell can deregulate many of cellular functions like deregulation of metabolic pathways, impairment of energy producing machinery of cell, signal transduction, activation of apoptotic pathways, misfolding of proteins as well as aggregation of proteins. So OS can be assumed as one of the major contributors to the progression of disease pathology in sCJD. For this reason, we decided to explore the role of OS in sCJD and also because the phenomenon of OS has been an area of less focus during the pathophysiology of sCJD as compared to Alzheimer's diseases (AD), Parkinson's diseases (PD) and Amyotrophic Lateral Sclerosis (ALS).

6.9 Role of DJ-1 in sCJD during OS

Protein deglycase (DJ-1) is one of the proteins found regulated relating to cellular stress conditions in our proteomics data set. Amongst all the proteins related to cellular stress conditions, DJ-1 has the highest peptide count (12) and sequence coverage (59,3%). It is found significantly upregulated both at mRNA and protein levels in both MM1 and VV2 subtypes of sCJD cases. Further exploration of OS based on DJ-1 role in OS in sCJD strengthens the hypothesis of presence of pronounced level of OS in sCJD. DJ-1 is known as a sensor of OS and for its role in protection against OS. Genetic mutation in DJ-1 gene (PARK7) is implicated in the early onset of familial form of Parkinson's disease. It has a conserved sequence throughout the evolution. DJ-1 implicates its neuroprotective function by regulating anti-oxidative, anti-apoptotic and anti-inflammatory pathways (Kahle et al., 2009). Many cellular mechanisms can potentiate the neuroprotective functions of DJ-1. During

oxidative stress DJ-1 acts as an ROS quencher, resulting in shift to its more acidic form due to oxidation at its Cys 106 residue and trans-localization to mitochondria as well as nucleus from the cytoplasm (Canet-Aviles et al., 2004;Junn et al., 2009). Oxidation of DJ-1 at Cys 106 residue to sulfinic acid is critical for DJ-1 to play its neuroprotective role by interacting with other proteins (Kato et al., 2013). But role of Cys 106 oxidation of DJ-1 in its nuclear trans-localization still remains unclear (Blackinton et al., 2009;Canet-Aviles et al., 2004;Junn et al., 2009). DJ-1 also functions as molecular chaperone during oxidative-stress by up-regulating HSP70, which prevents aggregation of alpha-synuclein and hence cell death by binding and stabilizing alpha-synuclein (Huang et al., 2006;Klucken et al., 2004;Zhou et al., 2006). So alpha-synuclein mediated cellular toxicity and aggregation is inhibited when DJ-1 is highly expressed in dopaminergic neurons (Zhou and Freed, 2005). Vesicular mono amine transporter-2 (VMAT2) is a protein responsible for the transport of neurotransmitters at synapses. VMAT2 also keeps cytoplasmic dopamine levels in control by storing the neurotransmitter in synaptic vesicles. DJ-1 increases cellular resistance against dopamine toxicity by upregulating the expression of VMAT2 (Ishikawa et al., 2012;Lev et al., 2013).

6.9.1 Role of DJ-1 in protection against OS by mediating mitochondrial mitophagy

Mitochondria continuously undergo fission and fusion processes to meet the varying energy demands of the cell which is considered to be a protective phenomenon against oxidative stress. (McCoy and Cookson, 2011) reported that cells devoid of DJ-1 had low mitochondrial fusion rate. DJ-1 is recruited to mitochondria during oxidative stress but any condition leading to the loss of function of DJ-1 can also lead to reduced membrane potential and increased fragmentation of mitochondria (Wang et al., 2012) whereas higher expressions of DJ-1 lead to sustained mitochondrial integrity resulting in increased resistance to oxidative insults (Irrcher et al., 2010;Krebiehl et al., 2010;Thomas et al., 2011;Wang et al., 2012).

6.9.2 Direct role of DJ-1 in protection against OS by mediating thioredoxin system

Thioredoxin reductase is the enzyme which catalyzes the reduction of thioredoxin (Mustacich et al., 2004) and Thioredoxin dependent peroxide reductase is found significantly upregulated in VV2 subtype based on our proteomic findings. It is an important component in the thioredoxin system. Thioredoxin (Trx) system is a small family of antioxidant enzymes involved in neuroprotection by alleviating oxidative stress (Bai et al., 2002;Takagi et al., 2000;Zhou et al., 2009). Trx loss leads to increased vulnerability to oxidative. Trx also protects the cells by regulating the activity of apoptosis signal-regulating kinase-1 (ASK1) (Saitoh et al., 1998). Thioredoxin system includes Trx1, thioredoxin reductase (TrxR) and

nicotinamide adenine dinucleotide phosphate (NADPH) and exerts a strong protein disulfide reductase function (Nakamura et al., 1997).

Apoptosis signal-regulating kinase 1 (ASK1) is a member of MAP kinase family and can activate c-Jun N-terminal kinase (JNK) and p38 mitogen-activated protein kinases in a Raf independent manner under various cellular stress conditions like oxidative stress, endoplasmic reticulum stress and calcium influx. Under normal cellular conditions, ASK1 is bound to Trx1, but under the influence of oxidative stress it can dissociate from Trx1 leading to its activation and hence cell death. Wild-type DJ-1 can inhibit the apoptotic potential of AKS1 by interacting with it and blocking its dissociation from Trx1: This neuroprotective function of DJ-1 is impaired in PD linked L166P mutant DJ-1. Cys106 residue of DJ-1 is essential for regulating ASK-1/Trx1 interaction (Im et al., 2010). Collectively, DJ-1-ASK1 interaction plays an important role in the anti-oxidant response by modulating the interaction between ASK1 and Trx1.

6.9.3 Direct role of DJ-1 in protection against OS by mediating Glutathione biosynthesis

Glutathione (GSH) is another antioxidant: protecting the cells from free radicals, peroxides, lipid peroxides and heavy metals (Pompella et al., 2003). DJ-1 also regulates the glutathione activity by increasing the expression of the enzyme glutamate cysteine ligase (GCL). GCL is the first enzyme of the pathway of cellular GSH biosynthesis (Zhou and Freed, 2005). Glutathione S transferase Mu 2 is a class of enzymes which protects the cells by detoxifying electrophilic compounds like carcinogens, drug residues, environmental toxins and toxic products of oxidative stress, in conjunction with glutathione (Li et al., 2014). GSTMu2 is found significantly upregulated both at transcriptional as well as translational levels in MM1 and VV2 subtypes of sCJD in present study.

6.9.4 Indirect role of DJ-1 in protection against OS by mediating Nrf2/ARE pathway

One of the proposed mechanism of action of protecting the cell against OS by DJ-1 is through regulating the activity of the transcription factor Nuclear factor erythroid-2 related factor 2 (Nrf2). Nrf2 induces the expression of antioxidation related elements (ARE) and is reported to be regulated by DJ-1 (Clements et al., 2006b). Upregulation in DJ-1 in response to oxidative stress expression leads to inactivation of Keap1 resulting in the release of Nrf2 from Keap1, inducing its translocation into the nucleus and thus activating ARE which is the main regulatory site of antioxidant expression (Cheng et al., 2013;Malhotra et al., 2008) (Figure. 6.1). Keap1 is the main regulator of Nrf2 activity by continuously ubiquinating Nrf2 in

cytoplasm and directing it to proteasomal degradation. But during oxidative stress, Keap1 is inactivated and Nrf2 expression is stabilized by DJ-1 (Clements et al., 2006a). Our results showing increased mRNA expression of Nrf2, decreased expression of ubiquinated-Nrf2 along with high expression of its activated form: phospho-Nrf2 confirm the activation of Nrf2 in sCJD (MM1 and VV2 subtype) cases for its downstream regulation of ARE. ARE encode detoxifying enzymes and antioxidant proteins, including NAD(P)H: quinone oxidoreductase 1, hemeoxygenase-1, glutathione S-transferase, glutathione cysteine ligase C, glutathione peroxidase and thioredoxin-dependent peroxide reductase.

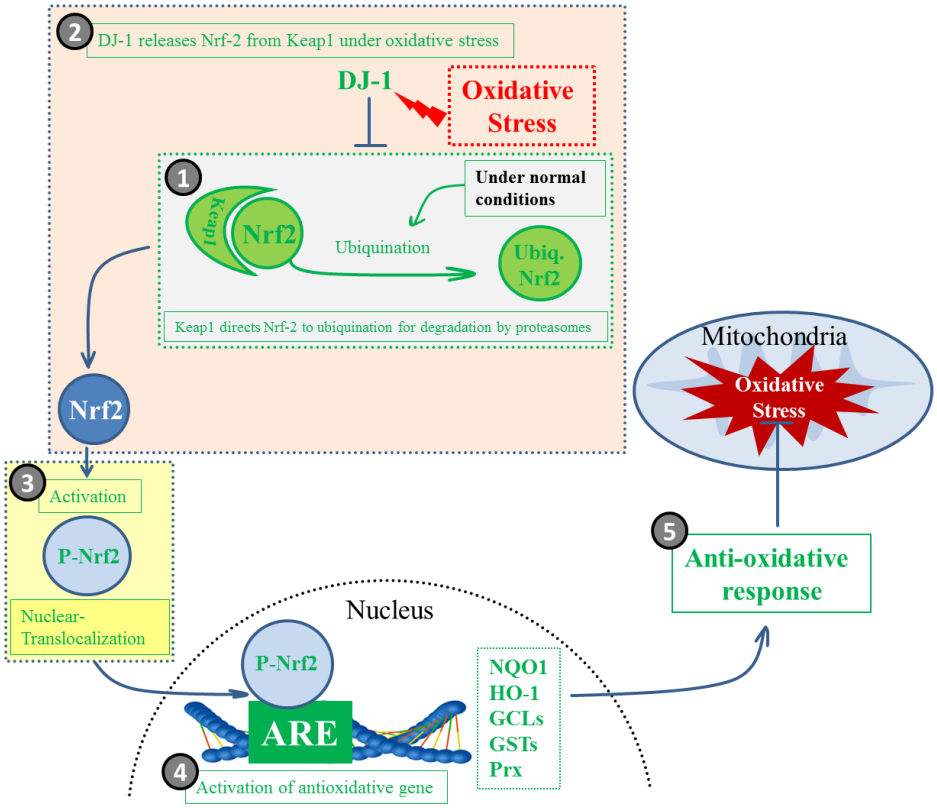

Figure 6-1: Mechanism of antioxidative response activation of DJ-1 by mediating Nrf2/ARE pathway

One of the mechanisms, by which DJ-1 protects the cells against oxidative stress is by regulating the activity of Nrf2 which leads to activation of antioxidative response elements (ARE) in the nucleus. **1-** Under normal cellular conditions, Nrf2 activity is inhibited by Keap1 who continuously ubiquinates Nrf2 and directs to proteasomal degradation, **2-** Under the effect of oxidative stress, DJ-1 is upregulated and it inhibits Keap1 activity and releases Nrf2 from Keap1 for its downstream functions, **3-** Nrf2 is phosphorylated which is necessary for its downstream activity and then it translocalizes to nucleus, **4-** In nucleus, phosphor-Nrf2 induces the expression of antioxidative genes NQO1, HO-1, GSLs, GSTs and Prx, **5-** Expression of these antioxidative genes then perform their functions in variety of ways to protect the cell against OS.

Increased expression of hemeoxygenase-1 at transcriptional level and increased expression of glutathione S-transferase and thioredoxin-dependent peroxide reductase both at transcriptional and translational levels confirm the activation of complete Nrf2/ARE pathway in sCJD (MM1 and VV2 subtype). In general, the target genes of Nrf2 are involved in glutathione synthesis, the elimination of ROS, xenobiotic metabolism, and drug transport (Chanas et al., 2002;Moinova and Mulcahy, 1999;Sekhar et al., 2003;Thimmulappa et al., 2002).

6.9.5 Aspects responsible for production of oxidative stress in sCJD

Possible aspects for the pronounced levels of oxidative stress in sCJD can be PrP^{SC} amyloid plaques, formed in brain tissues of patients with sCJD. These PrP^{SC} amyloid plaques are surrounded by reactive microglia (Block and Hong, 2005;Kim and de, 2005) which result in local inflammatory response and production of reactive oxygen (ROS) and nitrogen species (RNS).

Another aspect leading to oxidative stress in sCJD can be due to the conversion of PrP^{C} into PrP^{SC} leading to reduced total PrP^{C} levels in the brain cells. Since PrP^{C} is known to possess a SOD-like function, and conversion of PrP^{C} into PrP^{SC} during the pathophysiology of disease in sCJD also leads to reduced antioxidant capacity of brain cells leading to oxidative stress (Brown et al., 1997;Klamt et al., 2001).

This study gives a detailed overview of all the pathophysiological events during the course of the disease in sCJD. Furthermore, these results altogether can be helpful in attracting more efforts towards further exploration of the identified molecular regulations in order to find out early disease specific diagnostic markers and designing therapeutic strategies.

7 Conclusion

Based on these results we can speculate that oxidative stress is one of the major pathological factors during the course of the disease in MM1 and VV2 subtypes of sCJD which can deregulate other cellular activities as well. Furthermore, oxidative stress is present even during the presymptomatic stage of the disease in sCJD as shown by results from mice models of sCJD and it is also clearly evident from the results obtained from human CSF samples of sCJD patients that oxidative stress is present during the clinical stage of sCJD as well. Experimental results of DJ-1 show the potential implication of DJ-1 as a biomarker for the identification of oxidative stress even during the early stages of sCJD specifically. DJ-1 is commonly playing its anti-oxidative role (both directly by localizing to nucleus and indirectly by activating Nrf2/ARE pathway) in sCJD. Using antioxidative therapeutic strategies in future may be helpful not only in decreasing the progression rate of sCJD specifically but also at some point it may be helpful to overcome the pronounced levels of oxidative stress and to recover the cell from pathological condition. Furthermore, these results provide a broader overview of the whole regulated proteome during the course of disease in sCJD (MM1 and VV2 subtypes) in human, thus opening the new horizons for better understanding the pathophysiology of disease and redirecting the therapeutic strategies in right dimension.

8 Annexure

Regulation of spots used in validation of proteomics findings after mass-spectrometery.

Analysis of spot 164 with Delta2D

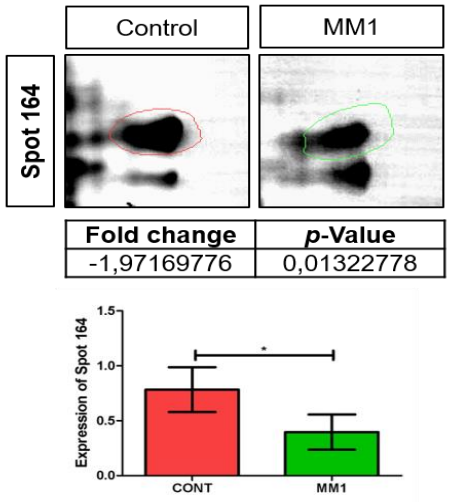

Fold change	*p*-Value
-1,97169776	0,01322778

Protein identification results by MS/MS

Spot	Proteins identified	Peptide	Sequence coverage
164	Pyruvate kinaseM1/2	2	6,03%
164	Dihydrolipoyl dehydrogenase	2	8,64%
164	Elongation factor 1-alpha 1	3	26,00%

Analysis of spot 373 with Delta2D

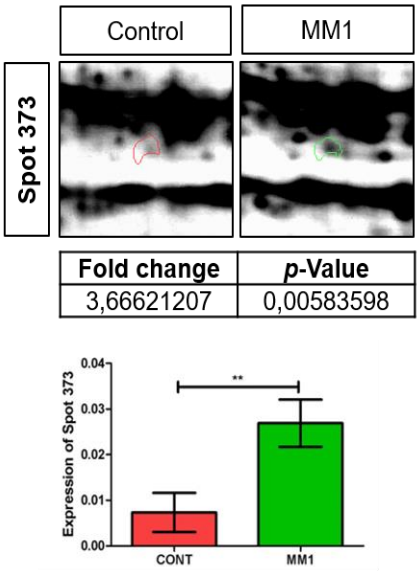

Fold change	*p*-Value
3,66621207	0,00583598

Protein identification results by MS/MS

Spot	Proteins identified	Peptide	Sequence coverage
373	Septin-6	9	22,40%

Analysis of spot 432 with Delta2D

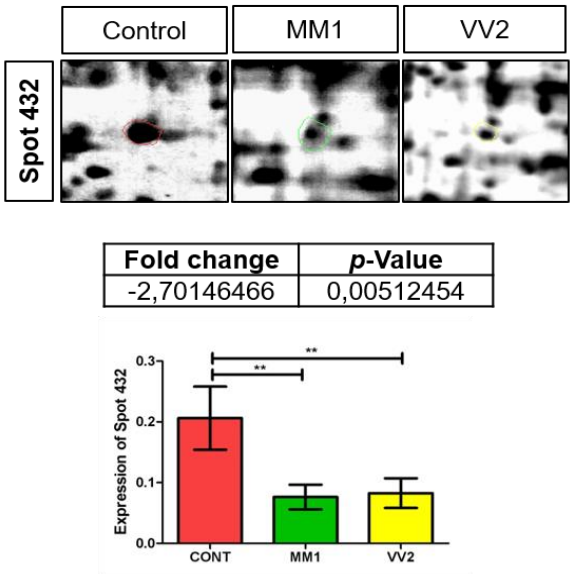

Fold change	*p*-Value
-2,70146466	0,00512454

Protein identification results by MS/MS

Spot	Proteins identified	Peptide	Sequence coverage
432	Guanine nucleotide-binding protein G(o) subunit alpha	2	6,50%
432	Protein phosphatase methylesterase 1	3	11,10%
432	Dihydrolipoyllysine-residue succinyltransferase	4	10,20%
432	TAR DNA-binding protein 43	4	11,60%
432	Creatine kinase B	4	13,10%
432	Actin, cytoplasmic 1	7	30,70%
432	Succinyl-CoA ligase subunit beta	31	40,00%

Analysis of spot 495 with Delta2D

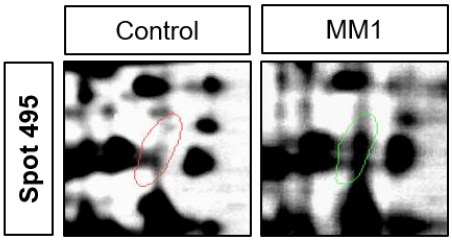

Fold change	*p*-Value
1,80697596	0,02977849

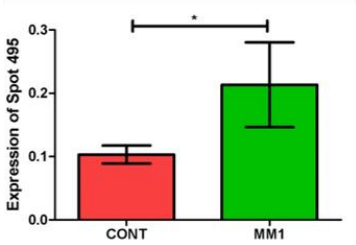

Protein identification results by MS/MS

Spot	Proteins identified	Peptide	Sequence coverage
495	NAD-dependent protein deacetylase sirtuin-2	2	4,88%
495	N(G),N(G)-dimethylarginine dimethylaminohydrolase 1	2	8,07%
495	Isocitrate dehydrogenase [NAD] subunit alpha	7	19,40%
495	L-lactate dehydrogenase B chain	10	34,10%

Analysis of spot 506 with Delta2D

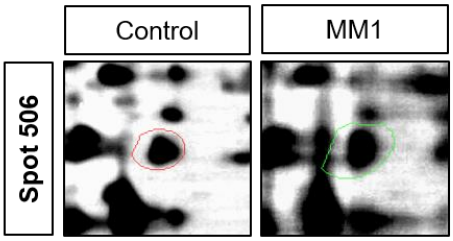

Fold change	*p*-Value
1,75852241	0,04910973

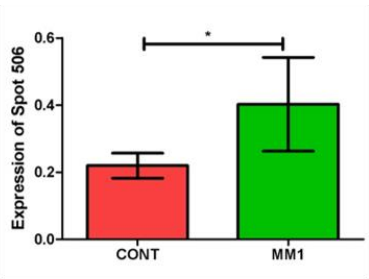

Protein identification results by MS/MS

Spot	Proteins identified	Peptide	Sequence coverage
506	m7GpppX diphosphatase	2	5,34%
506	Protein NDRG4	2	6,82%
506	Serine racemase	2	8,24%
506	Serine/threonine-protein phosphatase PP1-alpha catalytic subunit	2	8,48%
506	Heterogeneous nuclear ribonucleoprotein H3	3	8,96%
506	Vacuolar protein sorting-associated protein VTA1 homolog	3	12,40%
506	Protein kinase C delta-binding protein	3	13,80%
506	N-acetyl-D-glucosamine kinase	6	21,20%
506	Transaldolase	24	53,10%

Analysis of spot 742 with Delta2D

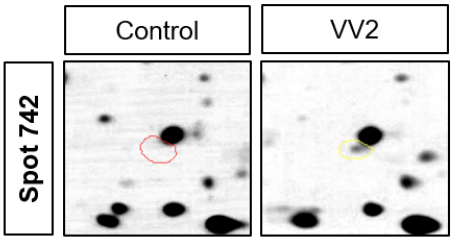

Fold change	*p*-Value
3,2964486	0,02282627

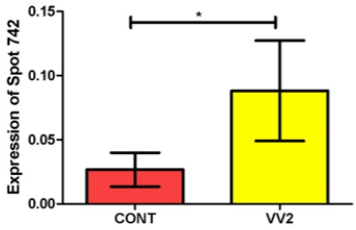

Protein identification results by MS/MS

Spot	Proteins identified	Peptide	Sequence coverage
742	Dehydrogenase/reductase SDR family member 11	2	9,62%
742	Glutathione S-transferase Mu 2	2	10,10%
742	Amphiphysin	3	3,88%
742	Alpha-synuclein	3	27,10%
742	Persulfide dioxygenase ETHE1	4	18,10%
742	Dihydropteridine reductase	4	20,10%
742	Heat shock protein beta-1	4	26,30%
742	Hypoxanthine-guanine phosphoribosyltransferase	5	30,70%
742	Peroxiredoxin-6	12	41,10%

Analysis of spot 773 with Delta2D

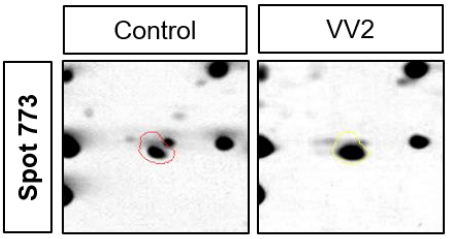

Fold change	*p*-Value
2,16567478	0,00033027

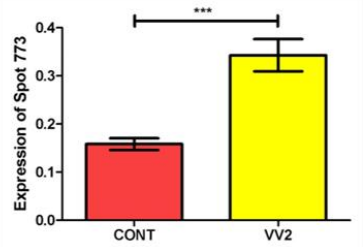

Protein identification results by MS/MS

Spot	Proteins identified	Peptide	Sequence coverage
773	Protein S100-A8	2	12,90%
773	Ig kappa chain C region	2	33,00%
773	Neutrophil defensin 1	3	20,20%
773	Mucin-5B	4	0,96%
773	Serum albumin	6	9,03%
773	Lysozyme C	6	30,40%
773	Ig alpha-1 chain C region	10	32,30%
773	Protein DJ-1	12	59,30%
773	Polymeric immunoglobulin receptor	13	16,50%

Analysis of spot 801 with Delta2D

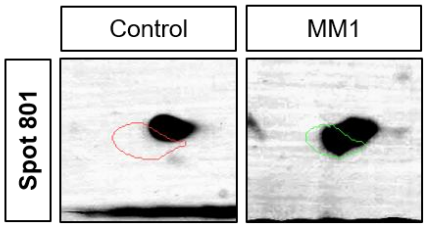

Fold change	*p*-Value
4,52334203	0,00209677

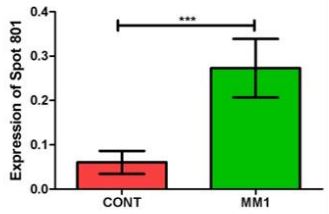

Protein identification by MS/MS

Spot	Proteins identified	Peptide	Sequence coverage
801	Superoxide dismutase [Cu-Zn]	11	69,50%

9 References Cited

Abramov, A. Y., J. Jacobson, F. Wientjes, J. Hothersall, L. Canevari, and M. R. Duchen, 2005, Expression and modulation of an NADPH oxidase in mammalian astrocytes: J.Neurosci., v. 25, no. 40, p. 9176-9184.

Agostinho, P., J. P. Lopes, Z. Velez, and C. R. Oliveira, 2008, Overactivation of calcineurin induced by amyloid-beta and prion proteins: Neurochem.Int., v. 52, no. 6, p. 1226-1233.

Alper, T., 1985, Scrapie agent unlike viruses in size and susceptibility to inactivation by ionizing or ultraviolet radiation: Nature, v. 317, no. 6039, p. 750.

Altmeppen, H. C., B. Puig, F. Dohler, D. K. Thurm, C. Falker, S. Krasemann, and M. Glatzel, 2012, Proteolytic processing of the prion protein in health and disease: Am.J.Neurodegener.Dis., v. 1, no. 1, p. 15-31.

Andersson, M. et al., 1994, Cerebrospinal fluid in the diagnosis of multiple sclerosis: a consensus report: J.Neurol.Neurosurg.Psychiatry, v. 57, no. 8, p. 897-902.

Bai, J., H. Nakamura, I. Hattori, M. Tanito, and J. Yodoi, 2002, Thioredoxin suppresses 1-methyl-4-phenylpyridinium-induced neurotoxicity in rat PC12 cells: Neurosci.Lett., v. 321, no. 1-2, p. 81-84.

Baker, C. A., Z. Y. Lu, I. Zaitsev, and L. Manuelidis, 1999a, Microglial activation varies in different models of Creutzfeldt-Jakob disease: J.Virol., v. 73, no. 6, p. 5089-5097.

Baker, C. A., D. Martin, and L. Manuelidis, 2002b, Microglia from Creutzfeldt-Jakob disease-infected brains are infectious and show specific mRNA activation profiles: J.Virol., v. 76, no. 21, p. 10905-10913.

Basler, K., B. Oesch, M. Scott, D. Westaway, M. Walchli, D. F. Groth, M. P. McKinley, S. B. Prusiner, and C. Weissmann, 1986, Scrapie and cellular PrP isoforms are encoded by the same chromosomal gene: Cell, v. 46, no. 3, p. 417-428.

Baulac, S. et al., 2009, Increased DJ-1 expression under oxidative stress and in Alzheimer's disease brains: Mol.Neurodegener., v. 4, p. 12.

Becker, M., J. Kuhse, and J. Kirsch, 2013, Effects of two elongation factor 1A isoforms on the formation of gephyrin clusters at inhibitory synapses in hippocampal neurons: Histochem.Cell Biol., v. 140, no. 6, p. 603-609.

Bellinger-Kawahara, C., J. E. Cleaver, T. O. Diener, and S. B. Prusiner, 1987a, Purified scrapie prions resist inactivation by UV irradiation: J.Virol., v. 61, no. 1, p. 159-166.

Bellinger-Kawahara, C., T. O. Diener, M. P. McKinley, D. F. Groth, D. R. Smith, and S. B. Prusiner, 1987b, Purified scrapie prions resist inactivation by procedures that hydrolyze, modify, or shear nucleic acids: Virology, v. 160, no. 1, p. 271-274.

Bessen, R. A., and R. F. Marsh, 1994, Distinct PrP properties suggest the molecular basis of strain variation in transmissible mink encephalopathy: J.Virol., v. 68, no. 12, p. 7859-7868.

Biasini, E., J. A. Turnbaugh, U. Unterberger, and D. A. Harris, 2012, Prion protein at the crossroads of physiology and disease: Trends Neurosci., v. 35, no. 2, p. 92-103.

Blackinton, J., M. Lakshminarasimhan, K. J. Thomas, R. Ahmad, E. Greggio, A. S. Raza, M. R. Cookson, and M. A. Wilson, 2009, Formation of a stabilized cysteine sulfinic acid is critical for the mitochondrial function of the parkinsonism protein DJ-1: J.Biol.Chem., v. 284, no. 10, p. 6476-6485.

Block, M. L., and J. S. Hong, 2005, Microglia and inflammation-mediated neurodegeneration: multiple triggers with a common mechanism: Prog.Neurobiol., v. 76, no. 2, p. 77-98.

Bolognani, F., and N. I. Perrone-Bizzozero, 2008, RNA-protein interactions and control of mRNA stability in neurons: J.Neurosci.Res., v. 86, no. 3, p. 481-489.

Bolton, D. C., M. P. McKinley, and S. B. Prusiner, 1984, Molecular characteristics of the major scrapie prion protein: Biochemistry, v. 23, no. 25, p. 5898-5906.

Brown, D. R., 2001, Copper and prion disease: Brain Res.Bull., v. 55, no. 2, p. 165-173.

Brown, D. R., C. Clive, and S. J. Haswell, 2001, Antioxidant activity related to copper binding of native prion protein: J.Neurochem., v. 76, no. 1, p. 69-76.

Brown, D. R., J. Herms, and H. A. Kretzschmar, 1994, Mouse cortical cells lacking cellular PrP survive in culture with a neurotoxic PrP fragment: Neuroreport, v. 5, no. 16, p. 2057-2060.

Brown, D. R., B. Schmidt, and H. A. Kretzschmar, 1996a, A neurotoxic prion protein fragment enhances proliferation of microglia but not astrocytes in culture: Glia, v. 18, no. 1, p. 59-67.

Brown, D. R., B. Schmidt, and H. A. Kretzschmar, 1996b, Role of microglia and host prion protein in neurotoxicity of a prion protein fragment: Nature, v. 380, no. 6572, p. 345-347.

Brown, D. R., W. J. Schulz-Schaeffer, B. Schmidt, and H. A. Kretzschmar, 1997, Prion protein-deficient cells show altered response to oxidative stress due to decreased SOD-1 activity: Exp.Neurol., v. 146, no. 1, p. 104-112.

Brown, G. C., and A. Bal-Price, 2003, Inflammatory neurodegeneration mediated by nitric oxide, glutamate, and mitochondria: Mol.Neurobiol., v. 27, no. 3, p. 325-355.

Bruce, M. E., 2003, TSE strain variation: Br.Med.Bull., v. 66, p. 99-108.

Budka, H., 2003, Neuropathology of prion diseases: Br.Med.Bull., v. 66, p. 121-130.

Canet-Aviles, R. M. et al., 2004, The Parkinson's disease protein DJ-1 is neuroprotective due to cysteine-sulfinic acid-driven mitochondrial localization: Proc.Natl.Acad.Sci.U.S.A, v. 101, no. 24, p. 9103-9108.

Carp, R. I., 1982, Transmission of scrapie by oral route: effect of gingival scarification: Lancet, v. 1, no. 8264, p. 170-171.

Chanas, S. A. et al., 2002, Loss of the Nrf2 transcription factor causes a marked reduction in constitutive and inducible expression of the glutathione S-transferase Gsta1, Gsta2, Gstm1, Gstm2, Gstm3 and Gstm4 genes in the livers of male and female mice: Biochem.J., v. 365, no. Pt 2, p. 405-416.

Cheng, X., S. J. Chapple, B. Patel, W. Puszyk, D. Sugden, X. Yin, M. Mayr, R. C. Siow, and G. E. Mann, 2013, Gestational diabetes mellitus impairs Nrf2-mediated adaptive antioxidant defenses and redox signaling in fetal endothelial cells in utero: Diabetes, v. 62, no. 12, p. 4088-4097.

Chesebro, B. et al., 1985, Identification of scrapie prion protein-specific mRNA in scrapie-infected and uninfected brain: Nature, v. 315, no. 6017, p. 331-333.

Cho, S., and G. Dawson, 2000, Palmitoyl protein thioesterase 1 protects against apoptosis mediated by Ras-Akt-caspase pathway in neuroblastoma cells: J.Neurochem., v. 74, no. 4, p. 1478-1488.

Choi, C. J., V. Anantharam, N. J. Saetveit, R. S. Houk, A. Kanthasamy, and A. G. Kanthasamy, 2007, Normal cellular prion protein protects against manganese-induced oxidative stress and apoptotic cell death: Toxicol.Sci., v. 98, no. 2, p. 495-509.

Clarke, M. C., and R. H. Kimberlin, 1984, Pathogenesis of mouse scrapie: distribution of agent in the pulp and stroma of infected spleens: Vet.Microbiol., v. 9, no. 3, p. 215-225.

Clements, C. M., R. S. McNally, B. J. Conti, T. W. Mak, and J. P. Ting, 2006a, DJ-1, a cancer- and Parkinson's disease-associated protein, stabilizes the antioxidant transcriptional master regulator Nrf2: Proc.Natl.Acad.Sci.U.S.A, v. 103, no. 41, p. 15091-15096.

Clements, C. M., R. S. McNally, B. J. Conti, T. W. Mak, and J. P. Ting, 2006b, DJ-1, a cancer- and Parkinson's disease-associated protein, stabilizes the antioxidant transcriptional master regulator Nrf2: Proc.Natl.Acad.Sci.U.S.A, v. 103, no. 41, p. 15091-15096.

Cole, S., and R. H. Kimberlin, 1985, Pathogenesis of mouse scrapie: dynamics of vacuolation in brain and spinal cord after intraperitoneal infection: Neuropathol.Appl.Neurobiol., v. 11, no. 3, p. 213-227.

Colling, S. B., M. Khana, J. Collinge, and J. G. Jefferys, 1997, Mossy fibre reorganization in the hippocampus of prion protein null mice: Brain Res., v. 755, no. 1, p. 28-35.

Collinge, J., M. Poulter, M. B. Davis, M. Baraitser, F. Owen, T. J. Crow, and A. E. Harding, 1991, Presymptomatic detection or exclusion of prion protein gene defects in families with inherited prion diseases: Am.J.Hum.Genet., v. 49, no. 6, p. 1351-1354.

Colton, C. A., M. Gbadegesin, D. A. Wink, K. M. Miranda, M. G. Espey, and S. Vicini, 2001, Nitroxyl anion regulation of the NMDA receptor: J.Neurochem., v. 78, no. 5, p. 1126-1134.

Criado, J. R. et al., 2005, Mice devoid of prion protein have cognitive deficits that are rescued by reconstitution of PrP in neurons: Neurobiol.Dis., v. 19, no. 1-2, p. 255-265.

Denkers, N. D. et al., 2013, Aerosol transmission of chronic wasting disease in white-tailed deer: J.Virol., v. 87, no. 3, p. 1890-1892.

Di, D. F., R. Sultana, G. F. Tiu, N. N. Scheff, M. Perluigi, C. Cini, and D. A. Butterfield, 2010, Protein levels of heat shock proteins 27, 32, 60, 70, 90 and thioredoxin-1 in amnestic mild cognitive impairment: an investigation on the role of cellular stress response in the progression of Alzheimer disease: Brain Res., v. 1333, p. 72-81.

Dringen, R., P. G. Pawlowski, and J. Hirrlinger, 2005, Peroxide detoxification by brain cells: J.Neurosci.Res., v. 79, no. 1-2, p. 157-165.

Duffy, P., J. Wolf, G. Collins, A. G. DeVoe, B. Streeten, and D. Cowen, 1974, Letter: Possible person-to-person transmission of Creutzfeldt-Jakob disease: N.Engl.J.Med., v. 290, no. 12, p. 692-693.

Eaton, C. J., I. E. Cabrera, J. A. Servin, S. J. Wright, M. P. Cox, and K. A. Borkovich, 2012, The guanine nucleotide exchange factor RIC8 regulates conidial germination through Galpha proteins in Neurospora crassa: PLoS.One., v. 7, no. 10, p. e48026.

Eckert, A., U. Keil, S. Kressmann, K. Schindowski, S. Leutner, S. Leutz, and W. E. Muller, 2003, Effects of EGb 761 Ginkgo biloba extract on mitochondrial function and oxidative stress: Pharmacopsychiatry, v. 36 Suppl 1, p. S15-S23.

Eghiaian, F., J. Grosclaude, S. Lesceu, P. Debey, B. Doublet, E. Treguer, H. Rezaei, and M. Knossow, 2004, Insight into the PrPC-->PrPSc conversion from the structures of antibody-bound ovine prion scrapie-susceptibility variants: Proc.Natl.Acad.Sci.U.S.A, v. 101, no. 28, p. 10254-10259.

Felton, L. M., C. Cunningham, E. L. Rankine, S. Waters, D. Boche, and V. H. Perry, 2005, MCP-1 and murine prion disease: separation of early behavioural dysfunction from overt clinical disease: Neurobiol.Dis., v. 20, no. 2, p. 283-295.

Fevrier, B., D. Vilette, F. Archer, D. Loew, W. Faigle, M. Vidal, H. Laude, and G. Raposo, 2004, Cells release prions in association with exosomes: Proc.Natl.Acad.Sci.U.S.A, v. 101, no. 26, p. 9683-9688.

Ford, M. J., L. J. Burton, H. Li, C. H. Graham, Y. Frobert, J. Grassi, S. M. Hall, and R. J. Morris, 2002, A marked disparity between the expression of prion protein and its message by neurones of the CNS: Neuroscience, v. 111, no. 3, p. 533-551.

Forloni, G., N. Angeretti, R. Chiesa, E. Monzani, M. Salmona, O. Bugiani, and F. Tagliavini, 1993, Neurotoxicity of a prion protein fragment: Nature, v. 362, no. 6420, p. 543-546.

Gajdusek, D. C., and V. Zigas, 1957, Degenerative disease of the central nervous system in New Guinea; the endemic occurrence of kuru in the native population: N.Engl.J.Med., v. 257, no. 20, p. 974-978.

Gambetti, P., Q. Kong, W. Zou, P. Parchi, and S. G. Chen, 2003, Sporadic and familial CJD: classification and characterisation: Br.Med.Bull., v. 66, p. 213-239.

Giese, A., M. H. Groschup, B. Hess, and H. A. Kretzschmar, 1995, Neuronal cell death in scrapie-infected mice is due to apoptosis: Brain Pathol., v. 5, no. 3, p. 213-221.

Gillessen, T., S. L. Budd, and S. A. Lipton, 2002, Excitatory amino acid neurotoxicity: Adv.Exp.Med.Biol., v. 513, p. 3-40.

Glatzel, M., F. L. Heppner, K. M. Albers, and A. Aguzzi, 2001, Sympathetic innervation of lymphoreticular organs is rate limiting for prion neuroinvasion: Neuron, v. 31, no. 1, p. 25-34.

Glaysher, B. R., and N. A. Mabbott, 2007, Role of the draining lymph node in scrapie agent transmission from the skin: Immunol.Lett., v. 109, no. 1, p. 64-71.

Goldfarb, L. G. et al., 1992, Fatal familial insomnia and familial Creutzfeldt-Jakob disease: disease phenotype determined by a DNA polymorphism: Science, v. 258, no. 5083, p. 806-808.

Gousset, K. et al., 2009, Prions hijack tunnelling nanotubes for intercellular spread: Nat.Cell Biol., v. 11, no. 3, p. 328-336.

Grassmann, A., H. Wolf, J. Hofmann, J. Graham, and I. Vorberg, 2013, Cellular aspects of prion replication in vitro: Viruses., v. 5, no. 1, p. 374-405.

Gray, F., H. Adle-Biassette, F. Chretien, T. Ereau, M. B. Delisle, and C. Vital, 1999a, [Neuronal apoptosis in human prion diseases]: Bull.Acad.Natl.Med., v. 183, no. 2, p. 305-320.

Gray, F., F. Chretien, H. Adle-Biassette, A. Dorandeu, T. Ereau, M. B. Delisle, N. Kopp, J. W. Ironside, and C. Vital, 1999b, Neuronal apoptosis in Creutzfeldt-Jakob disease: J.Neuropathol.Exp.Neurol., v. 58, no. 4, p. 321-328.

Ha, C. E., and N. V. Bhagavan, 2013, Novel insights into the pleiotropic effects of human serum albumin in health and disease: Biochim.Biophys.Acta, v. 1830, no. 12, p. 5486-5493.

Haraguchi, T. et al., 1989, Asparagine-linked glycosylation of the scrapie and cellular prion proteins: Arch.Biochem.Biophys., v. 274, no. 1, p. 1-13.

Harris, D. A., 2003, Trafficking, turnover and membrane topology of PrP: Br.Med.Bull., v. 66, p. 71-85.

Harris, D. A., M. T. Huber, D. P. van, S. L. Shyng, B. T. Chait, and R. Wang, 1993a, Processing of a cellular prion protein: identification of N- and C-terminal cleavage sites: Biochemistry, v. 32, no. 4, p. 1009-1016.

Harris, D. A., P. Lele, and W. D. Snider, 1993b, Localization of the mRNA for a chicken prion protein by in situ hybridization: Proc.Natl.Acad.Sci.U.S.A, v. 90, no. 9, p. 4309-4313.

Hay, B., R. A. Barry, I. Lieberburg, S. B. Prusiner, and V. R. Lingappa, 1987, Biogenesis and transmembrane orientation of the cellular isoform of the scrapie prion protein [published errratum appears in Mol Cell Biol 1987 May;7(5):2035]: Mol.Cell Biol., v. 7, no. 2, p. 914-920.

Haybaeck, J. et al., 2011, Aerosols transmit prions to immunocompetent and immunodeficient mice: PLoS.Pathog., v. 7, no. 1, p. e1001257.

Heese, K., C. Hock, and U. Otten, 1998, Inflammatory signals induce neurotrophin expression in human microglial cells: J.Neurochem., v. 70, no. 2, p. 699-707.

Heggebo, R., C. M. Press, G. Gunnes, M. J. Ulvund, M. A. Tranulis, and T. Lsverk, 2003, Detection of PrPSc in lymphoid tissues of lambs experimentally exposed to the scrapie agent: J.Comp Pathol., v. 128, no. 2-3, p. 172-181.

Heppner, F. L., A. D. Christ, M. A. Klein, M. Prinz, M. Fried, J. P. Kraehenbuhl, and A. Aguzzi, 2001, Transepithelial prion transport by M cells: Nat.Med., v. 7, no. 9, p. 976-977.

Hsuan, J., and S. Cockcroft, 2001, The PITP family of phosphatidylinositol transfer proteins: Genome Biol., v. 2, no. 9, p. REVIEWS3011.

Huang, C., H. Cheng, S. Hao, H. Zhou, X. Zhang, J. Gao, Q. H. Sun, H. Hu, and C. C. Wang, 2006, Heat shock protein 70 inhibits alpha-synuclein fibril formation via interactions with diverse intermediates: J.Mol.Biol., v. 364, no. 3, p. 323-336.

Huang, F. P., C. F. Farquhar, N. A. Mabbott, M. E. Bruce, and G. G. MacPherson, 2002, Migrating intestinal dendritic cells transport PrP(Sc) from the gut: J.Gen.Virol., v. 83, no. Pt 1, p. 267-271.

Ihara, M. et al., 2007, Sept4, a component of presynaptic scaffold and Lewy bodies, is required for the suppression of alpha-synuclein neurotoxicity: Neuron, v. 53, no. 4, p. 519-533.

Im, J. Y., K. W. Lee, E. Junn, and M. M. Mouradian, 2010, DJ-1 protects against oxidative damage by regulating the thioredoxin/ASK1 complex: Neurosci.Res., v. 67, no. 3, p. 203-208.

Imran, M., and S. Mahmood, 2011, An overview of human prion diseases: Virol.J., v. 8, p. 559.

Irrcher, I. et al., 2010, Loss of the Parkinson's disease-linked gene DJ-1 perturbs mitochondrial dynamics: Hum.Mol.Genet., v. 19, no. 19, p. 3734-3746.

Ishikawa, S., Y. Tanaka, K. Takahashi-Niki, T. Niki, H. Ariga, and S. M. Iguchi-Ariga, 2012, Stimulation of vesicular monoamine transporter 2 activity by DJ-1 in SH-SY5Y cells: Biochem.Biophys.Res.Commun., v. 421, no. 4, p. 813-818.

Itoh, K. et al., 1997, An Nrf2/small Maf heterodimer mediates the induction of phase II detoxifying enzyme genes through antioxidant response elements: Biochem.Biophys.Res.Commun., v. 236, no. 2, p. 313-322.

Jendroska, K., F. P. Heinzel, M. Torchia, L. Stowring, H. A. Kretzschmar, A. Kon, A. Stern, S. B. Prusiner, and S. J. DeArmond, 1991, Proteinase-resistant prion protein accumulation in Syrian hamster brain correlates with regional pathology and scrapie infectivity: Neurology, v. 41, no. 9, p. 1482-1490.

Jimenez-Huete, A., P. M. Lievens, R. Vidal, P. Piccardo, B. Ghetti, F. Tagliavini, B. Frangione, and F. Prelli, 1998, Endogenous proteolytic cleavage of normal and disease-associated isoforms of the human prion protein in neural and non-neural tissues: Am.J.Pathol., v. 153, no. 5, p. 1561-1572.

Junn, E., W. H. Jang, X. Zhao, B. S. Jeong, and M. M. Mouradian, 2009, Mitochondrial localization of DJ-1 leads to enhanced neuroprotection: J.Neurosci.Res., v. 87, no. 1, p. 123-129.

Kahle, P. J., J. Waak, and T. Gasser, 2009, DJ-1 and prevention of oxidative stress in Parkinson's disease and other age-related disorders: Free Radic.Biol.Med., v. 47, no. 10, p. 1354-1361.

Kanaani, J., S. B. Prusiner, J. Diacovo, S. Baekkeskov, and G. Legname, 2005, Recombinant prion protein induces rapid polarization and development of synapses in embryonic rat hippocampal neurons in vitro: J.Neurochem., v. 95, no. 5, p. 1373-1386.

Kato, I., H. Maita, K. Takahashi-Niki, Y. Saito, N. Noguchi, S. M. Iguchi-Ariga, and H. Ariga, 2013, Oxidized DJ-1 inhibits p53 by sequestering p53 from promoters in a DNA-binding affinity-dependent manner: Mol.Cell Biol., v. 33, no. 2, p. 340-359.

Kawano, T., 2007, Prion-derived copper-binding peptide fragments catalyze the generation of superoxide anion in the presence of aromatic monoamines: Int.J.Biol.Sci., v. 3, no. 1, p. 57-63.

Khacho, M., K. Mekhail, K. Pilon-Larose, A. Pause, J. Cote, and S. Lee, 2008, eEF1A is a novel component of the mammalian nuclear protein export machinery: Mol.Biol.Cell, v. 19, no. 12, p. 5296-5308.

Kim, S. U., and V. J. de, 2005, Microglia in health and disease: J.Neurosci.Res., v. 81, no. 3, p. 302-313.

Kimberlin, R. H., and C. A. Walker, 1989, Pathogenesis of scrapie in mice after intragastric infection: Virus Res., v. 12, no. 3, p. 213-220.

Kincaid, A. E., K. F. Hudson, M. W. Richey, and J. C. Bartz, 2012, Rapid transepithelial transport of prions following inhalation: J.Virol., v. 86, no. 23, p. 12731-12740.

Kinoshita, A., M. Kinoshita, H. Akiyama, H. Tomimoto, I. Akiguchi, S. Kumar, M. Noda, and J. Kimura, 1998a, Identification of septins in neurofibrillary tangles in Alzheimer's disease: Am.J.Pathol., v. 153, no. 5, p. 1551-1560.

Kinoshita, A., M. Kinoshita, H. Akiyama, H. Tomimoto, I. Akiguchi, S. Kumar, M. Noda, and J. Kimura, 1998b, Identification of septins in neurofibrillary tangles in Alzheimer's disease: Am.J.Pathol., v. 153, no. 5, p. 1551-1560.

Kinoshita, M., 2006, Diversity of septin scaffolds: Curr.Opin.Cell Biol., v. 18, no. 1, p. 54-60.

Kitamoto, T., T. Muramoto, S. Mohri, K. Doh-ura, and J. Tateishi, 1991, Abnormal isoform of prion protein accumulates in follicular dendritic cells in mice with Creutzfeldt-Jakob disease: J.Virol., v. 65, no. 11, p. 6292-6295.

Klamt, F., F. Dal-Pizzol, Conte da Frota ML Jr, R. Walz, M. E. Andrades, E. G. da Silva, R. R. Brentani, I. Izquierdo, and J. C. Fonseca Moreira, 2001, Imbalance of antioxidant defense in mice lacking cellular prion protein: Free Radic.Biol.Med., v. 30, no. 10, p. 1137-1144.

Klein, M. A., R. Frigg, A. J. Raeber, E. Flechsig, I. Hegyi, R. M. Zinkernagel, C. Weissmann, and A. Aguzzi, 1998, PrP expression in B lymphocytes is not required for prion neuroinvasion: Nat.Med., v. 4, no. 12, p. 1429-1433.

Klemm, H. M., J. M. Welton, C. L. Masters, G. M. Klug, A. Boyd, A. F. Hill, S. J. Collins, and V. A. Lawson, 2012, The prion protein preference of sporadic Creutzfeldt-Jakob disease subtypes: J.Biol.Chem., v. 287, no. 43, p. 36465-36472.

Klucken, J., Y. Shin, B. T. Hyman, and P. J. McLean, 2004, A single amino acid substitution differentiates Hsp70-dependent effects on alpha-synuclein degradation and toxicity: Biochem.Biophys.Res.Commun., v. 325, no. 1, p. 367-373.

Knight, R. S., and R. G. Will, 2004, Prion diseases: J.Neurol.Neurosurg.Psychiatry, v. 75 Suppl 1, p. i36-i42.

Krebiehl, G. et al., 2010, Reduced basal autophagy and impaired mitochondrial dynamics due to loss of Parkinson's disease-associated protein DJ-1: PLoS.One., v. 5, no. 2, p. e9367.

Lev, N., Y. Barhum, N. S. Pilosof, D. Ickowicz, H. Y. Cohen, E. Melamed, and D. Offen, 2013, DJ-1 protects against dopamine toxicity: implications for Parkinson's disease and aging: J.Gerontol.A Biol.Sci.Med.Sci., v. 68, no. 3, p. 215-225.

Liberski, P. P., and J. W. Ironside, 2004, An outline of the neuropathology of transmissible spongiform encephalopathies (prion diseases): Folia Neuropathol., v. 42 Suppl B, p. 39-58.

Linden, R., V. R. Martins, M. A. Prado, M. Cammarota, I. Izquierdo, and R. R. Brentani, 2008, Physiology of the prion protein: Physiol Rev., v. 88, no. 2, p. 673-728.

Llorens, F. et al., 2013, PrP mRNA and protein expression in brain and PrP(c) in CSF in Creutzfeldt-Jakob disease MM1 and VV2: Prion., v. 7, no. 5, p. 383-393.

Malhotra, D. et al., 2008, Decline in NRF2-regulated antioxidants in chronic obstructive pulmonary disease lungs due to loss of its positive regulator, DJ-1: Am.J.Respir.Crit Care Med., v. 178, no. 6, p. 592-604.

Mange, A., F. Beranger, K. Peoc'h, T. Onodera, Y. Frobert, and S. Lehmann, 2004, Alpha- and beta-cleavages of the amino-terminus of the cellular prion protein: Biol.Cell, v. 96, no. 2, p. 125-132.

Manson, J., J. D. West, V. Thomson, P. McBride, M. H. Kaufman, and J. Hope, 1992, The prion protein gene: a role in mouse embryogenesis?: Development, v. 115, no. 1, p. 117-122.

Martin-Lanneree, S., C. Lasbleiz, M. Sanial, S. Fouix, F. Besse, H. Tricoire, and A. Plessis, 2006, Characterization of the Drosophila myeloid leukemia factor: Genes Cells, v. 11, no. 12, p. 1317-1335.

Mathur, J., N. Mathur, B. Kernebeck, and M. Hulskamp, 2003, Mutations in actin-related proteins 2 and 3 affect cell shape development in Arabidopsis: Plant Cell, v. 15, no. 7, p. 1632-1645.

McBride, P. A., and M. Beekes, 1999, Pathological PrP is abundant in sympathetic and sensory ganglia of hamsters fed with scrapie: Neurosci.Lett., v. 265, no. 2, p. 135-138.

McCoy, M. K., and M. R. Cookson, 2011, DJ-1 regulation of mitochondrial function and autophagy through oxidative stress: Autophagy., v. 7, no. 5, p. 531-532.

McMahon, H. E., A. Mange, N. Nishida, C. Creminon, D. Casanova, and S. Lehmann, 2001, Cleavage of the amino terminus of the prion protein by reactive oxygen species: J.Biol.Chem., v. 276, no. 3, p. 2286-2291.

Mead, S., 2006, Prion disease genetics: Eur.J.Hum.Genet., v. 14, no. 3, p. 273-281.

Mhatre, M., R. A. Floyd, and K. Hensley, 2004, Oxidative stress and neuroinflammation in Alzheimer's disease and amyotrophic lateral sclerosis: common links and potential therapeutic targets: J.Alzheimers.Dis., v. 6, no. 2, p. 147-157.

Milhavet, O., and S. Lehmann, 2002, Oxidative stress and the prion protein in transmissible spongiform encephalopathies: Brain Res.Brain Res.Rev., v. 38, no. 3, p. 328-339.

Mohan, J., K. L. Brown, C. F. Farquhar, M. E. Bruce, and N. A. Mabbott, 2004, Scrapie transmission following exposure through the skin is dependent on follicular dendritic cells in lymphoid tissues: J.Dermatol.Sci., v. 35, no. 2, p. 101-111.

Moi, P., K. Chan, I. Asunis, A. Cao, and Y. W. Kan, 1994, Isolation of NF-E2-related factor 2 (Nrf2), a NF-E2-like basic leucine zipper transcriptional activator that binds to the tandem NF-E2/AP1 repeat of the beta-globin locus control region: Proc.Natl.Acad.Sci.U.S.A, v. 91, no. 21, p. 9926-9930.

Moinova, H. R., and R. T. Mulcahy, 1999, Up-regulation of the human gamma-glutamylcysteine synthetase regulatory subunit gene involves binding of Nrf-2 to an electrophile responsive element: Biochem.Biophys.Res.Commun., v. 261, no. 3, p. 661-668.

Molenaar, R. J., T. Radivoyevitch, J. P. Maciejewski, C. J. van Noorden, and F. E. Bleeker, 2014, The driver and passenger effects of isocitrate dehydrogenase 1 and 2 mutations in oncogenesis and survival prolongation: Biochim.Biophys.Acta, v. 1846, no. 2, p. 326-341.

Moller, T., C. Nolte, R. Burger, A. Verkhratsky, and H. Kettenmann, 1997, Mechanisms of C5a and C3a complement fragment-induced [Ca2+]i signaling in mouse microglia: J.Neurosci., v. 17, no. 2, p. 615-624.

Montrasio, F. et al., 2001, B lymphocyte-restricted expression of prion protein does not enable prion replication in prion protein knockout mice: Proc.Natl.Acad.Sci.U.S.A, v. 98, no. 7, p. 4034-4037.

Moreira, P. I. et al., 2005, Oxidative stress: the old enemy in Alzheimer's disease pathophysiology: Curr.Alzheimer Res., v. 2, no. 4, p. 403-408.

Moser, M., R. J. Colello, U. Pott, and B. Oesch, 1995, Developmental expression of the prion protein gene in glial cells: Neuron, v. 14, no. 3, p. 509-517.

Mustacich, D., A. Wagner, R. Williams, W. Bair, L. Barbercheck, S. P. Stratton, A. K. Bhattacharyya, and G. Powis, 2004, Increased skin carcinogenesis in a keratinocyte directed thioredoxin-1 transgenic mouse: Carcinogenesis, v. 25, no. 10, p. 1983-1989.

Nakada, N., S. Hongo, T. Ohki, A. Maeda, and M. Takeda, 2002, Molecular characterization of NDRG4/Bdm1 protein isoforms that are differentially regulated during rat brain development: Brain Res.Dev.Brain Res., v. 135, no. 1-2, p. 45-53.

Nakamaru-Ogiso, E., H. Han, A. Matsuno-Yagi, E. Keinan, S. C. Sinha, T. Yagi, and T. Ohnishi, 2010, The ND2 subunit is labeled by a photoaffinity analogue of asimicin, a potent complex I inhibitor: FEBS Lett., v. 584, no. 5, p. 883-888.

Nakamura, H., K. Nakamura, and J. Yodoi, 1997, Redox regulation of cellular activation: Annu.Rev.Immunol., v. 15, p. 351-369.

Neumann, M. et al., 2006, Ubiquitinated TDP-43 in frontotemporal lobar degeneration and amyotrophic lateral sclerosis: Science, v. 314, no. 5796, p. 130-133.

Nichols, T. A. et al., 2013, Intranasal inoculation of white-tailed deer (Odocoileus virginianus) with lyophilized chronic wasting disease prion particulate complexed to montmorillonite clay: PLoS.One., v. 8, no. 5, p. e62455.

Nishizuka, Y., 1986, Perspectives on the role of protein kinase C in stimulus-response coupling: J.Natl.Cancer Inst., v. 76, no. 3, p. 363-370.

Oesch, B. et al., 1985, A cellular gene encodes scrapie PrP 27-30 protein: Cell, v. 40, no. 4, p. 735-746.

Owen, J. B., W. O. Opii, C. Ramassamy, W. M. Pierce, and D. A. Butterfield, 2008, Proteomic analysis of brain protein expression levels in NF-kappabeta p50 -/- homozygous knockout mice: Brain Res., v. 1240, p. 22-30.

Padilla, D. et al., 2011, Sheep and goat BSE propagate more efficiently than cattle BSE in human PrP transgenic mice: PLoS.Pathog., v. 7, no. 3, p. e1001319.

Palmer, M. S., A. J. Dryden, J. T. Hughes, and J. Collinge, 1991, Homozygous prion protein genotype predisposes to sporadic Creutzfeldt-Jakob disease: Nature, v. 352, no. 6333, p. 340-342.

Pan, K. M. et al., 1993, Conversion of alpha-helices into beta-sheets features in the formation of the scrapie prion proteins: Proc.Natl.Acad.Sci.U.S.A, v. 90, no. 23, p. 10962-10966.

Parchi, P. et al., 1996, Molecular basis of phenotypic variability in sporadic Creutzfeldt-Jakob disease: Ann.Neurol., v. 39, no. 6, p. 767-778.

Parchi, P. et al., 2012, Consensus classification of human prion disease histotypes allows reliable identification of molecular subtypes: an inter-rater study among surveillance centres in Europe and USA: Acta Neuropathol., v. 124, no. 4, p. 517-529.

Parchi, P. et al., 1999, Classification of sporadic Creutzfeldt-Jakob disease based on molecular and phenotypic analysis of 300 subjects: Ann.Neurol., v. 46, no. 2, p. 224-233.

Parchi, P. et al., 2000, Genetic influence on the structural variations of the abnormal prion protein: Proc.Natl.Acad.Sci.U.S.A, v. 97, no. 18, p. 10168-10172.

Peden, A. H., and J. W. Ironside, 2004, Review: pathology of variant Creutzfeldt-Jakob disease: Folia Neuropathol., v. 42 Suppl A, p. 85-91.

Pereira, C., E. Ferreiro, S. M. Cardoso, and C. R. de Oliveira, 2004, Cell degeneration induced by amyloid-beta peptides: implications for Alzheimer's disease: J.Mol.Neurosci., v. 23, no. 1-2, p. 97-104.

Perrone-Bizzozero, N., and F. Bolognani, 2002, Role of HuD and other RNA-binding proteins in neural development and plasticity: J.Neurosci.Res., v. 68, no. 2, p. 121-126.

Polymenidou, M., K. Stoeck, M. Glatzel, M. Vey, A. Bellon, and A. Aguzzi, 2005, Coexistence of multiple PrPSc types in individuals with Creutzfeldt-Jakob disease: Lancet Neurol., v. 4, no. 12, p. 805-814.

Pompella, A., A. Visvikis, A. Paolicchi, T. De, V, and A. F. Casini, 2003, The changing faces of glutathione, a cellular protagonist: Biochem.Pharmacol., v. 66, no. 8, p. 1499-1503.

Power, J. H., S. Asad, T. K. Chataway, F. Chegini, J. Manavis, J. A. Temlett, P. H. Jensen, P. C. Blumbergs, and W. P. Gai, 2008, Peroxiredoxin 6 in human brain: molecular forms, cellular distribution and association with Alzheimer's disease pathology: Acta Neuropathol., v. 115, no. 6, p. 611-622.

Prusiner, S. B., and S. J. DeArmond, 1994, Prion diseases and neurodegeneration: Annu.Rev.Neurosci., v. 17, p. 311-339.

Prusiner, S. B., D. F. Groth, D. C. Bolton, S. B. Kent, and L. E. Hood, 1984, Purification and structural studies of a major scrapie prion protein: Cell, v. 38, no. 1, p. 127-134.

Prusiner, S. B., M. R. Scott, S. J. DeArmond, and F. E. Cohen, 1998, Prion protein biology: Cell, v. 93, no. 3, p. 337-348.

Puig, S., and D. J. Thiele, 2002, Molecular mechanisms of copper uptake and distribution: Curr.Opin.Chem.Biol., v. 6, no. 2, p. 171-180.

Puoti, G., A. Bizzi, G. Forloni, J. G. Safar, F. Tagliavini, and P. Gambetti, 2012, Sporadic human prion diseases: molecular insights and diagnosis: Lancet Neurol., v. 11, no. 7, p. 618-628.

Re, L., F. Rossini, F. Re, M. Bordicchia, A. Mercanti, O. S. Fernandez, and S. Barocci, 2006, Prion protein potentiates acetylcholine release at the neuromuscular junction: Pharmacol.Res., v. 53, no. 1, p. 62-68.

Riemer, C., I. Queck, D. Simon, R. Kurth, and M. Baier, 2000, Identification of upregulated genes in scrapie-infected brain tissue: J.Virol., v. 74, no. 21, p. 10245-10248.

Rivera-Milla, E. et al., 2006, Disparate evolution of prion protein domains and the distinct origin of Doppel- and prion-related loci revealed by fish-to-mammal comparisons: FASEB J., v. 20, no. 2, p. 317-319.

Rizo, J., and T. C. Sudhof, 2002, Snares and Munc18 in synaptic vesicle fusion: Nat.Rev.Neurosci., v. 3, no. 8, p. 641-653.

Ross, C. A., and M. A. Poirier, 2004, Protein aggregation and neurodegenerative disease: Nat.Med., v. 10 Suppl, p. S10-S17.

Saitoh, M., H. Nishitoh, M. Fujii, K. Takeda, K. Tobiume, Y. Sawada, M. Kawabata, K. Miyazono, and H. Ichijo, 1998, Mammalian thioredoxin is a direct inhibitor of apoptosis signal-regulating kinase (ASK) 1: EMBO J., v. 17, no. 9, p. 2596-2606.

Santuccione, A., V. Sytnyk, I. Leshchyns'ka, and M. Schachner, 2005, Prion protein recruits its neuronal receptor NCAM to lipid rafts to activate p59fyn and to enhance neurite outgrowth: J.Cell Biol., v. 169, no. 2, p. 341-354.

Sawada, M., A. Suzumura, H. Hosoya, T. Marunouchi, and T. Nagatsu, 1999, Interleukin-10 inhibits both production of cytokines and expression of cytokine receptors in microglia: J.Neurochem., v. 72, no. 4, p. 1466-1471.

Sayah, S., A. M. Ischenko, A. Zhakhov, A. S. Bonnard, and M. Fontaine, 1999, Expression of cytokines by human astrocytomas following stimulation by C3a and C5a anaphylatoxins: specific increase in interleukin-6 mRNA expression: J.Neurochem., v. 72, no. 6, p. 2426-2436.

Schmid, H. et al., 2006, Macroenzyme creatine kinase (CK) type 2 in HIV-infected patients is significantly associated with TDF and consists of ubiquitous mitochondrial CK: Antivir.Ther., v. 11, no. 8, p. 1071-1080.

Schmitt-Ulms, G. et al., 2001, Binding of neural cell adhesion molecules (N-CAMs) to the cellular prion protein: J.Mol.Biol., v. 314, no. 5, p. 1209-1225.

Schultz, J., A. Schwarz, S. Neidhold, M. Burwinkel, C. Riemer, D. Simon, M. Kopf, M. Otto, and M. Baier, 2004, Role of interleukin-1 in prion disease-associated astrocyte activation: Am.J.Pathol., v. 165, no. 2, p. 671-678.

Sekhar, K. R. et al., 2003, NADPH oxidase activity is essential for Keap1/Nrf2-mediated induction of GCLC in response to 2-indol-3-yl-methylenequinuclidin-3-ols: Cancer Res., v. 63, no. 17, p. 5636-5645.

Selvaggini, C. et al., 1993, Molecular characteristics of a protease-resistant, amyloidogenic and neurotoxic peptide homologous to residues 106-126 of the prion protein: Biochem.Biophys.Res.Commun., v. 194, no. 3, p. 1380-1386.

Sharief, M. K., A. Green, J. P. Dick, J. Gawler, and E. J. Thompson, 1999, Heightened intrathecal release of proinflammatory cytokines in Creutzfeldt-Jakob disease: Neurology, v. 52, no. 6, p. 1289-1291.

Shoshan-Barmatz, V., A. Israelson, D. Brdiczka, and S. S. Sheu, 2006, The voltage-dependent anion channel (VDAC): function in intracellular signalling, cell life and cell death: Curr.Pharm.Des, v. 12, no. 18, p. 2249-2270.

Shyng, S. L., J. E. Heuser, and D. A. Harris, 1994, A glycolipid-anchored prion protein is endocytosed via clathrin-coated pits: J.Cell Biol., v. 125, no. 6, p. 1239-1250.

Shyng, S. L., M. T. Huber, and D. A. Harris, 1993, A prion protein cycles between the cell surface and an endocytic compartment in cultured neuroblastoma cells: J.Biol.Chem., v. 268, no. 21, p. 15922-15928.

Silva-Adaya, D., M. E. Gonsebatt, and J. Guevara, 2014, Thioredoxin system regulation in the central nervous system: experimental models and clinical evidence: Oxid.Med.Cell Longev., v. 2014, p. 590808.

Silveira, J. R., G. J. Raymond, A. G. Hughson, R. E. Race, V. L. Sim, S. F. Hayes, and B. Caughey, 2005, The most infectious prion protein particles: Nature, v. 437, no. 7056, p. 257-261.

Stahl, N., M. A. Baldwin, R. Hecker, K. M. Pan, A. L. Burlingame, and S. B. Prusiner, 1992, Glycosylinositol phospholipid anchors of the scrapie and cellular prion proteins contain sialic acid: Biochemistry, v. 31, no. 21, p. 5043-5053.

Stahl, N., D. R. Borchelt, K. Hsiao, and S. B. Prusiner, 1987, Scrapie prion protein contains a phosphatidylinositol glycolipid: Cell, v. 51, no. 2, p. 229-240.

Stoeck, K., M. Bodemer, B. Ciesielczyk, B. Meissner, M. Bartl, U. Heinemann, and I. Zerr, 2005, Interleukin 4 and interleukin 10 levels are elevated in the cerebrospinal fluid of patients with Creutzfeldt-Jakob disease: Arch.Neurol., v. 62, no. 10, p. 1591-1594.

Stoeck, K., M. Bodemer, and I. Zerr, 2006, Pro- and anti-inflammatory cytokines in the CSF of patients with Creutzfeldt-Jakob disease: J.Neuroimmunol., v. 172, no. 1-2, p. 175-181.

Surka, M. C., C. W. Tsang, and W. S. Trimble, 2002a, The mammalian septin MSF localizes with microtubules and is required for completion of cytokinesis: Mol.Biol.Cell, v. 13, no. 10, p. 3532-3545.

Surka, M. C., C. W. Tsang, and W. S. Trimble, 2002b, The mammalian septin MSF localizes with microtubules and is required for completion of cytokinesis: Mol.Biol.Cell, v. 13, no. 10, p. 3532-3545.

Tahara, E. B., M. H. Barros, G. A. Oliveira, L. E. Netto, and A. J. Kowaltowski, 2007, Dihydrolipoyl dehydrogenase as a source of reactive oxygen species inhibited by caloric restriction and involved in Saccharomyces cerevisiae aging: FASEB J., v. 21, no. 1, p. 274-283.

Takagi, Y., I. Hattori, K. Nozaki, A. Mitsui, M. Ishikawa, N. Hashimoto, and J. Yodoi, 2000, Excitotoxic hippocampal injury is attenuated in thioredoxin transgenic mice: J.Cereb.Blood Flow Metab, v. 20, no. 5, p. 829-833.

Taraboulos, A., A. J. Raeber, D. R. Borchelt, D. Serban, and S. B. Prusiner, 1992, Synthesis and trafficking of prion proteins in cultured cells: Mol.Biol.Cell, v. 3, no. 8, p. 851-863.

Taylor, D. R., and N. M. Hooper, 2006, The prion protein and lipid rafts: Mol.Membr.Biol., v. 23, no. 1, p. 89-99.

Telling, G. C. et al., 1996, Evidence for the conformation of the pathologic isoform of the prion protein enciphering and propagating prion diversity: Science, v. 274, no. 5295, p. 2079-2082.

Thimmulappa, R. K., K. H. Mai, S. Srisuma, T. W. Kensler, M. Yamamoto, and S. Biswal, 2002, Identification of Nrf2-regulated genes induced by the chemopreventive agent sulforaphane by oligonucleotide microarray: Cancer Res., v. 62, no. 18, p. 5196-5203.

Thomas, K. J. et al., 2011, DJ-1 acts in parallel to the PINK1/parkin pathway to control mitochondrial function and autophagy: Hum.Mol.Genet., v. 20, no. 1, p. 40-50.

Tobler, I. et al., 1996, Altered circadian activity rhythms and sleep in mice devoid of prion protein: Nature, v. 380, no. 6575, p. 639-642.

Tsuchiya, N., M. Ochiai, K. Nakashima, T. Ubagai, T. Sugimura, and H. Nakagama, 2007, SND1, a component of RNA-induced silencing complex, is up-regulated in human colon cancers and implicated in early stage colon carcinogenesis: Cancer Res., v. 67, no. 19, p. 9568-9576.

Tsui-Pierchala, B. A., M. Encinas, J. Milbrandt, and E. M. Johnson, Jr., 2002, Lipid rafts in neuronal signaling and function: Trends Neurosci., v. 25, no. 8, p. 412-417.

Tumani, H., G. Shen, J. B. Peter, and W. Bruck, 1999, Glutamine synthetase in cerebrospinal fluid, serum, and brain: a diagnostic marker for Alzheimer disease?: Arch.Neurol., v. 56, no. 10, p. 1241-1246.

Tumani, H., A. Smirnov, S. Barchfeld, U. Olgemoller, K. Maier, P. Lange, W. Bruck, and R. Nau, 2000, Inhibition of glutamine synthetase in rabbit pneumococcal meningitis is associated with neuronal apoptosis in the dentate gyrus: Glia, v. 30, no. 1, p. 11-18.

Turk, E., D. B. Teplow, L. E. Hood, and S. B. Prusiner, 1988, Purification and properties of the cellular and scrapie hamster prion proteins: Eur.J.Biochem., v. 176, no. 1, p. 21-30.

Turnbull, S., B. J. Tabner, D. R. Brown, and D. Allsop, 2003, Copper-dependent generation of hydrogen peroxide from the toxic prion protein fragment PrP106-126: Neurosci.Lett., v. 336, no. 3, p. 159-162.

van Delft, M. F. et al., 2006, The BH3 mimetic ABT-737 targets selective Bcl-2 proteins and efficiently induces apoptosis via Bak/Bax if Mcl-1 is neutralized: Cancer Cell, v. 10, no. 5, p. 389-399.

van, E. B., I. Dobbeleir, W. M. De, L. E. De, U. Lubke, J. J. Martin, and P. Cras, 2004, Extracellular protein deposition correlates with glial activation and oxidative stress in Creutzfeldt-Jakob and Alzheimer's disease: Acta Neuropathol., v. 108, no. 3, p. 194-200.

Van, E. B., P. Pals, J. J. Martin, and P. Cras, 2002, Transmissible spongiform encephalopathies: the story of a pathogenic protein: Peptides, v. 23, no. 7, p. 1351-1359.

Vassallo, N., J. Herms, C. Behrens, B. Krebs, K. Saeki, T. Onodera, O. Windl, and H. A. Kretzschmar, 2005, Activation of phosphatidylinositol 3-kinase by cellular prion protein and its role in cell survival: Biochem.Biophys.Res.Commun., v. 332, no. 1, p. 75-82.

Vey, M., S. Pilkuhn, H. Wille, R. Nixon, S. J. DeArmond, E. J. Smart, R. G. Anderson, A. Taraboulos, and S. B. Prusiner, 1996, Subcellular colocalization of the cellular and scrapie prion proteins in caveolae-like membranous domains: Proc.Natl.Acad.Sci.U.S.A, v. 93, no. 25, p. 14945-14949.

Vidal, A. E., S. Boiteux, I. D. Hickson, and J. P. Radicella, 2001, XRCC1 coordinates the initial and late stages of DNA abasic site repair through protein-protein interactions: EMBO J., v. 20, no. 22, p. 6530-6539.

Vilches, S. et al., 2013, Neurotoxicity of prion peptides mimicking the central domain of the cellular prion protein: PLoS.One., v. 8, no. 8, p. e70881.

Waggoner, D. J., T. B. Bartnikas, and J. D. Gitlin, 1999, The role of copper in neurodegenerative disease: Neurobiol.Dis., v. 6, no. 4, p. 221-230.

Walter, E. D., M. Chattopadhyay, and G. L. Millhauser, 2006, The affinity of copper binding to the prion protein octarepeat domain: evidence for negative cooperativity: Biochemistry, v. 45, no. 43, p. 13083-13092.

Wandzioch, E., M. Pusey, A. Werda, S. Bail, A. Bhaskar, M. Nestor, J. J. Yang, and L. M. Rice, 2014, PME-1 modulates protein phosphatase 2A activity to promote the malignant phenotype of endometrial cancer cells: Cancer Res., v. 74, no. 16, p. 4295-4305.

Wang, X., T. G. Petrie, Y. Liu, J. Liu, H. Fujioka, and X. Zhu, 2012, Parkinson's disease-associated DJ-1 mutations impair mitochondrial dynamics and cause mitochondrial dysfunction: J.Neurochem., v. 121, no. 5, p. 830-839.

Watt, N. T., and N. M. Hooper, 2005, Reactive oxygen species (ROS)-mediated beta-cleavage of the prion protein in the mechanism of the cellular response to oxidative stress: Biochem.Soc.Trans., v. 33, no. Pt 5, p. 1123-1125.

Wedler, F. C., and B. R. Horn, 1976, Catalytic mechanisms of glutamine synthetase enzymes. Studies with analogs of possible intermediates and transition states: J.Biol.Chem., v. 251, no. 23, p. 7530-7538.

Weise, J., R. Sandau, S. Schwarting, O. Crome, A. Wrede, W. Schulz-Schaeffer, I. Zerr, and M. Bahr, 2006, Deletion of cellular prion protein results in reduced Akt activation, enhanced postischemic caspase-3 activation, and exacerbation of ischemic brain injury: Stroke, v. 37, no. 5, p. 1296-1300.

Westergard, L., H. M. Christensen, and D. A. Harris, 2007a, The cellular prion protein (PrP(C)): its physiological function and role in disease: Biochim.Biophys.Acta, v. 1772, no. 6, p. 629-644.

Westergard, L., H. M. Christensen, and D. A. Harris, 2007b, The cellular prion protein (PrP(C)): its physiological function and role in disease: Biochim.Biophys.Acta, v. 1772, no. 6, p. 629-644.

Will, R. G., 1994, Gene influences on Creutzfeldt-Jakob disease: Lancet, v. 344, no. 8933, p. 1310-1311.

Windl, O. et al., 1996, Genetic basis of Creutzfeldt-Jakob disease in the United Kingdom: a systematic analysis of predisposing mutations and allelic variation in the PRNP gene: Hum.Genet., v. 98, no. 3, p. 259-264.

Yamamoto, A. et al., 1998, Deficiency in protein L-isoaspartyl methyltransferase results in a fatal progressive epilepsy: J.Neurosci., v. 18, no. 6, p. 2063-2074.

Ye, H. et al., 2002, DNA binding is required for the apoptogenic action of apoptosis inducing factor: Nat.Struct.Biol., v. 9, no. 9, p. 680-684.

Yuan, J., and B. A. Yankner, 2000, Apoptosis in the nervous system: Nature, v. 407, no. 6805, p. 802-809.

Yun, S. W., M. Gerlach, P. Riederer, and M. A. Klein, 2006, Oxidative stress in the brain at early preclinical stages of mouse scrapie: Exp.Neurol., v. 201, no. 1, p. 90-98.

Yuste, V. J., I. Sanchez-Lopez, C. Sole, R. S. Moubarak, J. R. Bayascas, X. Dolcet, M. Encinas, S. A. Susin, and J. X. Comella, 2005, The contribution of apoptosis-inducing factor, caspase-activated DNase, and inhibitor of caspase-activated DNase to the nuclear phenotype and DNA degradation during apoptosis: J.Biol.Chem., v. 280, no. 42, p. 35670-35683.

Zabel, M. D. et al., 2007, Stromal complement receptor CD21/35 facilitates lymphoid prion colonization and pathogenesis: J.Immunol., v. 179, no. 9, p. 6144-6152.

Zafar, S., M. Schmitz, N. Younus, W. Tahir, M. Shafiq, F. Llorens, I. Ferrer, O. Andeoletti, and I. Zerr, 2015, Creutzfeldt-Jakob Disease Subtype-Specific Regional and Temporal Regulation of ADP Ribosylation Factor-1-Dependent Rho/MLC Pathway at Pre-Clinical Stage: J.Mol.Neurosci., v. 56, no. 2, p. 329-348.

Zafar, S., N. Younas, S. Correia, M. Shafiq, W. Tahir, M. Schmitz, I. Ferrer, O. Andreoletti, and I. Zerr, 2016, Strain-Specific Altered Regulatory Response of Rab7a and Tau in Creutzfeldt-Jakob Disease and Alzheimer's Disease: Mol.Neurobiol..

Zanata, S. M. et al., 2002, Stress-inducible protein 1 is a cell surface ligand for cellular prion that triggers neuroprotection: EMBO J., v. 21, no. 13, p. 3307-3316.

Zhang, J., and Q. M. Chen, 2013, Far upstream element binding protein 1: a commander of transcription, translation and beyond: Oncogene, v. 32, no. 24, p. 2907-2916.

Zhang, J., C. D. Keene, C. Pan, K. S. Montine, and T. J. Montine, 2008, Proteomics of human neurodegenerative diseases: J.Neuropathol.Exp.Neurol., v. 67, no. 10, p. 923-932.

Zhang, P., X. Hu, X. Xu, Y. Chen, and R. J. Bache, 2011, Dimethylarginine dimethylaminohydrolase 1 modulates endothelial cell growth through nitric oxide and Akt: Arterioscler.Thromb.Vasc.Biol., v. 31, no. 4, p. 890-897.

Zhang, P., X. Xu, X. Hu, H. Wang, J. Fassett, Y. Huo, Y. Chen, and R. J. Bache, 2013, DDAH1 deficiency attenuates endothelial cell cycle progression and angiogenesis: PLoS.One., v. 8, no. 11, p. e79444.

Zhou, F. et al., 2009, Attenuation of neuronal degeneration in thioredoxin-1 overexpressing mice after mild focal ischemia: Brain Res., v. 1272, p. 62-70.

Zhou, R. H., K. Kokame, Y. Tsukamoto, C. Yutani, H. Kato, and T. Miyata, 2001, Characterization of the human NDRG gene family: a newly identified member, NDRG4, is specifically expressed in brain and heart: Genomics, v. 73, no. 1, p. 86-97.

Zhou, W., and C. R. Freed, 2005, DJ-1 up-regulates glutathione synthesis during oxidative stress and inhibits A53T alpha-synuclein toxicity: J.Biol.Chem., v. 280, no. 52, p. 43150-43158.

Zhou, W., M. Zhu, M. A. Wilson, G. A. Petsko, and A. L. Fink, 2006, The oxidation state of DJ-1 regulates its chaperone activity toward alpha-synuclein: J.Mol.Biol., v. 356, no. 4, p. 1036-1048.

10 PUBLICATIONS

[1] **Tahir W**, Zafar S, Llorens F, Arora A, Thüne K, Schmitz M, Gotzmann N, Kruse N, Mollenhauer B, Torres JM, Andréoletti O, Ferrer I, Zerr I. Cerebellum alterations in molecular subtypes of sporadic Creutzfeldt–Jakob disease with DJ-1 as a key regulator of Oxidative stress. 2016 (Manuscript in preparation).

[2] Arora AS, Zafar S, Llorens F, Mihm S, Kumar P, **Tahir W**, Thune K, Rosemol G, Schmitz M, Zerr I. Proteome profiling of Prion protein (PrP^{C}) knockout mice liver revealed a role of PrPC in lipid metabolism. Electrophoresis 2016 (Submitted).

[3] Zafar S, Younas N, Sheikh N, **Tahir W**, Shafiq M, Schmitz M, Grewe V, Ferrer I, Andreoletti O, Zerr I. Alteration of cofilin-1 activity: early critical response of LIMK-APP-SSH1 1 pathway in MM1 and VV2 subtype specific Creutzfeldt-Jakob disease. 2016 (Submitted).

[4] Llorens F, Thune K, Schmitz M, Ansoleaga B, Frau-Mendez MA, Cramm M, **Tahir W**, Gotzmann N, Berjaoui S, Carmona M, Silva CJ, Fernandez-Vega I, Zarranz JJ, Zerr I, Ferrer I. Identification of new molecular alterations in Fatal Familial Insomnia. Hum Mol Genet 2016.

[5] Zafar S, Younas N, Correia S, Shafiq M, **Tahir W**, Schmitz M, Ferrer I, Andreoletti O, Zerr I. Strain-Specific Altered Regulatory Response of Rab7a and Tau in Creutzfeldt-Jakob Disease and Alzheimer's Disease. Mol Neurobiol 2016.

[6] Zafar S, Schmitz M, Younus N, **Tahir W**, Shafiq M, Llorens F, Ferrer I, Andeoletti O, Zerr I. Creutzfeldt-Jakob Disease Subtype-Specific Regional and Temporal Regulation of ADP Ribosylation Factor-1-Dependent Rho/MLC Pathway at Pre-Clinical Stage. J Mol Neurosci 2015;56(2):329-48.

[7] Arora AS, Zafar S, Kollmar O, Llorens F, **Tahir W**, Vanselow S, Kumar P, Schmerr MJ, Schmitz M, Zerr I. Application of capillary immunoelectrophoresis revealed an age- and gender-dependent regulated expression of PrPC in liver. Electrophoresis 2015;36(24):3026-33.

[8] Zafar S, Asif AR, Ramljak S, **Tahir W**, Schmitz M, Zerr I. Anchorless 23-230 PrPC interactomics for elucidation of PrPC protective role. Mol Neurobiol 2014;49(3):1385-99.

ABSTRACTS/ POSTERS/TALKS

[1] **Poster: Tahir, W.,** Zafar, S., Nesslar, S., Arora, A., Shafiq, M., Schmitz, M., Stadelmann, C., and Zerr, I. 2013. Characterization of truncated forms of cellular prion protein under inflammatory and demyelinating stress condition by proteomic analysis of the Spinal Cord. Prion 2013. Banf. Alberta. Canada.

[2] **Poster:** Zafar, S., Asif, AR., Ramljak, S., Tahir**, W.,** Schmitz, M., and Zerr, I. Targeted interactomics to characterize anchorless 23-230 form of PrP^{C}. Prion 2013. Banf. Alberta. Canada.

[3] **Poster: Tahir, W.,** Zafar, S., Arora, A., Younus, N., Llorens, F., Schmitz, M., Ferrer, I., and Zerr, I. 2015. Characterization of differential proteome expression of MM1 and VV2 subtypes of sporadic Creutzfeldt-Jakob disease (sCJD) in Cerebellum. Prion 2015. Colorado. USA.

[4] **Abstract/ Talk: Tahir, W.,** Zafar, S., Schmitz, M., Llorens, F., Ferrer, I., and Zerr, I. 2015. Cross talk on the role of PARK7 (DJ-1) in pathophysiology of sporadic Creutzfeldt-Jakob diseases (CJD) in cerebellum in MM1 and VV2 subtypes. 4rth Iberian Congress on Prions, Lisbon. Portugal.

[5] **Poster:** Younas, N., Zafar S., Shafiq M., **Tahir, W.,** Schmitz M., Ferrer I., Andréoletti O., and Zerr I. Early response of Cofilin1 pathway in Creutzfeldt Jakob disease. Prion 2016. Tokyo. Japan.

11 Curriculum Vitae

First Name:	Waqas
Last Name:	Tahir
Date of Birth:	30.03.1984
Place of Birth:	Pakpattan, Pakistan
Nationality:	Pakistani

EDUCATION

04/2013- 03/2016 **PhD (Biology)**

Prion Research Group, Department of Neurology, University of Medicine Goettingen. Goerge August University, Goettingen, Germany.

Title: Identification and characterization of proteomic regulations in the cerebellum region of brain in MM1 and VV2 subtypes of sporadic Creutzfeldt-Jakob disease (sCJD).

10/2009- 12/2011 **Master of Philosophy (M.Phil.) Molecular Biology & Biotechnology**

Institute of Biochemistry and Biotechnology, UVAS, Lahore, Pakistan

Title: Evaluation of POU1F1 as Candidate gene to have influence on milk production in Red Sindhi and Dhani cattle through SNP detection.

01/2003- 03/2008 **DVM (Doctor of Veterinary Medicine)**

University of Veterinary & Animal sciences, Lahore, Pakistan

08/1999- 10/2002 **Higher Secondary School Certificate / F. Sc. (Pre-medical)**

Pakpattan, Pakistan

04/1998- 08/1999 **Secondary School Certificate / Matriculation (10th Grade)**

Pakpattan, Pakistan

WORK EXPERIENCE

05/2012- 07/2016 **Research Assistant**

Prion Research Group, Department of Neurology, University of Medicine Goettingen. Goettingen, Germany

10/2009-10/2011 **Master Thesis**

Institute of Biochemistry and Biotechnology, UVAS, Lahore, Pakistan

12 Acknowledgement

I owe my great acknowledgement to all those people who have contributed and helped in making this dissertation possible.

My first heartiest gratitude is to our group supervisor/ leader, **Prof. Dr. Inga Zerr**. I feel immensely lucky to have a group supervisor/ leader who gave me the opportunity to work with all freedom to explore at my own and always gave helpful and positive suggestions regarding my work. I could learn from her, how to think and question scientifically to be a critical researcher for doing a better research and science. Her patience and support in response to my mistakes helped me to be even more responsible researcher. Big heartfelt thanks to you for your support and confidence in me; Prof. Dr. Inga Zerr.

My next gratitude is to my supervisor; **Dr. Saima Zafar**, for showing her trust in me, supporting my work and ideas and all non- and scientific discussions.

Prof. Dr. Karsten Hanisch (late) was one of the best people whom I met during my dissertation period. He was my thesis committee member. I find my words very smaller for describing my gratitude for him. He was an exceptional human being, greatly knowledgful researcher and an encouraging supervisor. I am always saddened on his demise. You will be always remembered.

I owe my sincere gratitudes to the members of my thesis committee; **Prof. Dr. Mikael Simons** for his critical reviews and **PD Dr. Michael Hoppert** for his encouragement and kind suggestions during thesis committee meetings.

I would like to express my deep gratitude to **Dr. Franc Llorens** for his constructive criticisms and comments at different stages of my research along with thought provoking discussions, support and encouragement during my trip to Lisbon which had been very exciting in the beginning but a night-mare for me in the end. I am also thankful to **Dr. Matthias Schmitz** for his friendly suggestions and discussions, **Dr. Katrin Dittmar** for her friendly gestures, **Dr. Maria Cramn** (Miss Perfectionist) for sharing her expert opinions and **Barbara Ciesielczyk** for her patience and co-operation during my early days when I did not know German and she did not know English and Urdu.

I want to pay my appreciation and acknowledgment to **Dr. Walter Schluz-Schäffer** for his precise scientific discussions and expert opinions on related topics which enriched my knowledge in the area, **Dr. Uwe Hahmann** for being always ready to listen, help and make things possible for me to work in S2 lab, **Dr. Niels Kurse** for sharing his expertise on ECL based ELISA and **Dr. Arne Wrede** for his demonstration on using fluorescent microscope.

I don't want to forget **Dr. Olivier Andréoletti** for developing and providing mice models of sCJD, **Dr. Hassan Dihazi** for giving antibodies and letting me use fluorescent scanner, **Dr. Andre Fischer** and **Dr. Stefen Bonn** for sharing their lab facilities as well. So big acknowledgment for you all guys for your kind co-operation ever.

Especial thanks to **Maja Schneider-Dominco** and **Jolanthe Ehrlich** for being always there with their smiles to help and guide.

I also appreciate and thank for an unforgettable love and friendly time from all of my colleagues and friends including Mohsin, Neelum, Katrin, Tobias, Umer, Susane, Angela, Eriton, Ting, Niccolo, Viviane, Kerim, Zaheer and Niamat. Wish you all the best for your future endeavours. You all are rocking.

I am also grateful to **Dr. Aman Arora,** for everything which you did to facilitate me, my work, all non- and scientific discussions and for receiving me at Bahnof on my first day of arrival in Goettingen. This was the only time, which I remember when you were right in time. Big thanks for this.

Very importantly, there is one person, **Nadine Gotzmann;** whose suggestions, support and encouragement helped me to keep myself sane throughout these difficult years of ups and downs. Special heartfelt gratitude to you for being always right there with patience, love and care and even bigger "stomach-felt" thanks for delicious coconut cake. You are a star.

Finally, I want to pay my special heartfelt gratitude to my beloved parents for their unconditional affection, support, encouragement and prayers throughout my life. I also want to appreciate and thank for the love, support and prayers of my all other beloved family members.

Waqas Tahir.